US012082868B2

(12) **United States Patent**
Chen

(10) **Patent No.: US 12,082,868 B2**
(45) **Date of Patent: *Sep. 10, 2024**

(54) **MULTI-POLE SYNCHRONOUS PULMONARY ARTERY RADIOFREQUENCY ABLATION CATHETER**

(71) Applicant: **Pulnovo Medical (Wuxi) Co., Ltd.**, Jiangsu (CN)

(72) Inventor: **Shaoliang Chen**, Nanjing (CN)

(73) Assignee: **PULNOVO MEDICAL (WUXI) CO., LTD.**, Wuxi (CN)

(*) Notice: Subject to any disclaimer, the term of this patent is extended or adjusted under 35 U.S.C. 154(b) by 0 days.

This patent is subject to a terminal disclaimer.

(21) Appl. No.: **18/203,726**

(22) Filed: **May 31, 2023**

(65) **Prior Publication Data**

US 2023/0380881 A1 Nov. 30, 2023

Related U.S. Application Data

(63) Continuation-in-part of application No. 17/357,720, filed on Jun. 24, 2021, which is a continuation of (Continued)

(30) **Foreign Application Priority Data**

Nov. 13, 2012 (CN) 201210453470.4
Mar. 27, 2013 (CN) 201310103141.1

(51) **Int. Cl.**
A61B 18/00 (2006.01)
A61B 18/12 (2006.01)
(Continued)

(52) **U.S. Cl.**
CPC ***A61B 18/1206*** (2013.01); ***A61B 18/1492*** (2013.01); ***A61N 1/06*** (2013.01);
(Continued)

(58) **Field of Classification Search**
CPC A61B 2015/00386; A61B 2018/00577; A61B 2018/1467; A61B 2018/1407;
(Continued)

(56) **References Cited**

U.S. PATENT DOCUMENTS

5,263,493 A 11/1993 Avitall
5,643,197 A 7/1997 Brucker et al.
(Continued)

FOREIGN PATENT DOCUMENTS

AU 2007290727 B2 1/2012
AU 2015287691 B2 4/2019
(Continued)

OTHER PUBLICATIONS

Benza, et al. Predicting survival in pulmonary arterial hypertension: insights from the Registry to Evaluate Early and Long-Term Pulmonary Arterial Hypertension Disease Management (REVEAL). Circulation. Jul. 13, 2010;122(2):164-72. doi: 10.1161/CIRCULATIONAHA.109.898122. Epub Jun. 28, 2010.
(Continued)

Primary Examiner — Jaymi E Della
(74) *Attorney, Agent, or Firm* — WILSON SONSINI GOODRICH & ROSATI

(57) **ABSTRACT**

A multi-pole synchronous pulmonary artery radiofrequency ablation catheter may comprise a control handle, a catheter body and an annular ring. One end of the catheter body may be flexible, and the flexible end of the catheter body may be connected to the annular ring. The other end of the catheter body may be connected to the control handle. A shape memory wire may be arranged in the annular ring. One end of the shape memory wire may extend to an end of the annular ring and the other end of the shape memory wire may pass through a root of the annular ring and be fixed on the flexible end of the catheter body. The annular ring may
(Continued)

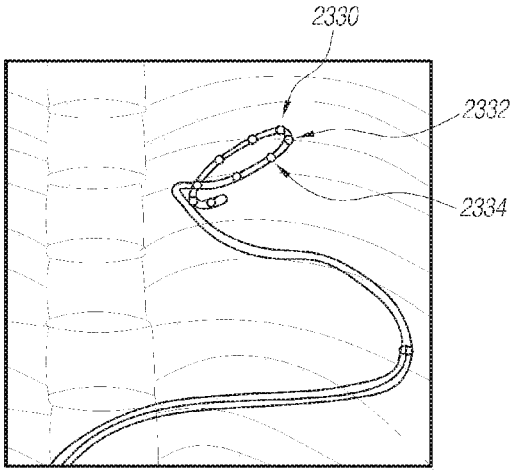

be provided with an electrode group. The device can be used to treat pulmonary hypertension or heart failure with pulmonary denervation.

13 Claims, 44 Drawing Sheets

Related U.S. Application Data

application No. 15/873,721, filed on Jan. 17, 2018, now Pat. No. 11,241,267, which is a continuation of application No. 14/672,013, filed on Mar. 27, 2015, now Pat. No. 9,918,776, which is a continuation of application No. 14/666,214, filed on Mar. 23, 2015, now Pat. No. 9,827,036, which is a continuation-in-part of application No. 14/530,588, filed on Oct. 31, 2014, now abandoned, and a continuation-in-part of application No. 14/079,230, filed on Nov. 13, 2013, now abandoned.

(60) Provisional application No. 62/023,781, filed on Jul. 11, 2014.

(51) **Int. Cl.**

A61B 18/14	(2006.01)
A61N 1/06	(2006.01)
A61B 17/00	(2006.01)
A61B 17/32	(2006.01)

(52) **U.S. Cl.**

CPC *A61B 2017/00867* (2013.01); *A61B 2017/320069* (2017.08); *A61B 2018/00029* (2013.01); *A61B 2018/00214* (2013.01); *A61B 2018/00345* (2013.01); *A61B 2018/00357* (2013.01); *A61B 2018/00375* (2013.01); *A61B 2018/00404* (2013.01); *A61B 2018/00434* (2013.01); *A61B 2018/00577* (2013.01); *A61B 2018/00613* (2013.01); *A61B 2018/00642* (2013.01); *A61B 2018/00702* (2013.01); *A61B 2018/00791* (2013.01); *A61B 2018/00797* (2013.01); *A61B 2018/00916* (2013.01); *A61B 2018/00988* (2013.01); *A61B 2018/124* (2013.01); *A61B 2018/1407* (2013.01); *A61B 2018/144* (2013.01); *A61B 2018/1467* (2013.01); *A61B 2218/002* (2013.01)

(58) **Field of Classification Search**

CPC A61B 2018/00404; A61B 2018/00434; A61B 2018/00375; A61B 18/1492

See application file for complete search history.

(56) **References Cited**

U.S. PATENT DOCUMENTS

5,715,817	A	2/1998	Stevens-Wright et al.
5,782,900	A	7/1998	De La Rama et al.
5,797,905	A	8/1998	Fleischman et al.
5,830,214	A	11/1998	Flom et al.
5,833,604	A	11/1998	Houser et al.
5,836,947	A	11/1998	Fleischman et al.
5,913,856	A	6/1999	Chia et al.
5,919,188	A	7/1999	Shearon et al.
5,938,694	A	8/1999	Jaraczewski et al.
6,064,902	A	5/2000	Haissaguerre et al.
6,090,104	A	7/2000	Webster, Jr.
6,096,036	A	8/2000	Bowe et al.
6,115,626	A	9/2000	Whayne et al.
6,123,702	A	9/2000	Swanson et al.
6,198,974	B1	3/2001	Webster, Jr.
6,237,886	B1	5/2001	Katsumata et al.
6,292,695	B1	9/2001	Webster, Jr. et al.
6,411,852	B1	6/2002	Danek et al.
6,493,589	B1	12/2002	Medhkour et al.
6,532,378	B2	3/2003	Saksena et al.
6,564,096	B2	5/2003	Mest
6,575,969	B1	6/2003	Rittman, III et al.
6,690,971	B2	2/2004	Schauerte et al.
7,260,431	B2	8/2007	Libbus et al.
7,269,457	B2	9/2007	Shafer et al.
7,363,076	B2	4/2008	Yun et al.
7,367,951	B2	5/2008	Bennett et al.
7,587,238	B2	9/2009	Moffitt et al.
7,616,990	B2	11/2009	Chavan et al.
7,623,926	B2	11/2009	Rossing et al.
7,630,760	B2	12/2009	Libbus et al.
7,660,628	B2	2/2010	Libbus et al.
7,664,548	B2	2/2010	Amurthur et al.
7,711,430	B2	5/2010	Errico et al.
7,715,915	B1	5/2010	Ryu et al.
7,734,355	B2	6/2010	Cohen et al.
7,744,618	B2	6/2010	Shuros et al.
7,783,353	B2	8/2010	Libbus et al.
7,789,877	B2	9/2010	Vanney
7,801,604	B2	9/2010	Brockway et al.
7,826,899	B1	11/2010	Ryu et al.
7,828,795	B2	11/2010	Privitera et al.
7,899,527	B2	3/2011	Yun et al.
7,925,342	B2	4/2011	Amurthur et al.
7,937,147	B2	5/2011	Sih et al.
8,019,435	B2	9/2011	Hastings et al.
8,027,724	B2	9/2011	Wei et al.
8,032,215	B2	10/2011	Libbus et al.
8,052,668	B2	11/2011	Sih
8,073,538	B2	12/2011	Peters et al.
8,088,127	B2	1/2012	Mayse et al.
8,116,883	B2	2/2012	Williams et al.
8,126,559	B2	2/2012	Libbus
8,229,564	B2	7/2012	Rezai
8,249,705	B1	8/2012	Kieval et al.
8,369,954	B2	2/2013	Stack et al.
8,442,638	B2	5/2013	Libbus et al.
8,483,832	B2	7/2013	Simon
8,527,064	B2	9/2013	Zhang et al.
8,585,601	B2	11/2013	Sverdlik et al.
8,620,400	B2	12/2013	De La Rama et al.
8,652,201	B2	2/2014	Oberti et al.
8,672,917	B2	3/2014	Sigg et al.
8,696,581	B2	4/2014	Sverdlik et al.
8,702,619	B2	4/2014	Wang
8,808,345	B2	8/2014	Clark et al.
8,840,601	B2	9/2014	Salahieh et al.
8,911,439	B2	12/2014	Mayse et al.
8,929,990	B2	1/2015	Moffitt et al.
8,983,609	B2	3/2015	Rezai et al.
8,986,231	B2	3/2015	Gertner et al.
9,005,100	B2	4/2015	Gnanashanmugam et al.
9,023,034	B2	5/2015	Jenson et al.
9,028,391	B2	5/2015	Gnanashanmugam et al.
9,028,417	B2	5/2015	Sverdlik et al.
9,028,485	B2	5/2015	Edmunds et al.
9,072,894	B2	7/2015	Chin et al.
9,084,609	B2	7/2015	Smith
9,089,350	B2	7/2015	Willard
9,126,044	B2	9/2015	Kramer et al.
9,283,031	B2	3/2016	Janssen et al.
9,326,786	B2	5/2016	Sverdlik et al.
9,345,900	B2	5/2016	Wu et al.
9,427,277	B2	8/2016	Swanson et al.
9,522,035	B2	12/2016	Highsmith
9,566,456	B2	2/2017	Sverdlik et al.
9,649,153	B2	5/2017	Mayse et al.
9,820,800	B2	11/2017	Chen
9,827,036	B2	11/2017	Chen
9,833,623	B2	12/2017	Gnanashanmugam et al.
9,872,720	B2	1/2018	Chen
9,918,776	B2	3/2018	Chen
10,357,304	B2	7/2019	Sverdlik et al.
10,368,893	B2	8/2019	Sverdlik et al.

(56) **References Cited**

U.S. PATENT DOCUMENTS

10,518,112	B2	12/2019	Gilad
10,874,454	B2	12/2020	Chen
10,933,259	B2	3/2021	Sverdlik et al.
10,946,197	B2	3/2021	Yun et al.
10,967,160	B2	4/2021	Sverdlik et al.
11,007,001	B1	5/2021	Carignan et al.
11,241,267	B2	2/2022	Chen
11,318,331	B2	5/2022	Shabtay et al.
11,357,447	B2	6/2022	Sverdlik et al.
11,395,694	B2	7/2022	Hata et al.
11,534,631	B2	12/2022	Gilad
11,717,346	B2	8/2023	Grasse et al.
2001/0031987	A1	10/2001	Saksena et al.
2002/0065514	A1	5/2002	Rashidi
2002/0120304	A1	8/2002	Mest
2004/0133197	A1	7/2004	Utley et al.
2005/0004440	A1	1/2005	Vanney
2005/0004565	A1	1/2005	Vanney
2005/0010095	A1	1/2005	Stewart et al.
2005/0113822	A1	5/2005	Fuimaono et al.
2005/0153885	A1	7/2005	Yun et al.
2005/0261672	A1	11/2005	Deem et al.
2005/0283148	A1	12/2005	Janssen et al.
2006/0041277	A1	2/2006	Deem et al.
2006/0074272	A1	4/2006	Diubaldi
2006/0116737	A1	6/2006	Libbus
2006/0167498	A1	7/2006	Dilorenzo
2006/0217772	A1	9/2006	Libbus et al.
2006/0241366	A1	10/2006	Falwell et al.
2007/0032835	A1	2/2007	Rittman et al.
2007/0038055	A1	2/2007	Fuimaono et al.
2007/0060921	A1	3/2007	Janssen et al.
2007/0083193	A1	4/2007	Werneth et al.
2007/0083194	A1	4/2007	Kunis et al.
2007/0129720	A1	6/2007	Demarais et al.
2007/0129760	A1	6/2007	Demarais et al.
2007/0142879	A1	6/2007	Greenberg et al.
2007/0191904	A1	8/2007	Libbus et al.
2007/0225641	A1	9/2007	Schneider et al.
2007/0255379	A1	11/2007	Williams et al.
2008/0255642	A1	10/2008	Zarins et al.
2008/0281312	A1	11/2008	Werneth et al.
2008/0306570	A1	12/2008	Rezai et al.
2009/0024124	A1	1/2009	Lefler et al.
2009/0062873	A1	3/2009	Wu et al.
2009/0118780	A1	5/2009	Dilorenzo
2009/0177262	A1	7/2009	Oberti et al.
2009/0216290	A1	8/2009	Ruse et al.
2009/0228078	A1	9/2009	Zhang et al.
2009/0248119	A1	10/2009	Libbus et al.
2009/0254142	A1	10/2009	Edwards et al.
2010/0057074	A1	3/2010	Roman et al.
2010/0094196	A1	4/2010	Nash et al.
2010/0113928	A1	5/2010	Thapliyal et al.
2010/0114095	A1	5/2010	Janssen et al.
2010/0137860	A1	6/2010	Demarais et al.
2010/0152726	A1	6/2010	Cadouri et al.
2010/0168548	A1	7/2010	Govari et al.
2010/0217347	A1	8/2010	Swoyer et al.
2010/0222859	A1	9/2010	Govari et al.
2010/0228317	A1	9/2010	Libbus et al.
2010/0241188	A1	9/2010	Errico et al.
2010/0249568	A1	9/2010	Stehr et al.
2010/0249773	A1	9/2010	Clark et al.
2010/0249859	A1	9/2010	Dilorenzo
2010/0268307	A1	10/2010	Demarais et al.
2010/0274221	A1	10/2010	Sigg et al.
2010/0286684	A1	11/2010	Hata et al.
2010/0286734	A1	11/2010	Yun et al.
2010/0298905	A1	11/2010	Simon
2011/0034915	A1	2/2011	Ibrahim et al.
2011/0082537	A1	4/2011	Moffitt et al.
2011/0112400	A1	5/2011	Emery et al.
2011/0118725	A1	5/2011	Mayse et al.
2011/0152855	A1	6/2011	Mayse et al.
2011/0160720	A1	6/2011	Johnson
2011/0166482	A1	7/2011	Stack et al.
2011/0178569	A1	7/2011	Parnis et al.
2011/0200171	A1	8/2011	Beetel et al.
2011/0202098	A1	8/2011	Demarais et al.
2011/0207758	A1	8/2011	Sobotka et al.
2011/0257561	A1	10/2011	Gertner et al.
2011/0257622	A1	10/2011	Salahieh et al.
2011/0257708	A1	10/2011	Kramer et al.
2011/0276103	A1	11/2011	Maile et al.
2011/0301587	A1	12/2011	Deem et al.
2011/0301664	A1	12/2011	Rezai
2011/0301679	A1	12/2011	Rezai et al.
2011/0306851	A1	12/2011	Wang
2012/0029505	A1	2/2012	Jenson
2012/0029509	A1	2/2012	Smith
2012/0029510	A1	2/2012	Haverkost
2012/0029511	A1	2/2012	Smith et al.
2012/0029512	A1	2/2012	Willard et al.
2012/0065554	A1	3/2012	Pikus
2012/0078129	A1	3/2012	Bailin
2012/0095371	A1	4/2012	Sverdlik et al.
2012/0116382	A1	5/2012	Ku et al.
2012/0123258	A1	5/2012	Willard
2012/0123406	A1	5/2012	Edmunds et al.
2012/0143294	A1	6/2012	Clark et al.
2012/0157992	A1	6/2012	Smith et al.
2012/0157993	A1	6/2012	Jenson et al.
2012/0158104	A1	6/2012	Huynh et al.
2012/0165815	A1	6/2012	Collins et al.
2012/0172680	A1	7/2012	Gelfand et al.
2012/0172870	A1	7/2012	Jenson et al.
2012/0184952	A1	7/2012	Jenson et al.
2012/0215106	A1	8/2012	Sverdlik et al.
2012/0232551	A1	9/2012	Swanson et al.
2012/0272839	A1	11/2012	Kaneko
2012/0277839	A1	11/2012	Kramer et al.
2012/0290024	A1	11/2012	Zhang et al.
2012/0294424	A1	11/2012	Chin et al.
2012/0302909	A1	11/2012	Mayse et al.
2013/0110104	A1	5/2013	Corvi et al.
2013/0131743	A1	5/2013	Yamasaki et al.
2013/0165922	A1	6/2013	Falwell et al.
2013/0204068	A1*	8/2013	Gnanashanmugam A61B 18/18 601/3
2013/0204242	A1	8/2013	Sverdlik et al.
2013/0211396	A1	8/2013	Sverdlik et al.
2013/0211437	A1	8/2013	Sverdlik et al.
2013/0218054	A1	8/2013	Sverdlik et al.
2013/0218068	A1	8/2013	Sverdlik et al.
2013/0317375	A1	11/2013	Garcia et al.
2014/0179993	A1	6/2014	Alexander et al.
2014/0180277	A1	6/2014	Chen
2014/0187894	A1	7/2014	Bui et al.
2015/0057599	A1	2/2015	Chen
2016/0128767	A1	5/2016	Azamian et al.
2018/0326227	A1	11/2018	Sverdlik et al.
2019/0290350	A1	9/2019	Sverdlik et al.
2019/0308003	A1	10/2019	Sverdlik et al.
2019/0366130	A1	12/2019	Sverdlik et al.
2020/0238107	A1	7/2020	Shabtay et al.
2021/0178194	A1	6/2021	Sverdlik et al.
2021/0338305	A1	11/2021	Chen
2022/0241617	A1	8/2022	Shabtay et al.
2022/0287634	A1	9/2022	Sverdlik et al.
2023/0037695	A1	2/2023	Carignan et al.

FOREIGN PATENT DOCUMENTS

AU	2019204804	B2	7/2020
CN	101797181	A	8/2010
CN	102119009	A	7/2011
CN	102198015	A	9/2011
CN	102641153	A	8/2012
CN	102686179	A	9/2012
CN	102908191	A	2/2013
CN	103142304	A	6/2013
CN	202982207	U	6/2013

(56) **References Cited**

FOREIGN PATENT DOCUMENTS

CN	103908334	A	7/2014
CN	103908336	A	7/2014
EP	0467422	B1	12/1997
EP	0916360	A2	5/1999
EP	1637086	A1	3/2006
EP	1637086	B1	9/2010
EP	2380518	A2	10/2011
EP	2712567	A1	4/2014
JP	2000500363	A	1/2000
JP	2002065693	A	3/2002
JP	2006504473	A	2/2006
JP	2008245767	A	10/2008
JP	2009543607	A	12/2009
JP	2011224364	A	11/2011
JP	2013510676	A	3/2013
KR	20130103763	A	9/2013
KR	20140088087	A	7/2014
RU	2074645	C1	3/1997
RU	2102090	C1	1/1998
RU	2503408	C2	1/2014
SU	1119663	A1	10/1984
SU	1412745	A1	7/1988
SU	1734708	A1	5/1992
WO	WO-9301862	A1	2/1993
WO	WO-9505771	A1	3/1995
WO	WO-9733526	A2	9/1997
WO	WO-9965561	A1	12/1999
WO	WO-0137723	A2	5/2001
WO	WO-0137925	A2	5/2001
WO	WO-2007018751	A2	2/2007
WO	WO-2010110785	A1	9/2010
WO	WO-2011075328	A1	6/2011
WO	WO-2011091069	A1	7/2011
WO	WO-2011139589	A2	11/2011
WO	WO-2012052920	A1	4/2012
WO	WO-2012052921	A1	4/2012
WO	WO-2012052922	A1	4/2012
WO	WO-2012052924	A1	4/2012
WO	WO-2012052926	A2	4/2012
WO	WO-2012052927	A1	4/2012
WO	WO-2012068268	A2	5/2012
WO	WO-2012120495	A2	9/2012
WO	WO-2012149341	A1	11/2012
WO	WO-2012149511	A2	11/2012
WO	WO-2012154800	A1	11/2012
WO	WO-2012149511	A3	2/2013
WO	WO-2013090848	A1	6/2013
WO	WO-2013111136	A2	8/2013
WO	WO-2013157011	A2	10/2013
WO	WO-2012068268	A3	4/2014
WO	WO-2014075415	A1	5/2014
WO	WO-2015193889	A1	12/2015
WO	WO-2016007851	A1	1/2016
WO	WO-2016007851	A8	2/2017
WO	WO-2016084081	A8	5/2017
WO	WO-2018173047	A1	9/2018
WO	WO-2018173052	A1	9/2018
WO	WO-2018173053	A1	9/2018
WO	WO-2021205450	A1	10/2021
WO	WO-2022269545	A2	12/2022

OTHER PUBLICATIONS

Brace. Radiofrequency and microwave ablation of the liver, lung, kidney, and bone: what are the differences? Curr Probl Diagn Radiol. May-Jun. 2009;38(3):135-43. doi: 10.1067/j.cpradiol.2007.10.001.

Chen, et al. Percutaneous pulmonary artery denervation completely abolishes experimental pulmonary arterial hypertension in vivo. EuroIntervention. Jun. 22, 2013;9(2):269-76. doi: 10.4244/EIJV912A43.

Chen. Pulmonary artery denervaion to treat pulmonary arterial hypertension unresponive to medication: a single-center, prospective, first-in-man PADN1 study. Nanjing First Hospital, Nanjing Medical University, Nanjing, China. TCT2012. Oct. 22, 2012. 23 pages.

Chen, SL. et al., Hemodynamic, functional, and clinical responses to pulmonary artery denervation in patients with pulmonary arterial hypertension of different causes: phase II results from the Pulmonary Artery Denervation-1 study. Circ Cardiovasc Interv. Nov. 2015;8(11):e002837. doi: 10.1161/CIRCINTERVENTIONS.115.002837.

Chen, SL. et al., Response to Letter Regarding Article, "Hemodynamic, Functional, and Clinical Responses to Pulmonary Artery Denervation in Patients With Pulmonary Arterial Hypertension of Different Causes: Phase II Results From the Pulmonary Artery Denervation-1 Study". Circ Cardiovasc Interv. Jan. 2016;9(1):e003463. doi: 10.1161/CIRCINTERVENTIONS.115.003463. No abstract available.

Chen, SL. et al., Pericardial effusion is correlated with clinical outcome after pulmonary artery denervation for pulmonary arterial hypertension. Oncotarget. Dec. 20, 2016. doi: 10.18632/oncotarget.14031. [Epub ahead of print].

Chinese application No. CN20131103141 filed Mar. 27, 2013 with English Translation.

Chinese Clinical Trial Register (ChiCTR): "First-in-Man of Pulmonary artery denervation for treatment of pulmonary artery hypertention: the PADN-1 trial" dated Apr. 6, 2012, http://www.chictr.org/en/proj/show.aspx?proj=2741 (3 pages).

Chinese Clinical Trial Register (ChiCTR): "Percutaneous pulmonary arterial denervation for treatment of chronic heart failure with secondary pulmonary hypertension" dated Nov. 2, 2012, http://www.chictr.org/en/proj/show.aspx? proj=3677 (3 pages).

Chinese Clinical Trial Register (ChiCTR): "Pulmonary Artery Denervation in Patients with Pulmonary Artery Hypertention (The PADN-2 trial): a randomised controlled trial" dated Apr. 12, 2012, http://www.chictr.org/en/proj/ show.aspx?proj=2756 (4 pages).

Cruz, et al. Cardiopulmonary Effects Following Endoscopic Thoracic Sympathectomy . European Journal of Cardio-Thoracic Surgery, Published by Elsevier BV. (2009) 491-496.

EP15818364.0 Extended Search Report dated Mar. 9, 2018.

European search report and opinion dated Nov. 18, 2015 for EP Application No. 13840133.

Farber, et al.Predicting outcomes in pulmonary arterial hypertension based on the 6-minute walk distance. J Heart Lung Transplant. Mar. 2015;34(3):362-8. doi: 10.1016/j.healun.2014.08.020. Epub Aug. 28, 2014.

Farber. Validation of the 6-minute walk in patients with pulmonary arterial hypertension: trying to fit a square PEG into a round hole? Circulation. Jul. 17, 2012;126(3):258-60. doi: 10.1161/CIRCULATIONAHA.112.118547. Epub Jun. 13, 2012.

Flues, et al. Cardiac and pulmonary arterial remodeling after sinoaortic denervation in normotensive rats. Auton Neurosci. Jan. 26, 2012;166(1-2):47-53. doi: 10.1016/j.autneu.2011.10.005. Epub Nov. 13, 2011. (Abstract).

Fritz, et al. Baseline and follow-up 6-min walk distance and brain natriuretic peptide predict 2-year mortality in pulmonary arterial hypertension. Chest. Feb. 1, 2013;143(2):315-23.

Frost, et al.Evaluation of the predictive value of a clinical worsening definition using 2-year outcomes in patients with pulmonary arterial hypertension: a REVEAL Registry analysis. Chest. Nov. 2013;144(5):1521-9. doi: 10.1378/chest.12-3023.

Galie, et al. A meta-analysis of randomized controlled trials in pulmonary arterial hypertension. Eur Heart J. Feb. 2009;30(4):394-403. doi: 10.1093/eurheartj/ehp022. Epub Jan. 20, 2009.

Galie, et al. Guidelines for the diagnosis and treatment of pulmonary hypertension: the Task Force for the Diagnosis and Treatment of Pulmonary Hypertension of the European Society of Cardiology (ESC) and the European Respiratory Society (ERS), endorsed by the International Society of Heart and Lung Transplantation (ISHLT). Eur Heart J. Oct. 2009;30(20):2493-537. doi: 10.1093/eurheartj/ehp297. Epub Aug. 27, 2009.

Galie, et al. New treatment strategies for pulmonary arterial hypertension: hopes or hypes? J Am Coll Cardiol. Sep. 17, 2013;62(12):1101-2. doi: 10.1016/j.jacc.2013.06.032. Epub Jul. 10, 2013.

(56) **References Cited**

OTHER PUBLICATIONS

Galie, et al.Tadalafil therapy for pulmonary arterial hypertension. Circulation. Jun. 9, 2009;119(22):2894-903. doi: 10.1161/CIRCULATIONAHA.108.839274. Epub May 26, 2009.

Garutti, et al. Surgical upper thoracic sympathectomy reduces arterial oxygenation during one-lung ventilation. J Cardiothorac Vasc Anesth. Oct. 2005;19(5):703-4.

Hiremath, et al. Exercise improvement and plasma biomarker changes with intravenous treprostinil therapy for pulmonary arterial hypertension: a placebo-controlled trial. J Heart Lung Transplant. Feb. 2010;29(2):137-49. doi: 10.1016/j.healun.2009.09.005.

Humbert, et al. Survival in patients with idiopathic, familial, and anorexigen-associated pulmonary arterial hypertension in the modern management era. Circulation. Jul. 13, 2010;122(2):156-63. doi: 10.1161/CIRCULATIONAHA.109.911818. Epub Jun. 28, 2010.

International search report and written opinion dated Aug. 22, 2013 for PCT/CN2013/073338.

International search report and written opinion dated Nov. 23, 2015 for PCT/US2015/039930.

Juratsch, et al. Experimental pulmonary hypertension produced by surgical and chemical denervation of the pulmonary vasculature. Chest. Apr. 1980;77(4):525-30.

Lang, et al. Recommendations for chamber quantification: a report from the American Society of Echocardiography's Guidelines and Standards Committee and the Chamber Quantification Writing Group, developed in conjunction with the European Association of Echocardiography, a branch of the European Society of Cardiology. J Am Soc Echocardiogr. Dec. 2005;18(12):1440-63.

LSI-Life Science Intelligence, Martin Grasse, Gradient Denervation Technologies—Pulmonary Hypertension Treatment | LSI Europe '22. Nov. 12, 2012, www.youtube.com/watch?v=Hft79H2MxUs.

McLaughlin, et al. End points and clinical trial design in pulmonary arterial hypertension. J Am Coll Cardiol. Jun. 30, 2009;54(1 Suppl):S97-107. doi: 10.1016/j.jacc.2009.04.007.

McLaughlin, et al. Prognosis of pulmonary arterial hypertension: ACCP evidence-based clinical practice guidelines. Chest. Jul. 2004;126(1 Suppl):78S-92S.

McLaughlin, et al. Randomized study of adding inhaled iloprost to existing bosentan in pulmonary arterial hypertension. Am J Respir Crit Care Med. Dec. 1, 2006;174(11):1257-63. Epub Aug. 31, 2006.

Mereles, et al. Exercise and respiratory training improve exercise capacity and quality of life in patients with severe chronic pulmonary hypertension. Circulation. Oct. 3, 2006;114(14):1482-9. Epub Sep. 18, 2006.

Naeije, et al. Pulmonary vascular responses to surgical chemodenervation and chemical sympathectomy in dogs. J Appl Physiol (1985). Jan. 1989;66(1):42-50. (Abstract).

Notice of Allowance dated Mar. 26, 2021 for U.S. Appl. No. 15/873,721.

Notice of Allowance dated Jun. 29, 2021 for U.S. Appl. No. 15/873,721.

Notice of Allowance dated Jul. 15, 2020 for U.S. Appl. No. 15/228,358.

Notice of allowance dated Aug. 16, 2016 for U.S. Appl. No. 14/672,021.

Notice of Allowance dated Sep. 11, 2017 for U.S. Appl. No. 14/672,010.

Notice of Allowance dated Sep. 14, 2017 for U.S. Appl. No. 14/672,021.

Notice of Allowance dated Sep. 19, 2017 and Sep. 7, 2017 for U.S. Appl. No. 14/666,214.

Notice of Allowance dated Sep. 22, 2017 for U.S. Appl. No. 14/672,021.

Notice of Allowance dated Sep. 24, 2019 for U.S. Appl. No. 15/228,358.

Notice of Allowance dated Oct. 13, 2017 for U.S. Appl. No. 14/672,021.

Notice of Allowance dated Oct. 13, 2017 for U.S. Appl. No. 14/672,010.

Notice of Allowance dated Oct. 13, 2017 for U.S. Appl. No. 14/666,214.

Notice of Allowance dated Oct. 18, 2017 for U.S. Appl. No. 14/672,013.

Notice of Allowance dated Nov. 2, 2017 for U.S. Appl. No. 14/672,013.

Notice of allowance dated Nov. 22, 2017 for U.S. Appl. No. 14/672,021.

Notice of Allowance dated Dec. 11, 2017 for U.S. Appl. No. 14/672,013.

Odero, et al. Left cardiac sympathetic denervation for the prevention of life-threatening arrhythmias: the surgical supraclavicular approach to cervicothoracic sympathectomy. Heart Rhythm. Aug. 2010;7(8):1161-5. doi: 10.1016/j.hrthm.2010.03.046. Epub Jun. 9, 2010.

Office action dated Jan. 5, 2015 for U.S. Appl. No. 14/530,588.

Office action dated Jan. 21, 2016 for U.S. Appl. No. 14/672,021.

Office action dated Feb. 4, 2016 for U.S. Appl. No. 14/079,230.

Office action dated Feb. 26, 2016 for U.S. Appl. No. 14/672,013.

Office action dated May 28, 2019 for U.S. Appl. No. 15/228,358.

Office action dated Jul. 14, 2015 for U.S. Appl. No. 14/666,214.

Office action dated Jul. 31, 2015 for U.S. Appl. No. 14/530,588.

Office action dated Aug. 5, 2015 for U.S. Appl. No. 14/672,010.

Office Action dated Aug. 31, 2017 for U.S. Appl. No. 14/672,013.

Office action dated Sep. 15, 2015 for U.S. Appl. No. 14/672,021.

Office action dated Oct. 8, 2015 for U.S. Appl. No. 14/672,013.

Office Action dated Oct. 21, 2016 for U.S. Appl. No. 14/530,588.

Office action dated Oct. 28, 2015 for U.S. Appl. No. 14/666,214.

Office action dated Dec. 9, 2020 for U.S. Appl. No. 15/873,721.

Office action dated Dec. 21, 2015 for U.S. Appl. No. 14/672,010.

Ommen, et al. Assessment of right atrial pressure with 2-dimensional and Doppler echocardiography: a simultaneous catheterization and echocardiographic study. Mayo Clin Proc. Jan. 2000;75(1):24-9.

Pokushalov, et al. A randomized comparison of pulmonary vein isolation with versus without concomitant renal artery denervation in patients with refractory symptomatic atrial fibrillation and resistant hypertension. J Am Coll Cardiol. Sep. 25, 2012;60(13):1163-70. doi: 10.1016/j.jacc.2012.05.036. Epub Sep. 5, 2012.

Savarese, et al. Do changes of 6-minute walk distance predict clinical events in patients with pulmonary arterial hypertension? A meta-analysis of 22 randomized trials. J Am Coll Cardiol. Sep. 25, 2012;60(13):1192-201. doi: 10.1016/j.jacc.2012.01.083.

Tei, et al. Noninvasive Doppler-derived myocardial performance index: correlation with simultaneous measurements of cardiac catheterization measurements. J Am Soc Echocardiogr. Mar. 1997;10(2):169-78.

Zhang, H. et al., Pulmonary artery denervation for treatment of a patient with pulmonary hypertension secondary to left heart disease. Pulm Circ. Jun. 2016;6(2):240-3. doi: 10.1086/685550.

Zhang, H. et al., Pulmonary Artery Denervation Significantly Increases 6-Min Walk Distance for Patients With Combined Pre- and Post-Capillary Pulmonary Hypertension Associated With Left Heart Failure. JACC: Cardiovascular Interventions, 12(3):274-284 (2019).

Zhang, YJ. et al., Pulmonary arterial hypertension: pharmacologic therapies and potential pulmonary artery denervation treatment. EuroIntervention. May 2013;9 Suppl R:R149-54. doi: 10.4244/EIJV9SRA25. Review.

Zhou, et al. Pulmonary Artery Denervation Attenuates Pulmonary Arterial Remodeling in Dogs With Pulmonary Arterial Hypertension Induced by Dehydrogenized Monocrotaline. JACC Cardiovasc Interv. Dec. 28, 2015;8(15):2013-23. doi: 10.1016/j.jcin.2015.09.015.

EP22155626.9 Extended European Search Report dated Apr. 28, 2022.

SG10201800251Y Search Report and Written Opinion dated Jan. 20, 2022.

U.S. Appl. No. 17/357,720 Office Action dated Apr. 25, 2024.

* cited by examiner

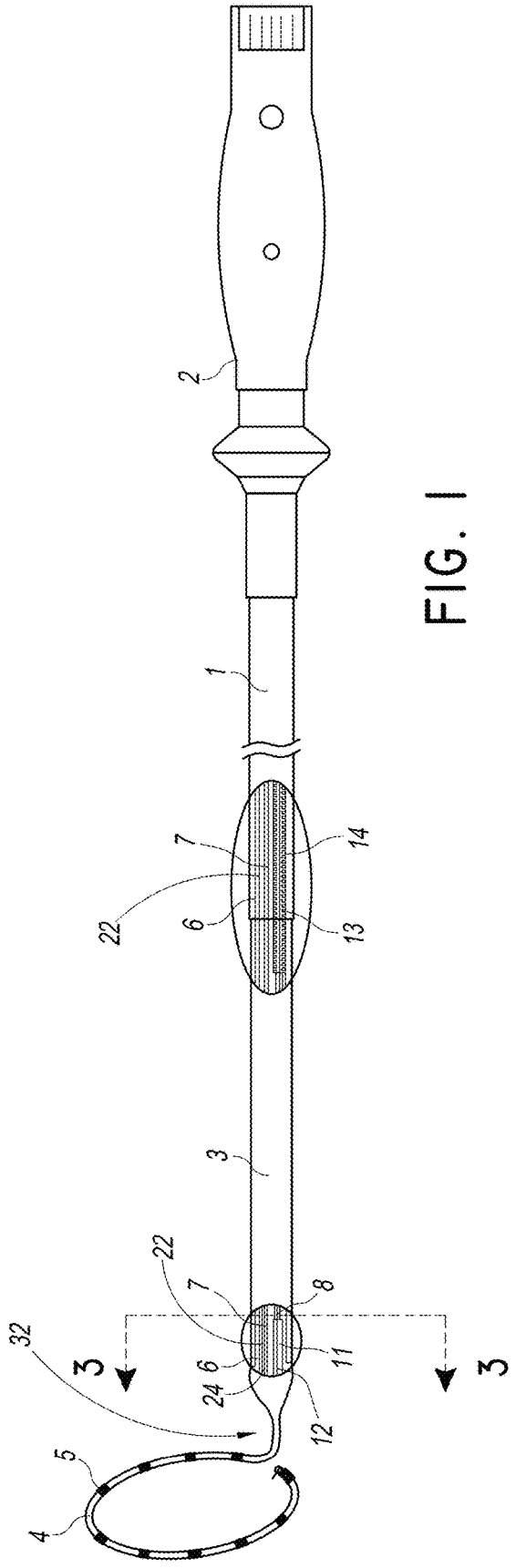

FIG. 1

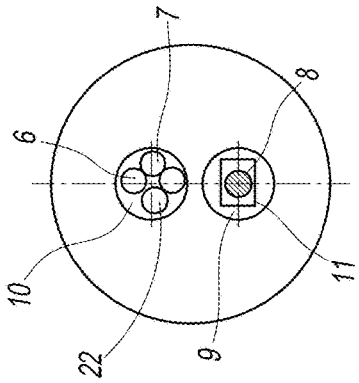

FIG. 3

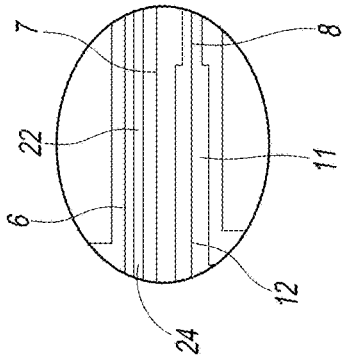

FIG. 2

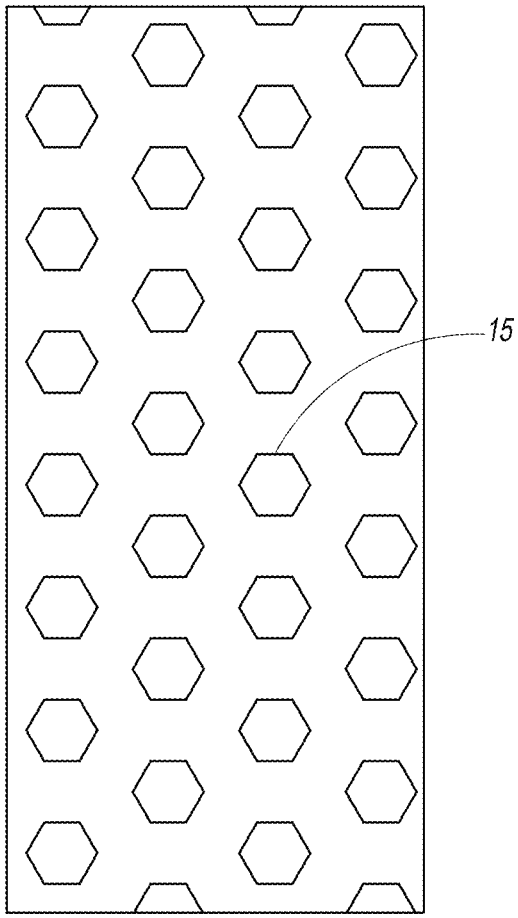

FIG. 4

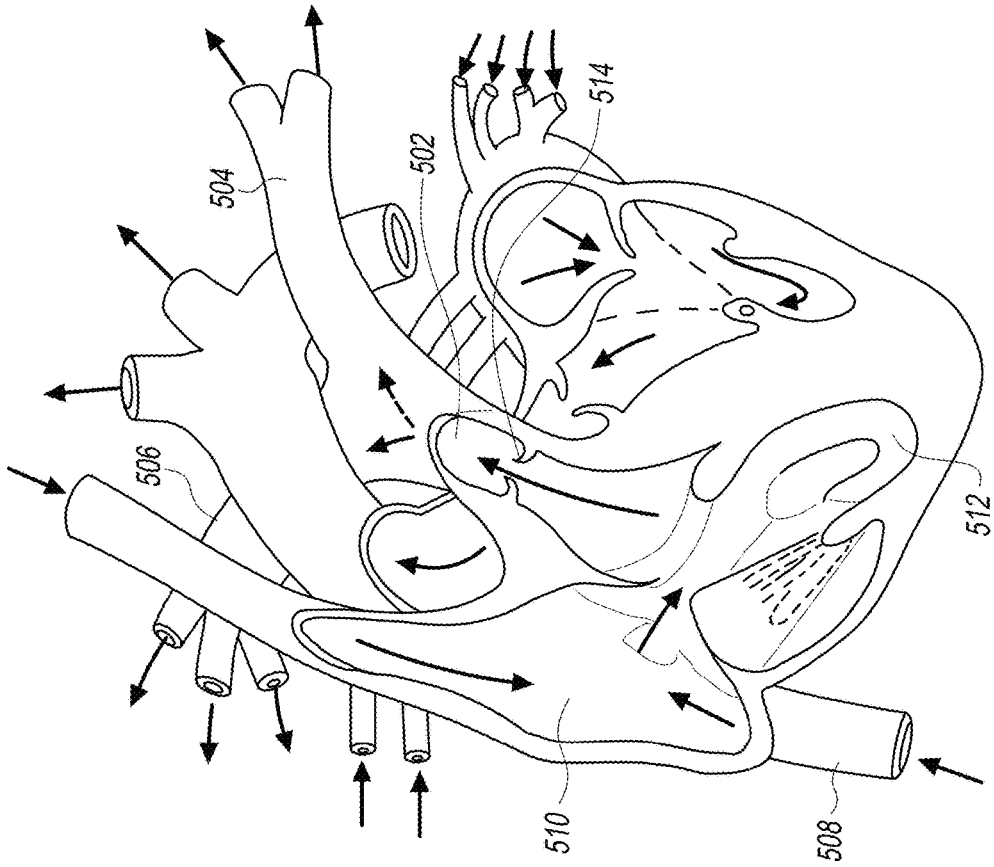

FIG. 5

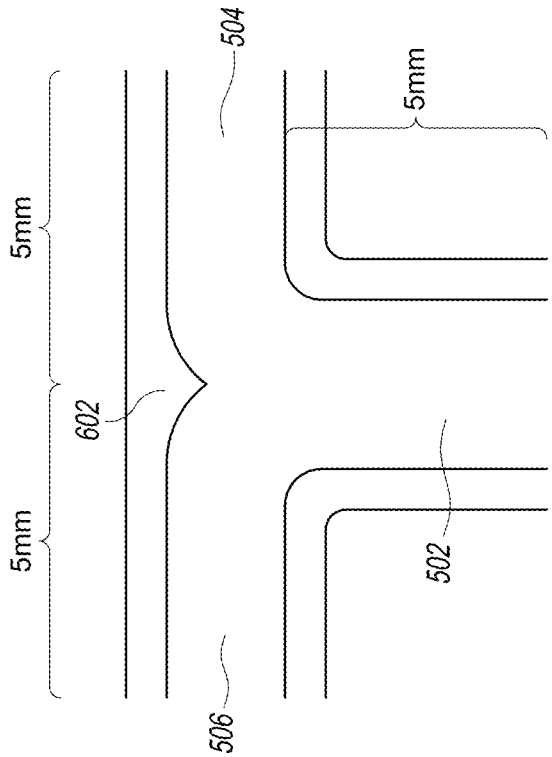

FIG. 6

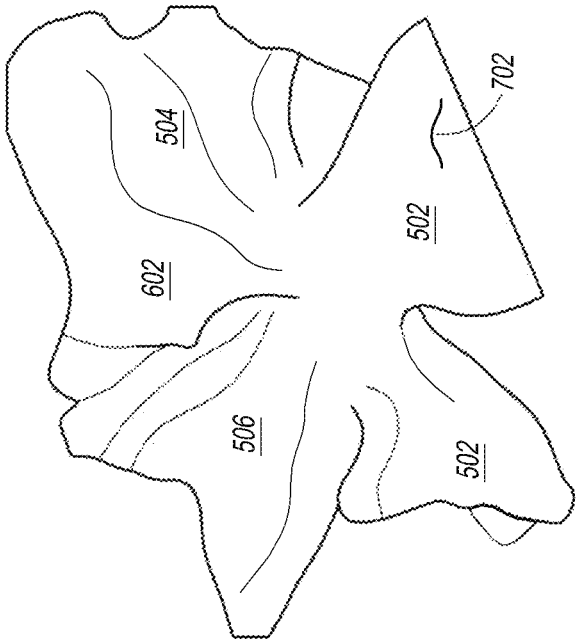

FIG. 7B

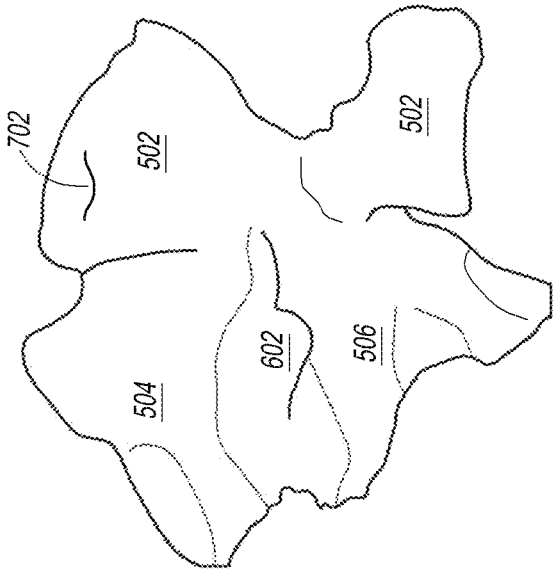

FIG. 7A

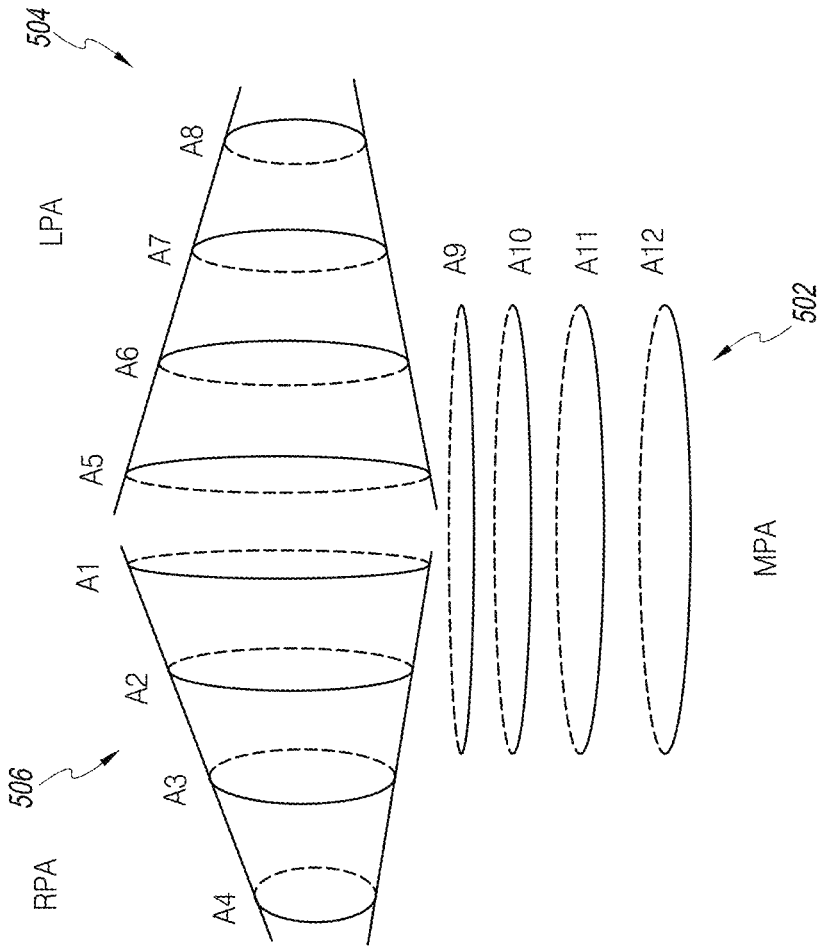

FIG. 8

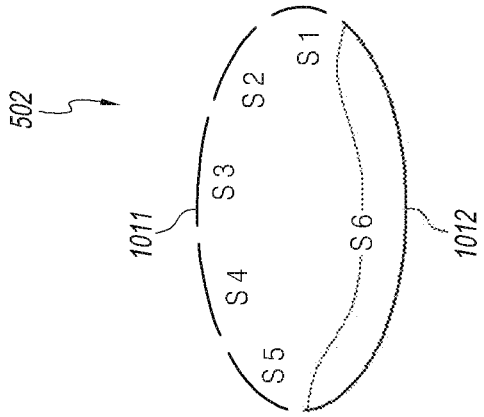

FIG. 9C

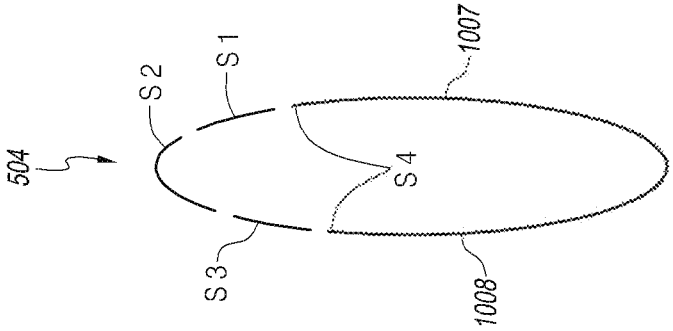

FIG. 9B

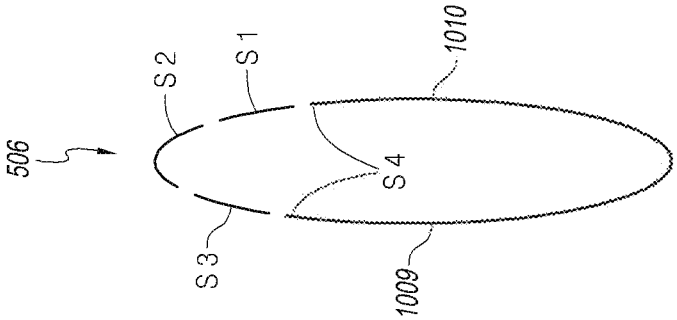

FIG. 9A

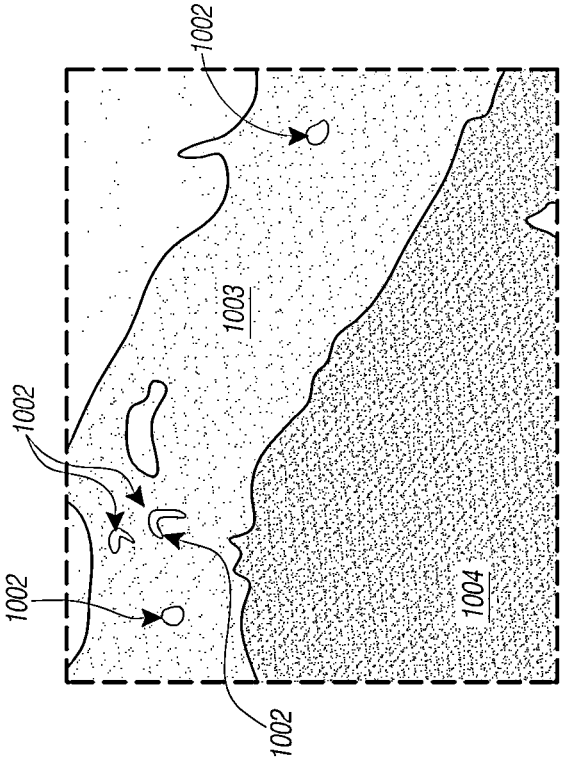

FIG. 10B

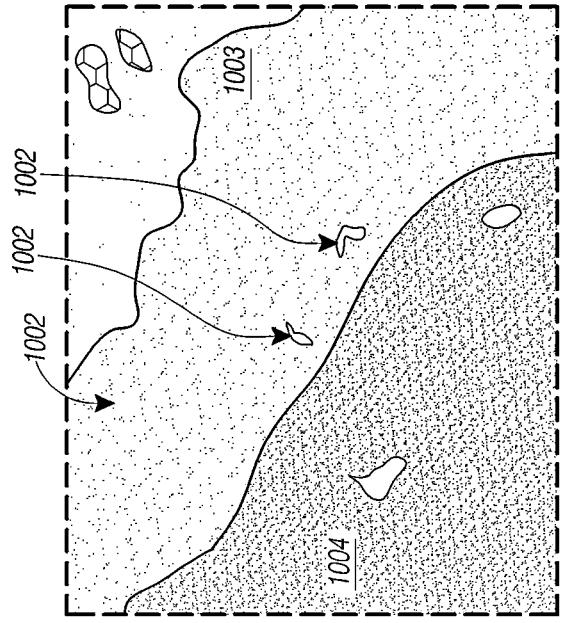

FIG. 10A

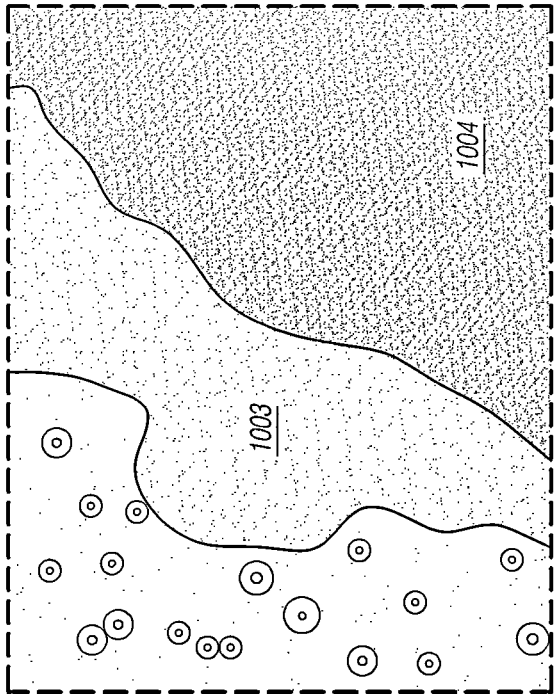

FIG. 10D

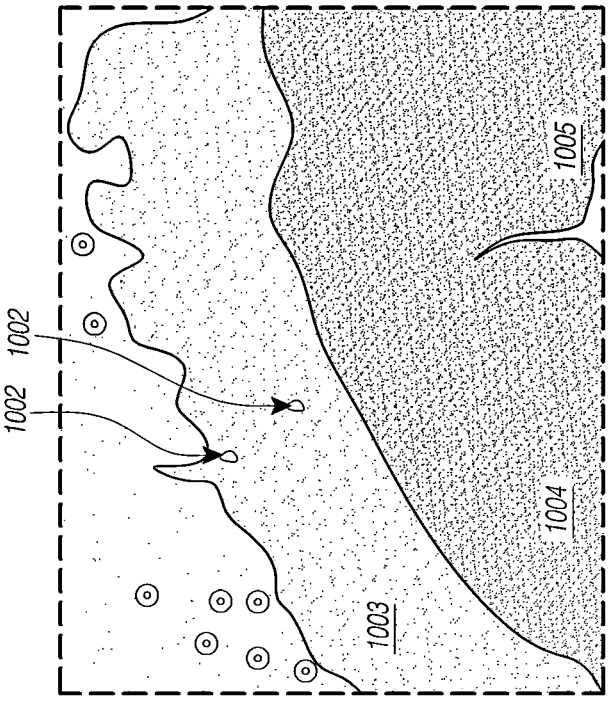

FIG. 10C

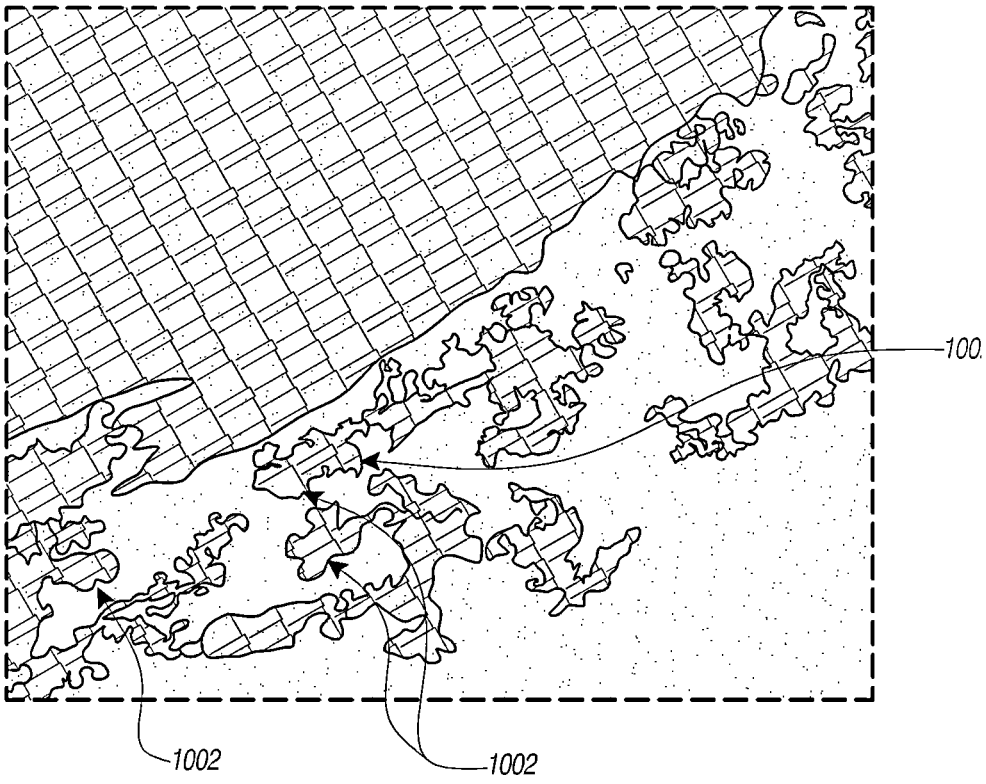

FIG. 11

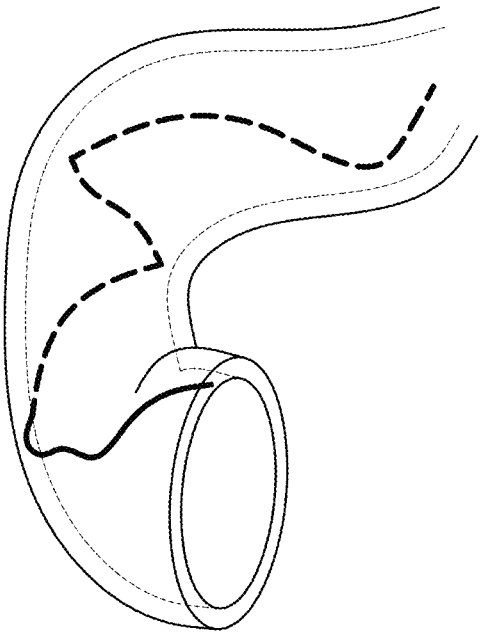

FIG. 13

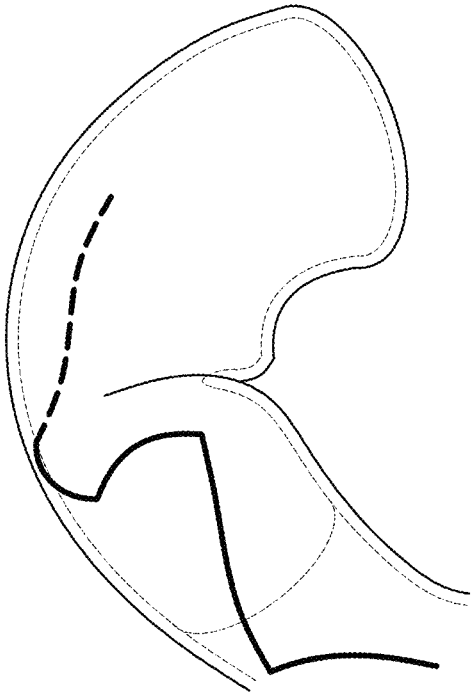

FIG. 12

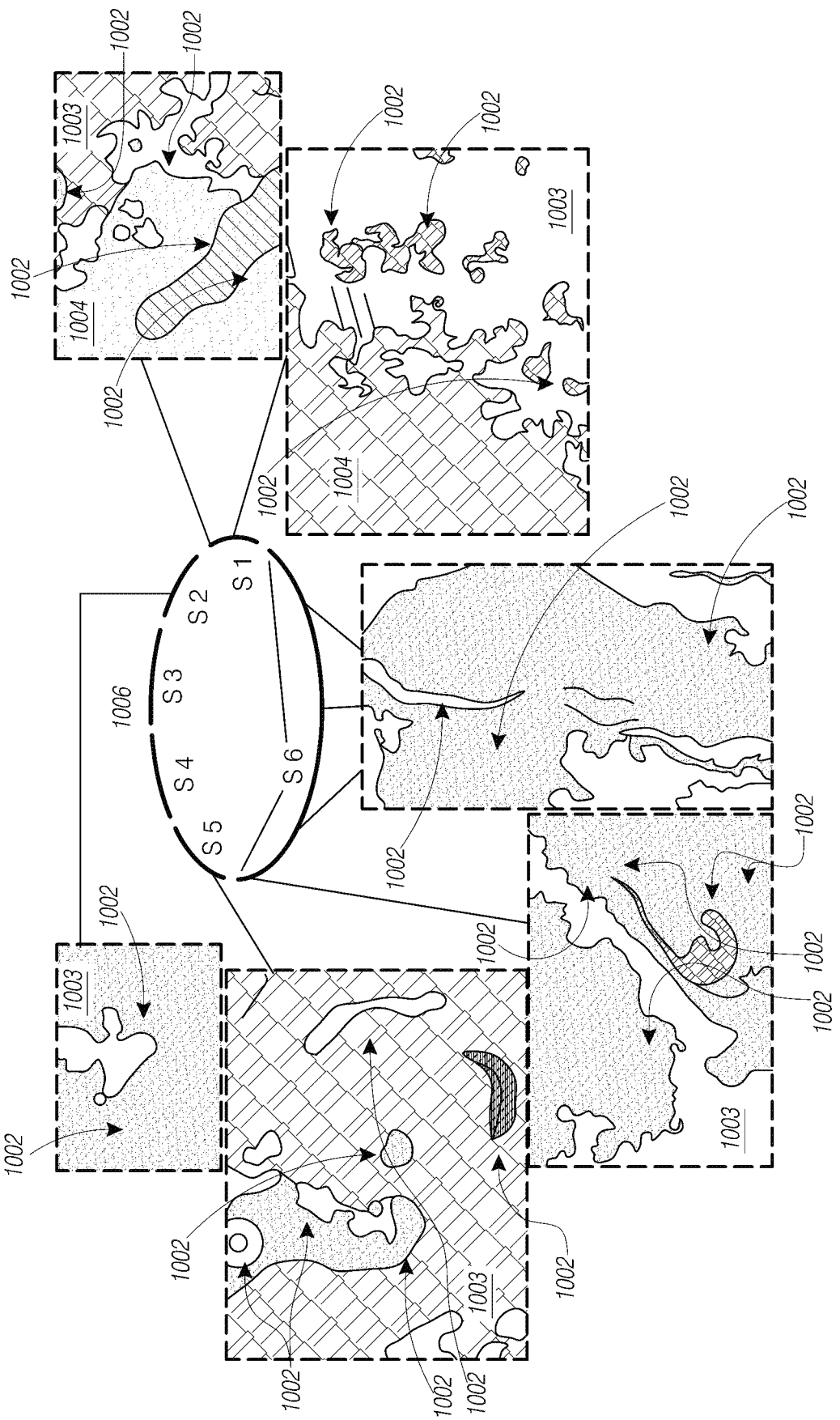

FIG. 14A

	Systolic Pulmonary Artery Pressure (mmHg)			Mean Pulmonary Artery Pressure (mmHg)		
Parameter	Before surgery	during surgery	Decline	Before surgery	during surgery	Decline
Parameter Status 1 Temperature <50° Energy 8-10W Ablation 120s	96	94	2.1%	56	54	3.6%
Parameter Status 2 Temperature 50°~60° Energy 8-10W Ablation 120s	88	64	27.3%	52	36	31%
Parameter Status 3 Temperature 40°~45° Energy <8W Ablation 120s	86	86	0%	54	53	1.9%
Parameter Status 4 Temperature 50°~60° Energy 8-10W Ablation 60s	86	78	9.3%	54	49	11.1%

FIG. 14B

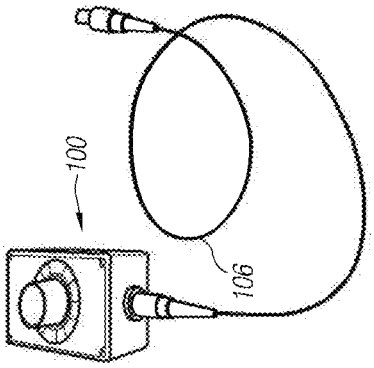

FIG. 15C

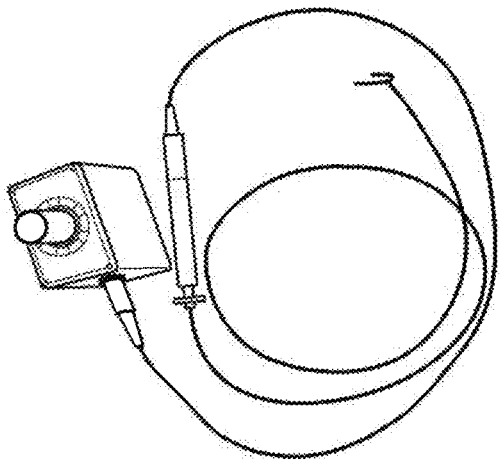

FIG. 15E

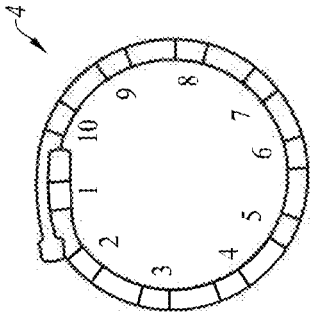

FIG. 15B

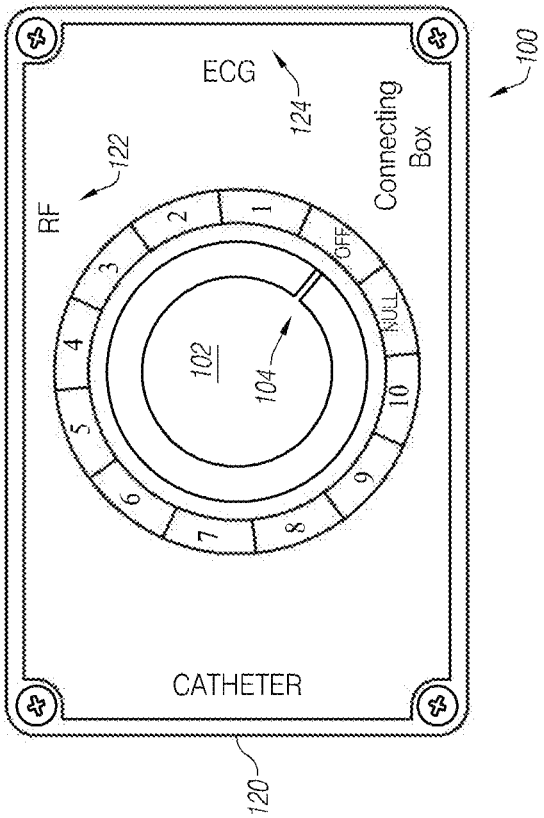

FIG. 15D

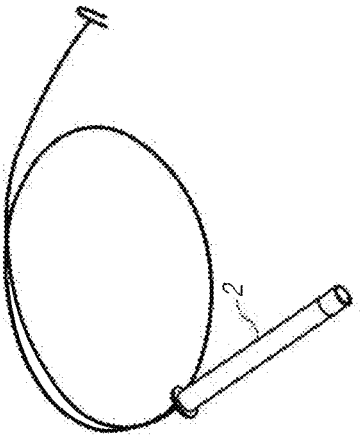

FIG. 15A

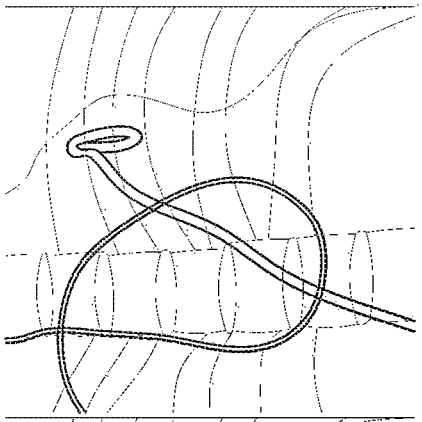

FIG. 16D

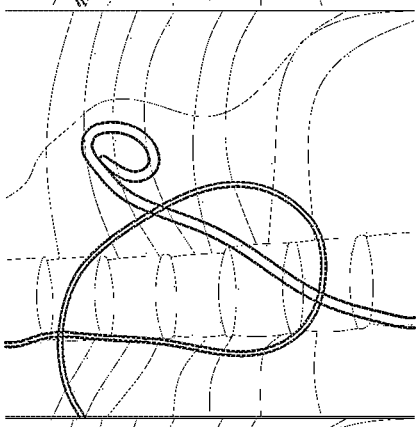

FIG. 16C

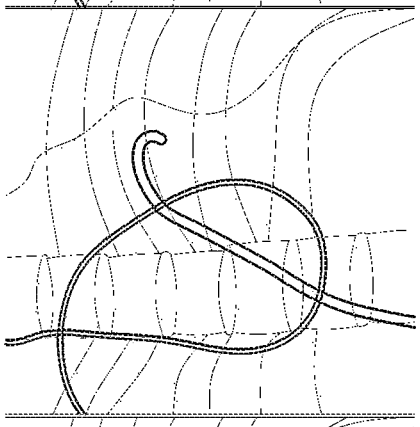

FIG. 16B

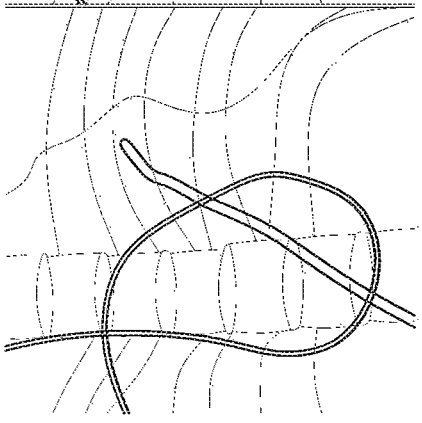

FIG. 16A

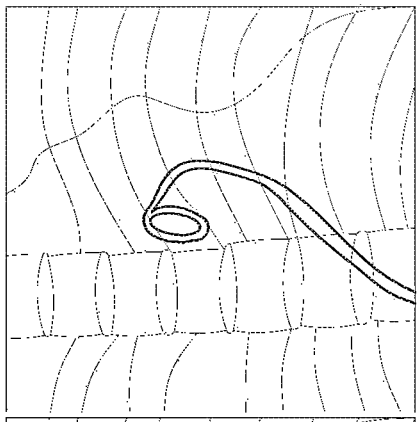

FIG. 16H

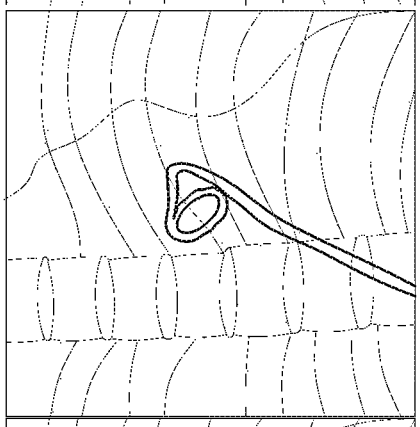

FIG. 16G

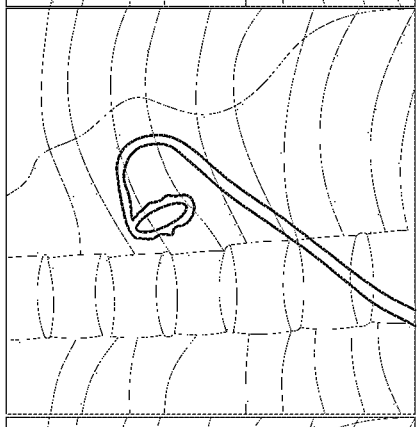

FIG. 16F

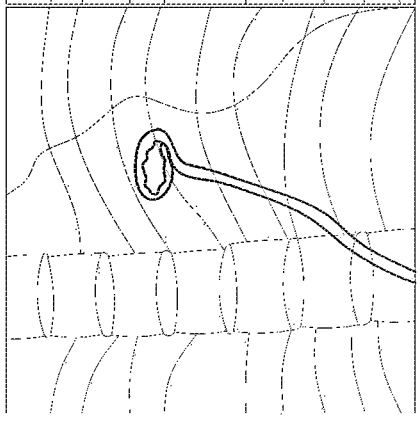

FIG. 16E

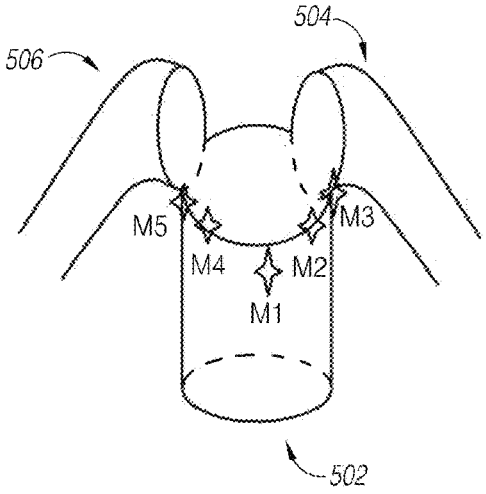

FIG. 17A

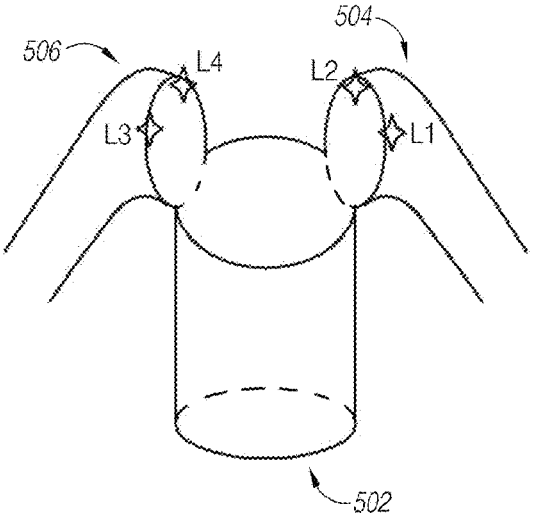

FIG. 17B

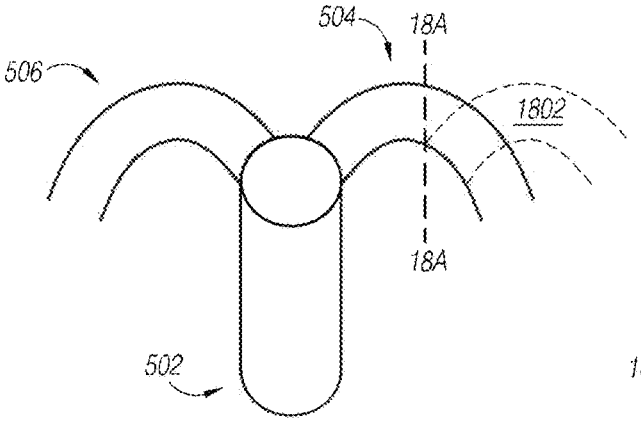

FIG. 18A

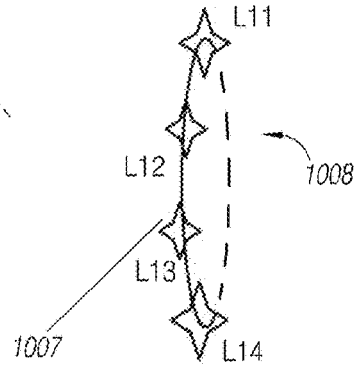

FIG. 18B

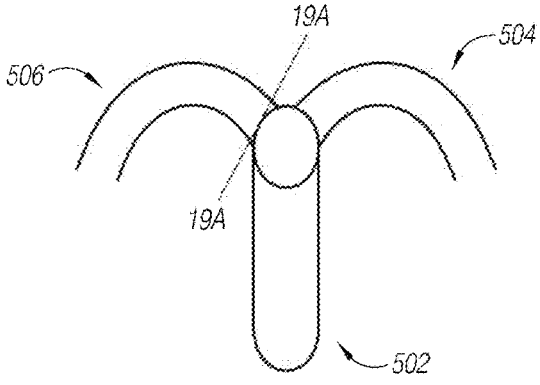

FIG. 19A

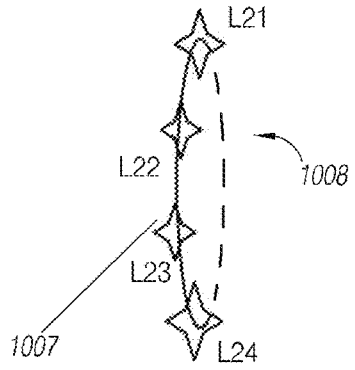

FIG. 19B

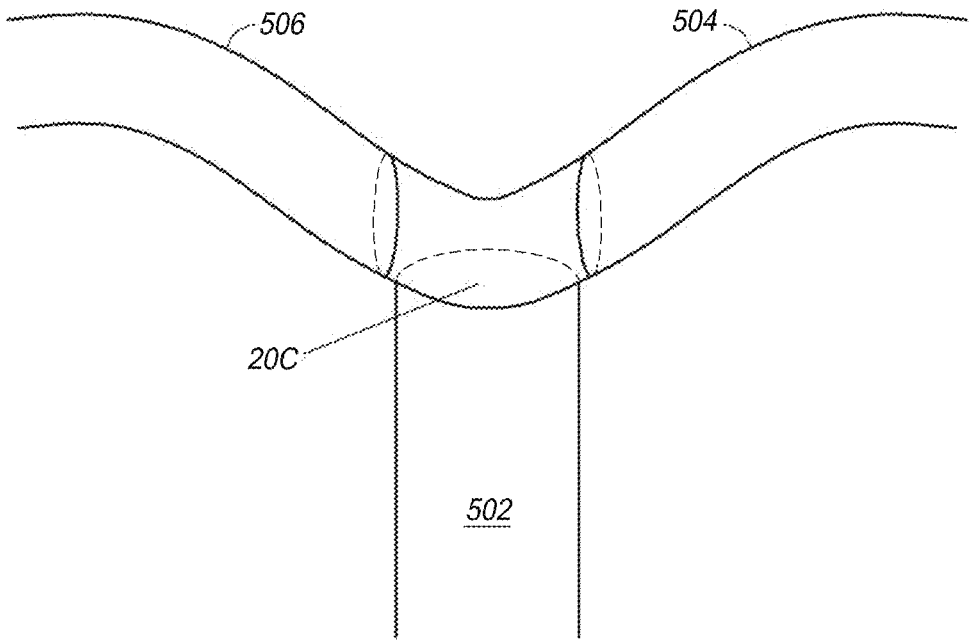

FIG. 20

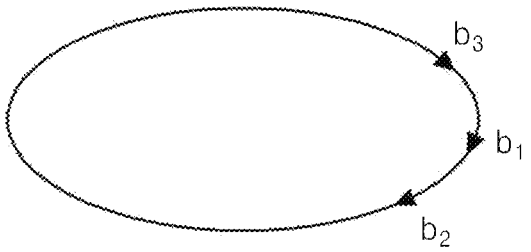

FIG. 21

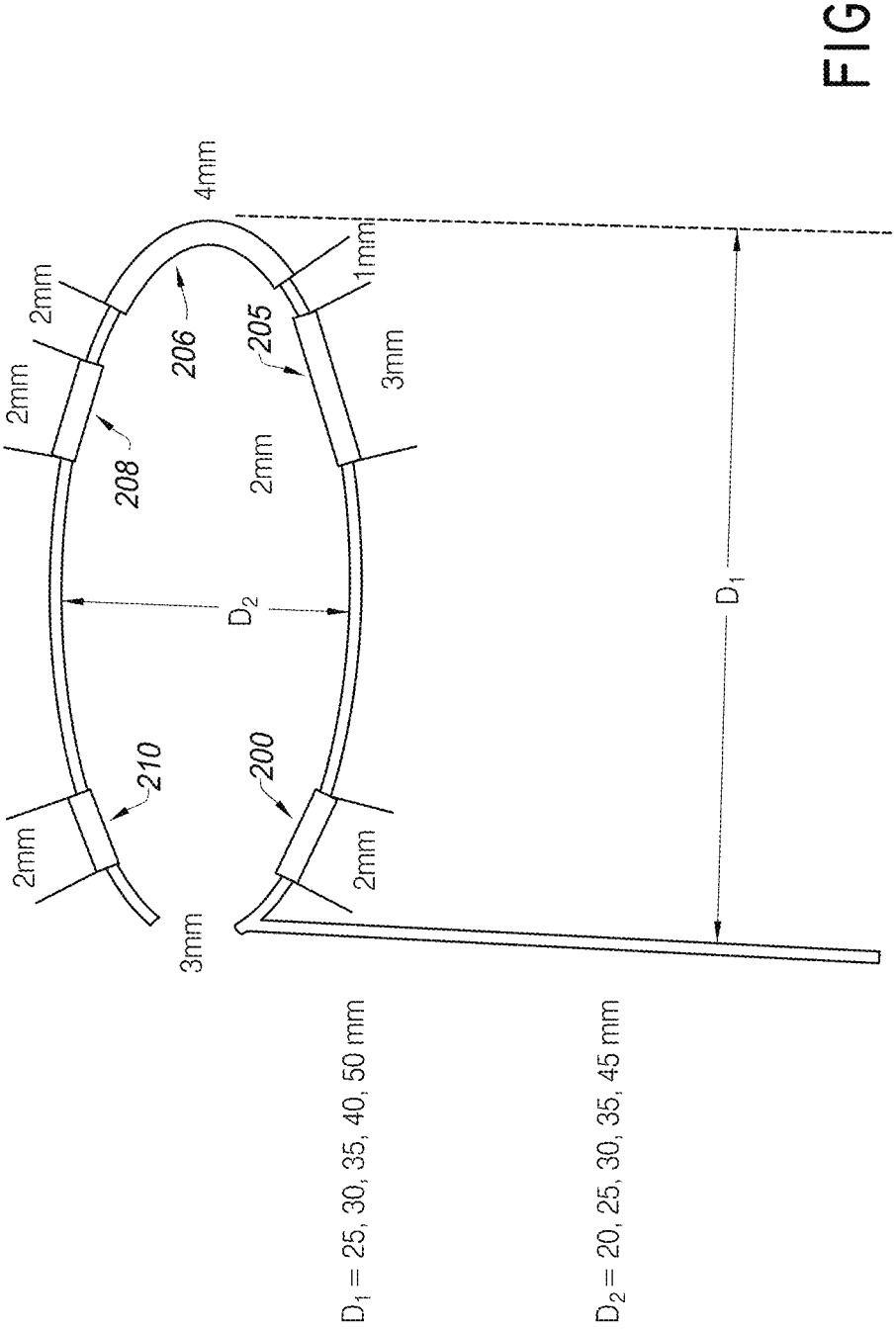
204
4mm
1mm
2mm
2mm
206
205
3mm
208
2mm
D_2
D_1
210
200
2mm
2mm
3mm
D_1 = 25, 30, 35, 40, 50 mm
D_2 = 20, 25, 30, 35, 45 mm

FIG. 22A

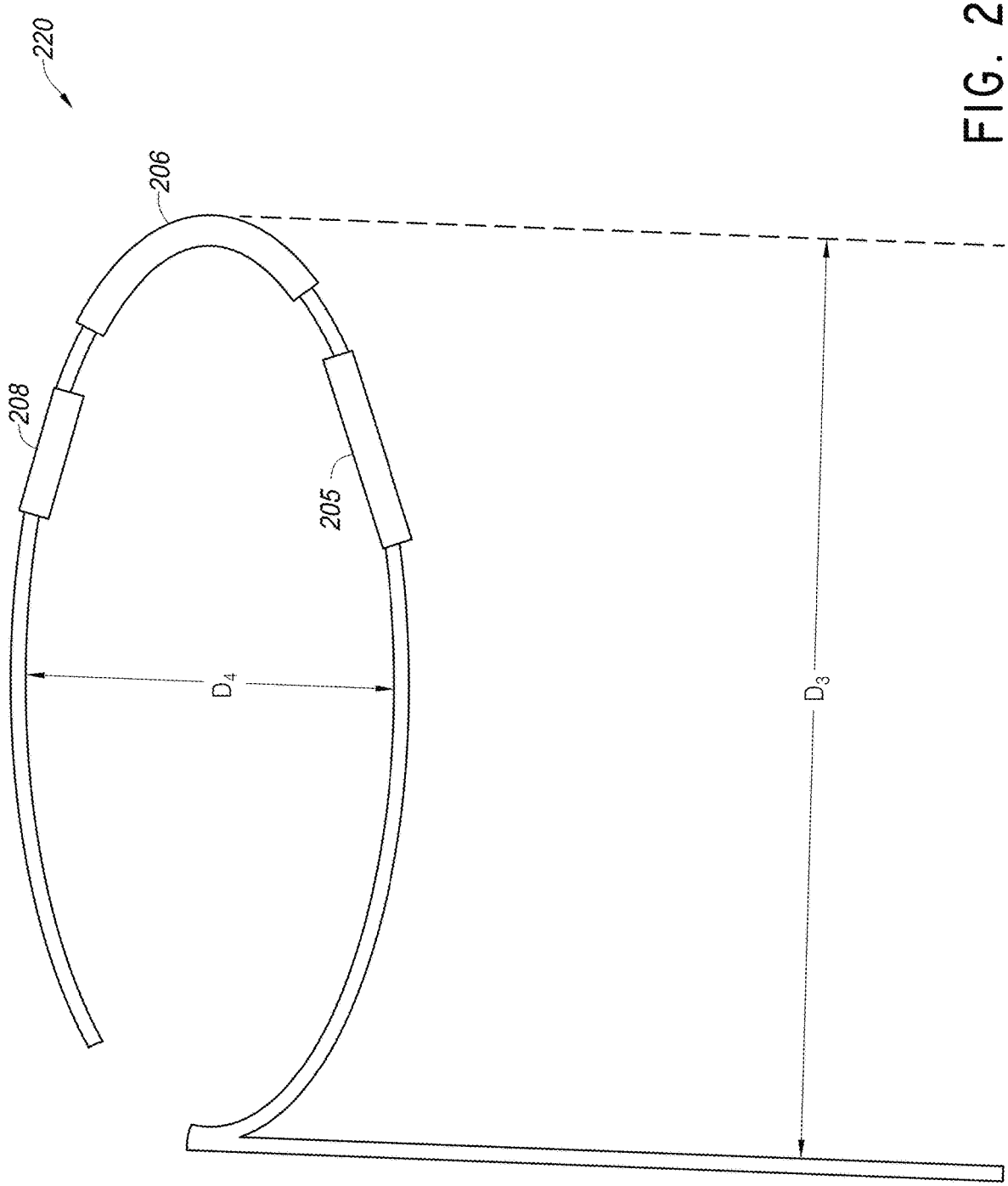

FIG. 22B

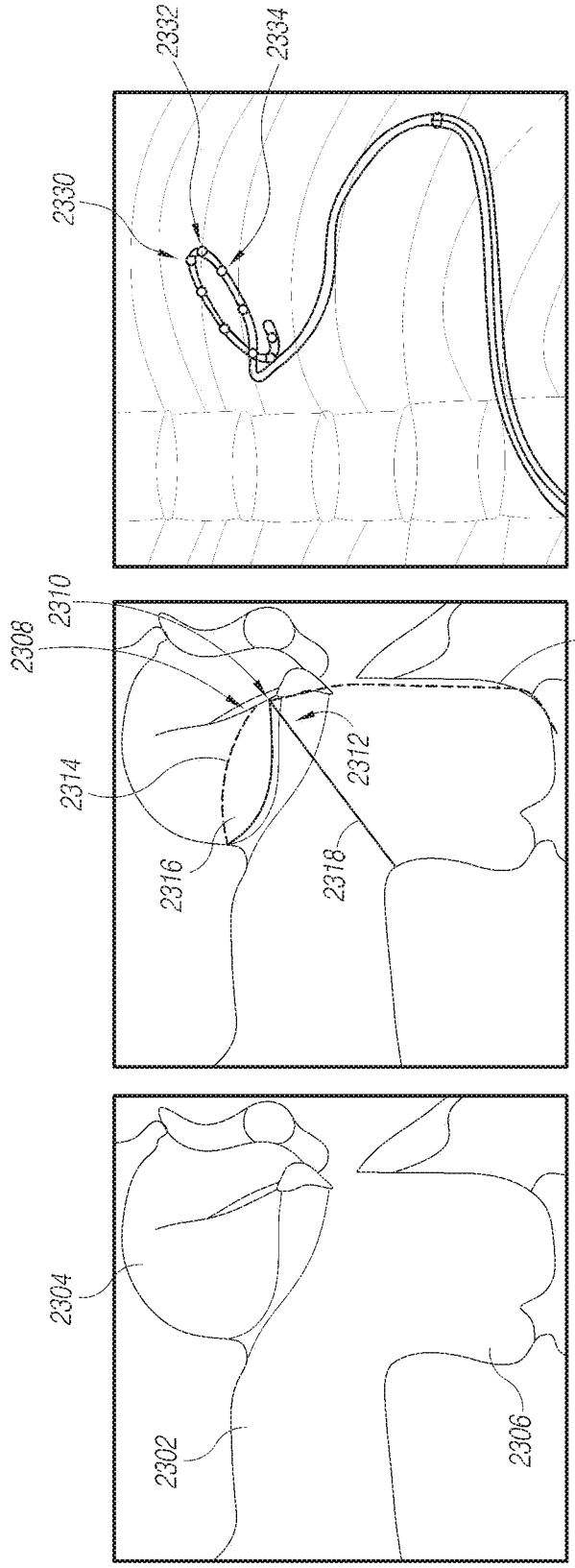

FIG. 23C

FIG. 23B

FIG. 23A

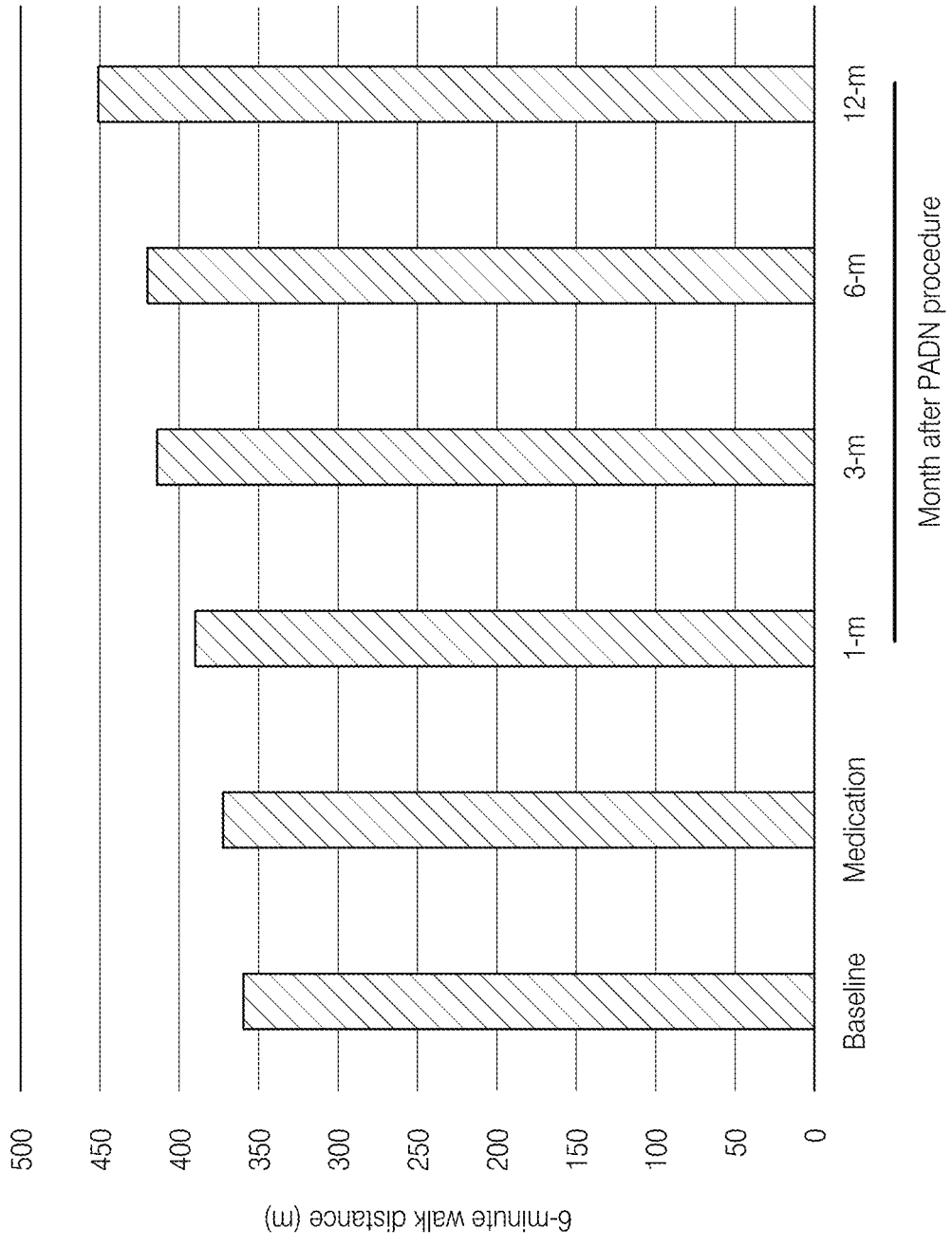
6-minute walk distance (m)
500
450
400
350
300
250
200
150
100
50
0
Baseline
Medication
1-m
3-m
6-m
12-m
Month after PADN procedure

FIG. 24A

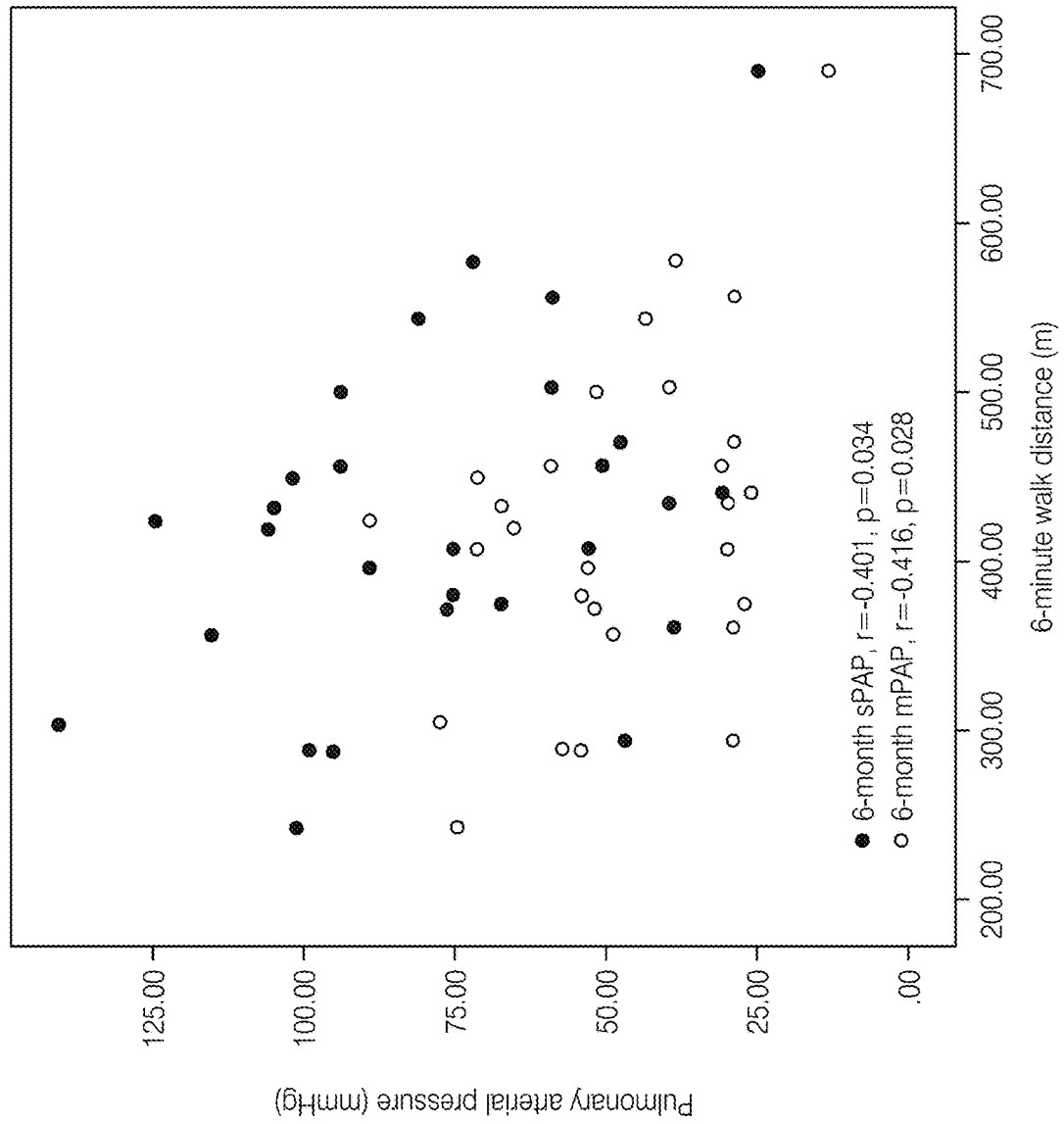
Pulmonary arterial pressure (mmHg)
125.00
100.00
75.00
50.00
25.00
.00
200.00
300.00
400.00
500.00
600.00
700.00
6-minute walk distance (m)
6-month sPAP, r=-0.401, p=0.034
6-month mPAP, r=-0.416, p=0.028

FIG. 24B

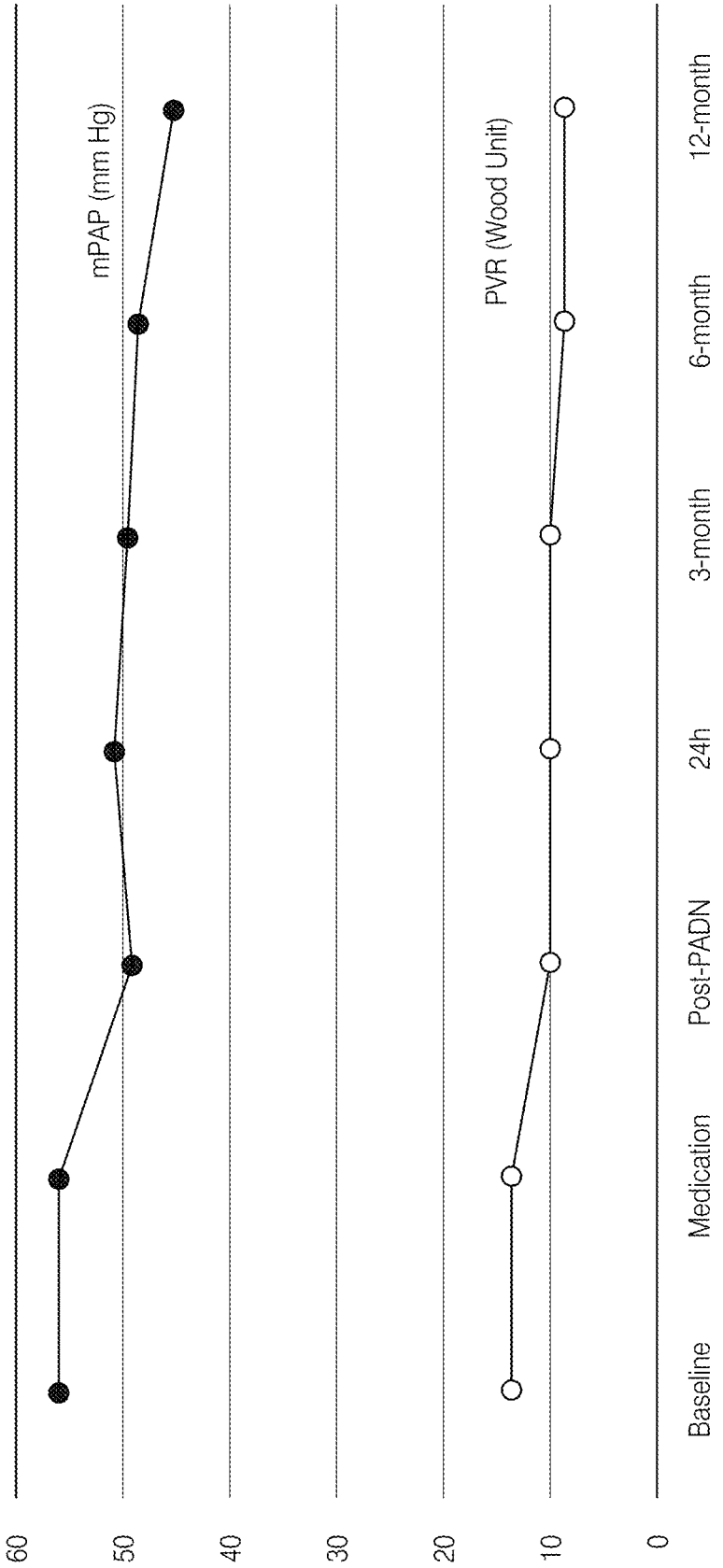
mPAP (mm Hg)
PVR (Wood Unit)
60
50
40
30
20
10
0
Baseline
Medication
Post-PADN
24h
3-month
6-month
12-month

FIG. 24C

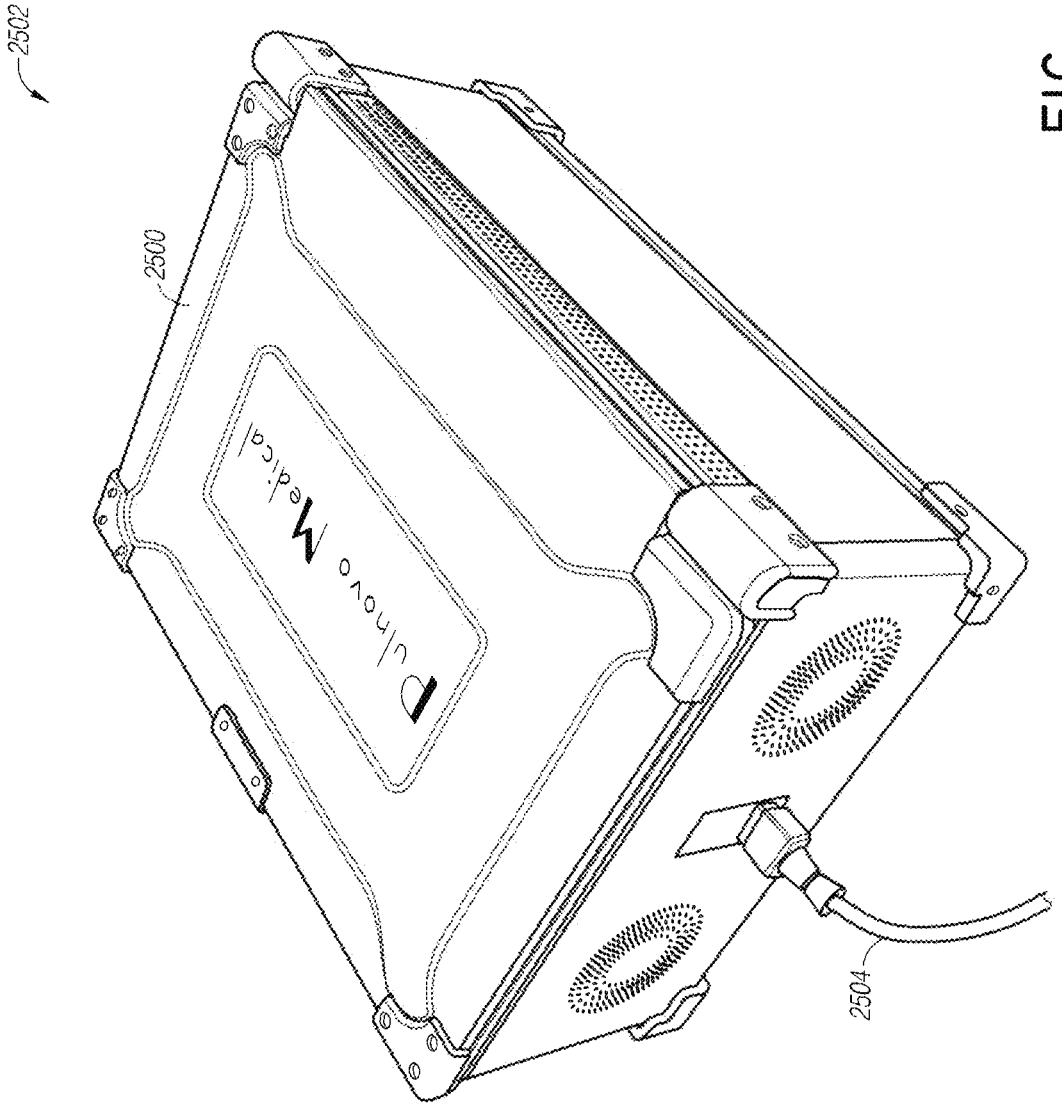

FIG. 25A

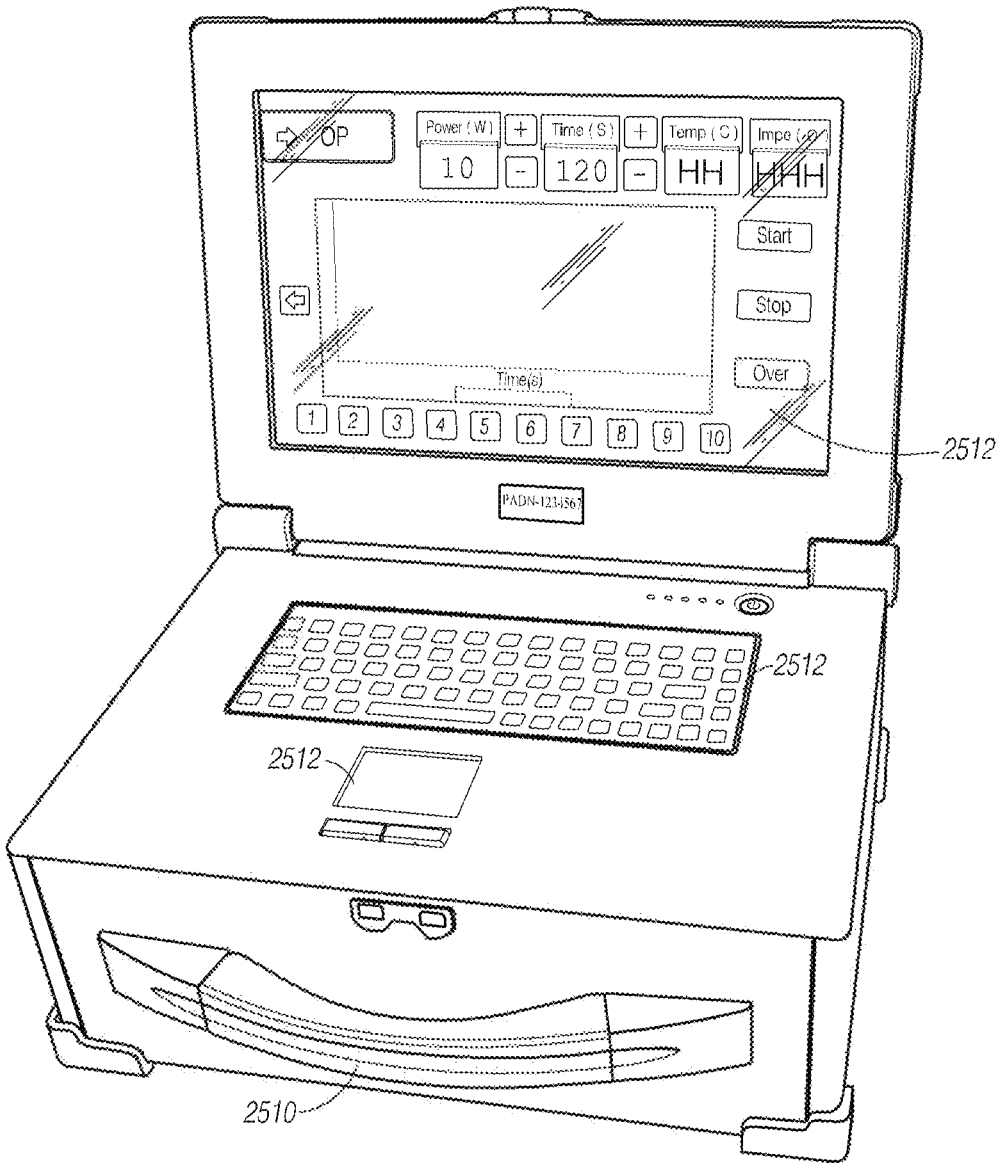
OP
Power (W)
Time (S)
Temp (C)
10
120
HH
HHH
Start
Stop
Over
Time(s)
1
2
3
4
5
6
7
8
9
10
PADN-123456?
2512
2512
2512
2510

FIG. 25B

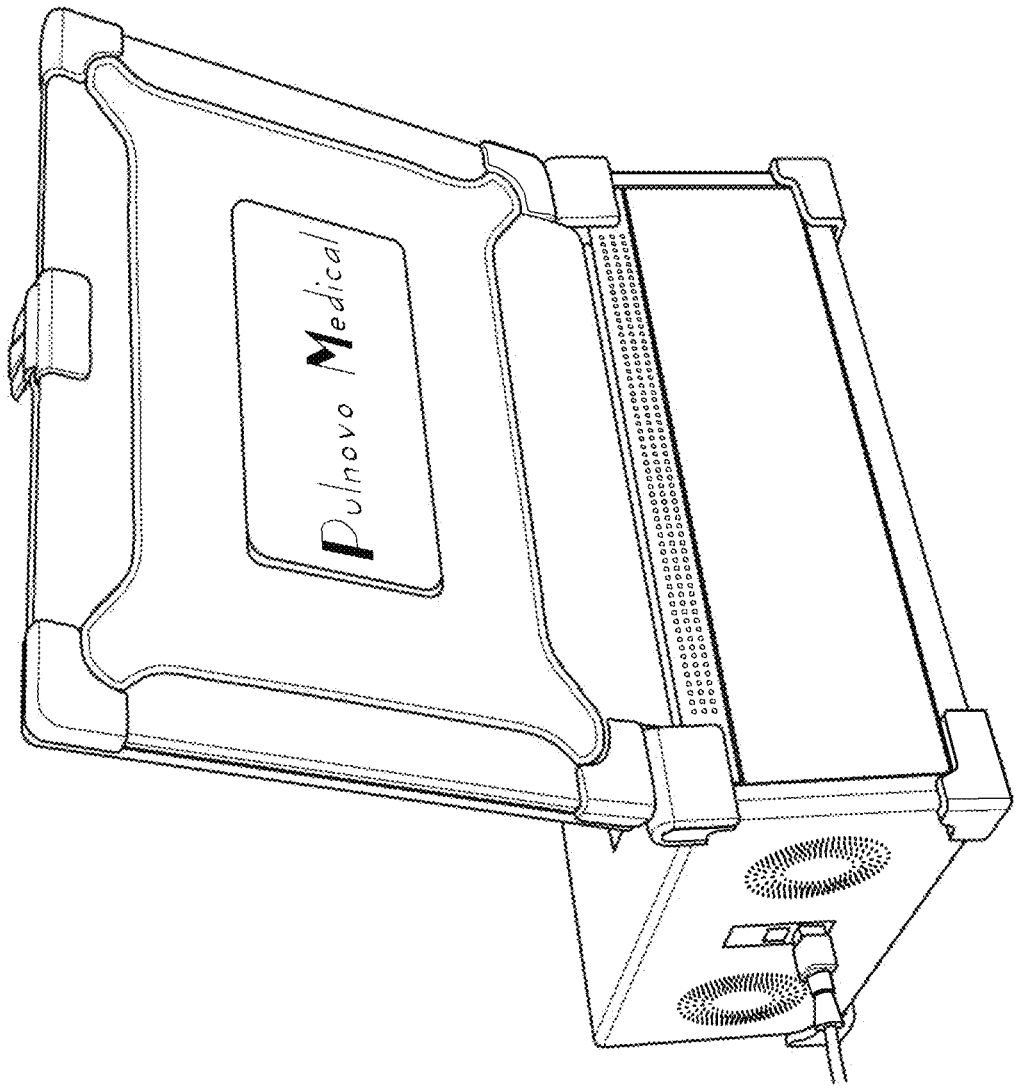

FIG. 25C

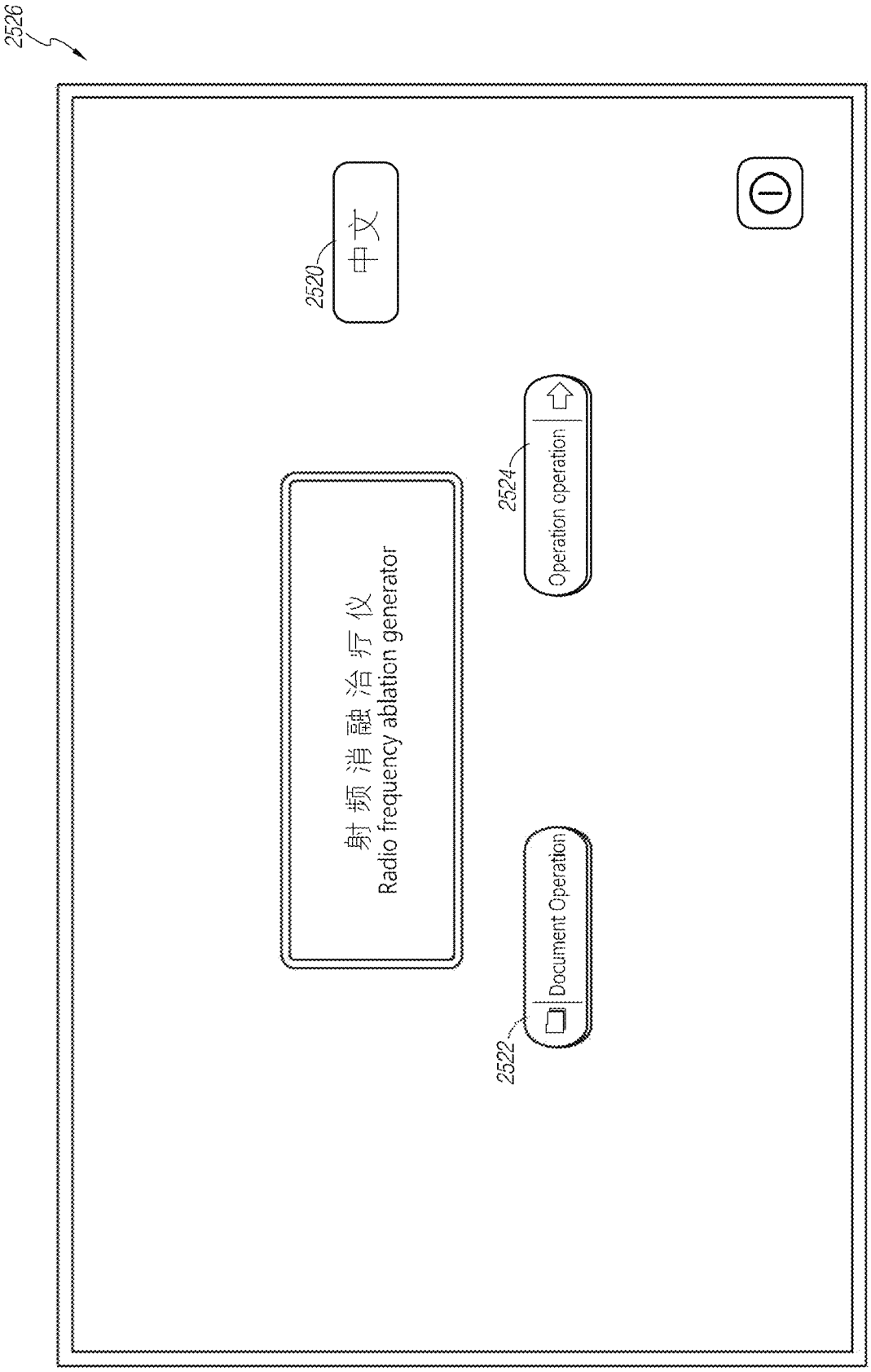
2526
2520
中文
射频消融治疗仪
Radio frequency ablation generator
2524
Operation operation
2522
Document Operation

FIG. 25D

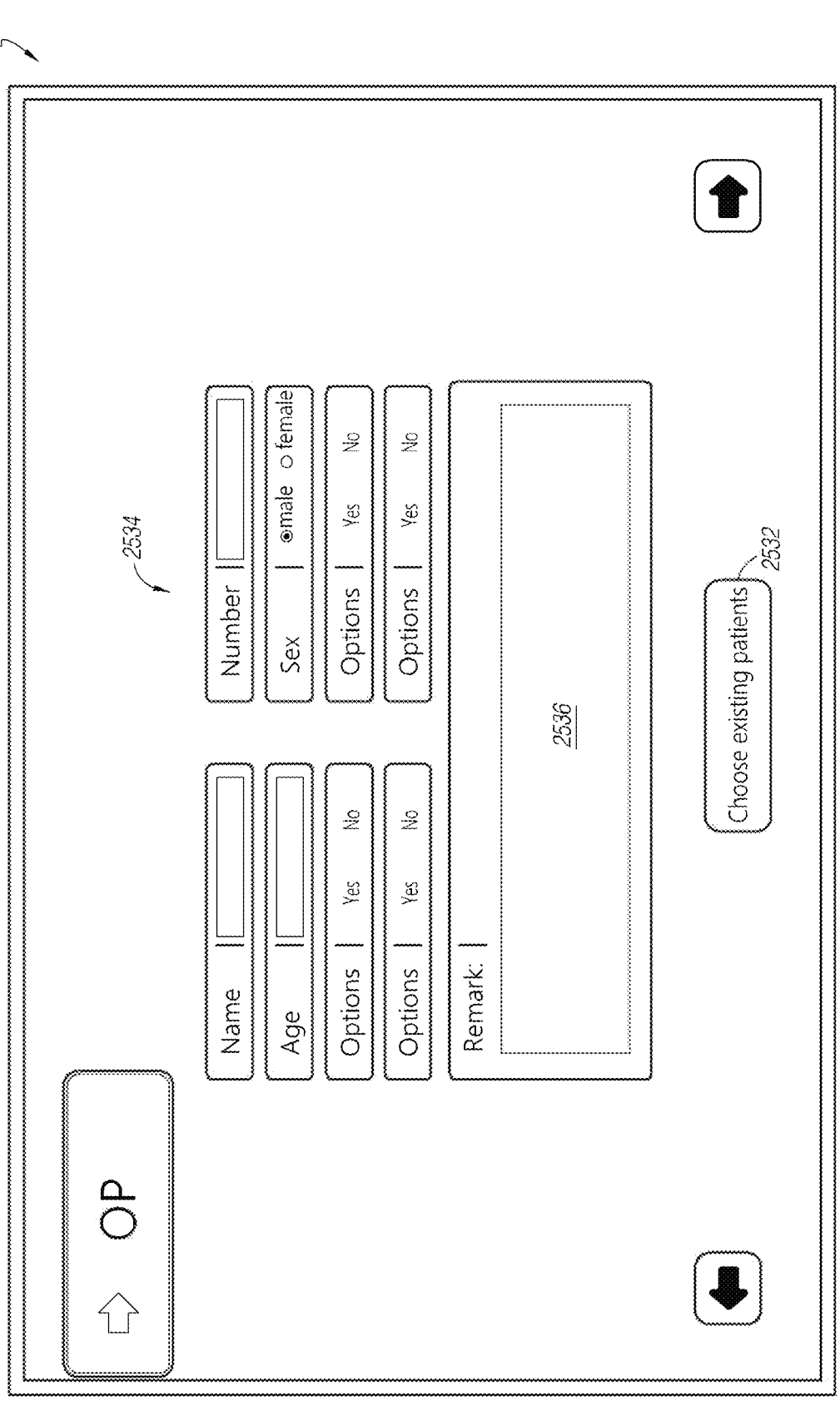
2530
OP
Name
Age
Options
Yes
No
Options
Yes
No
2534
Number
Sex
male
female
Options
Yes
No
Options
Yes
No
Remark:
2536
Choose existing patients
2532

FIG. 25E

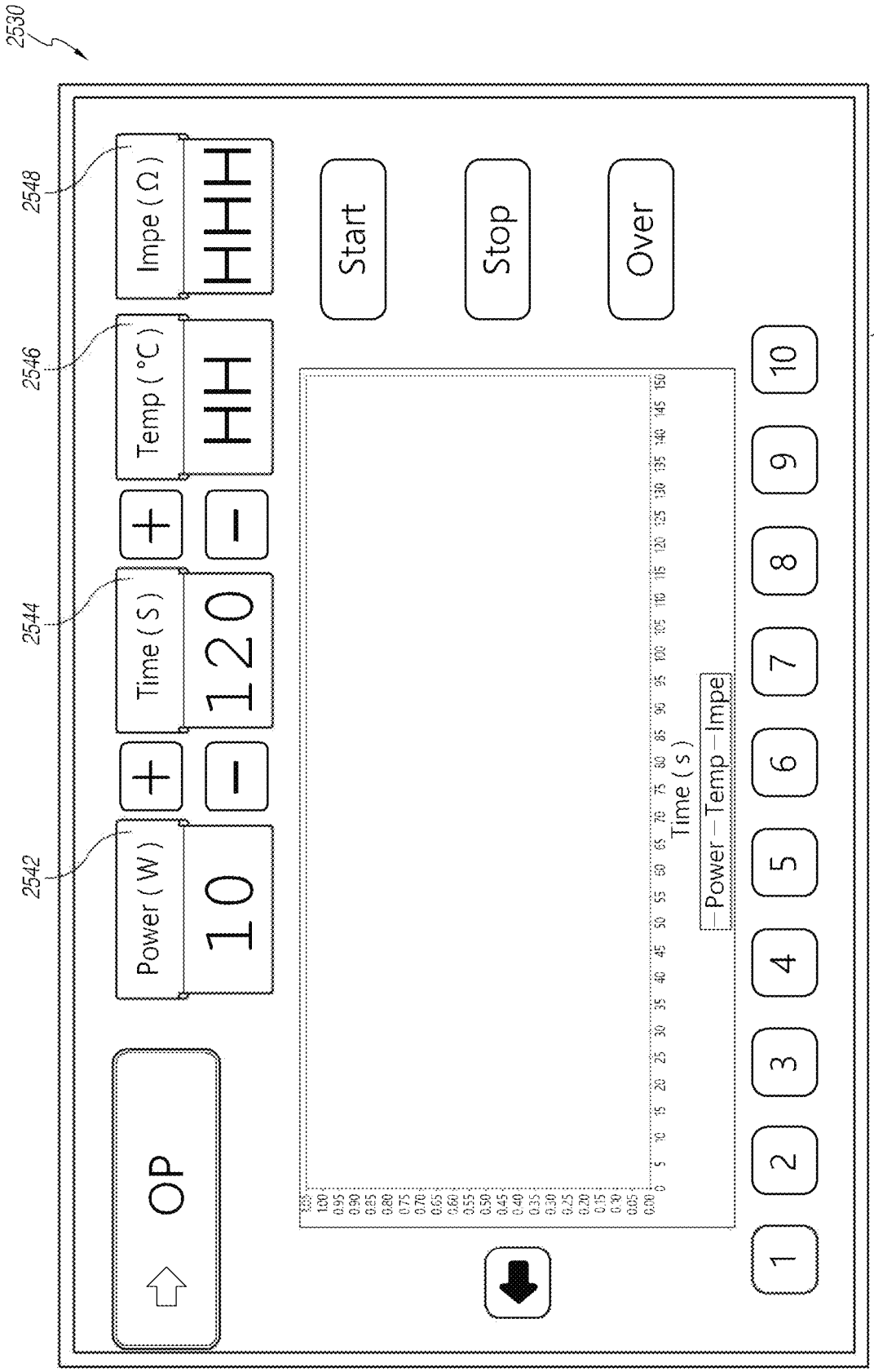
2530
2548
2546
2544
2542
2540
Impe (Ω)
HHH
Temp (°C)
HH
Time (S)
120
Power (W)
10
+
−
Start
Stop
Over
OP
Power
Temp
Impe
Time (s)
1
2
3
4
5
6
7
8
9
10

FIG. 25F

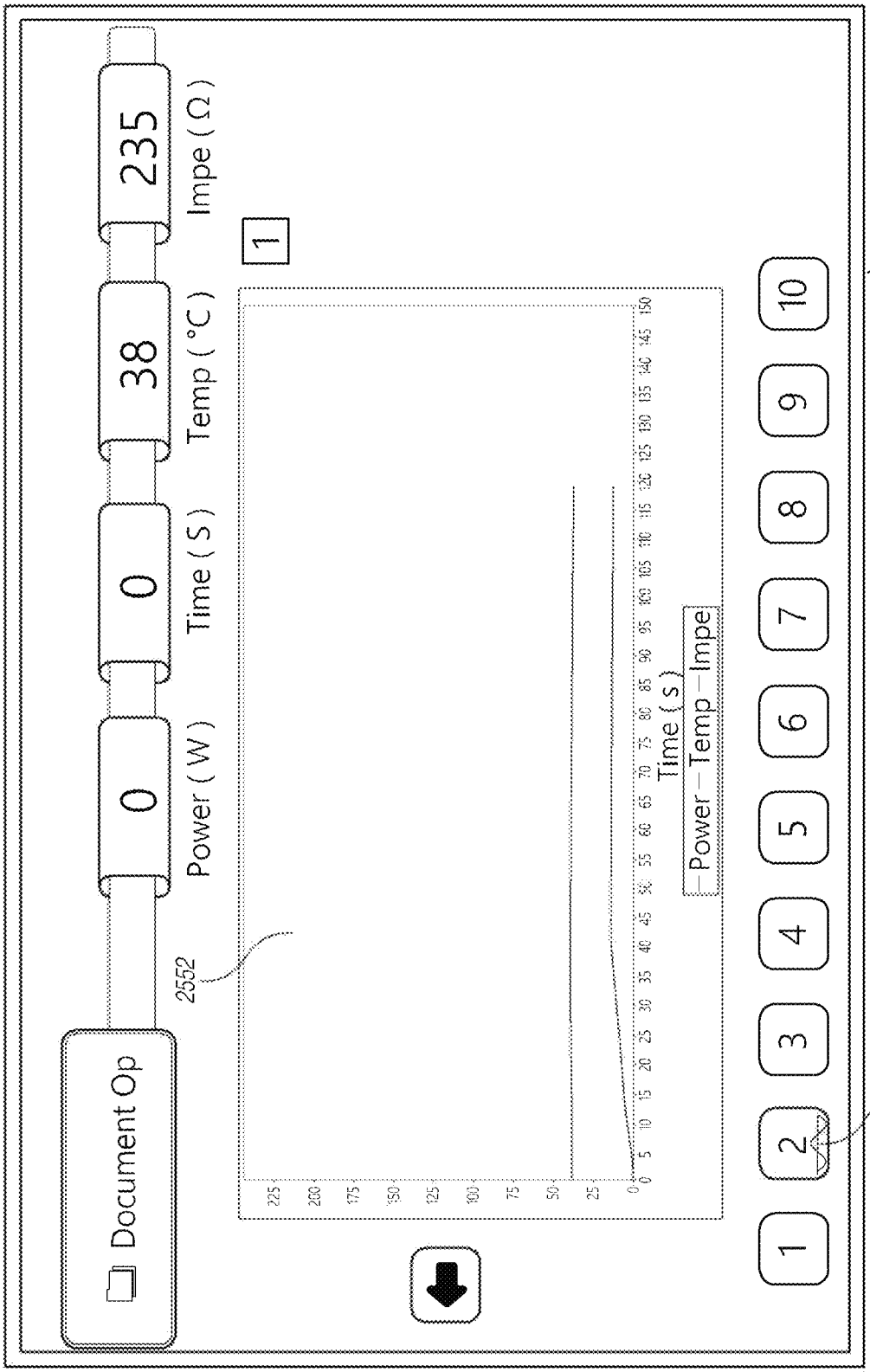
Document Op
0
Power (W)
0
Time (S)
38
Temp (°C)
235
Impe (Ω)
1
2552
Power—Temp—Impe
Time (s)
2550
2570
1
2
3
4
5
6
7
8
9
10

FIG. 25G

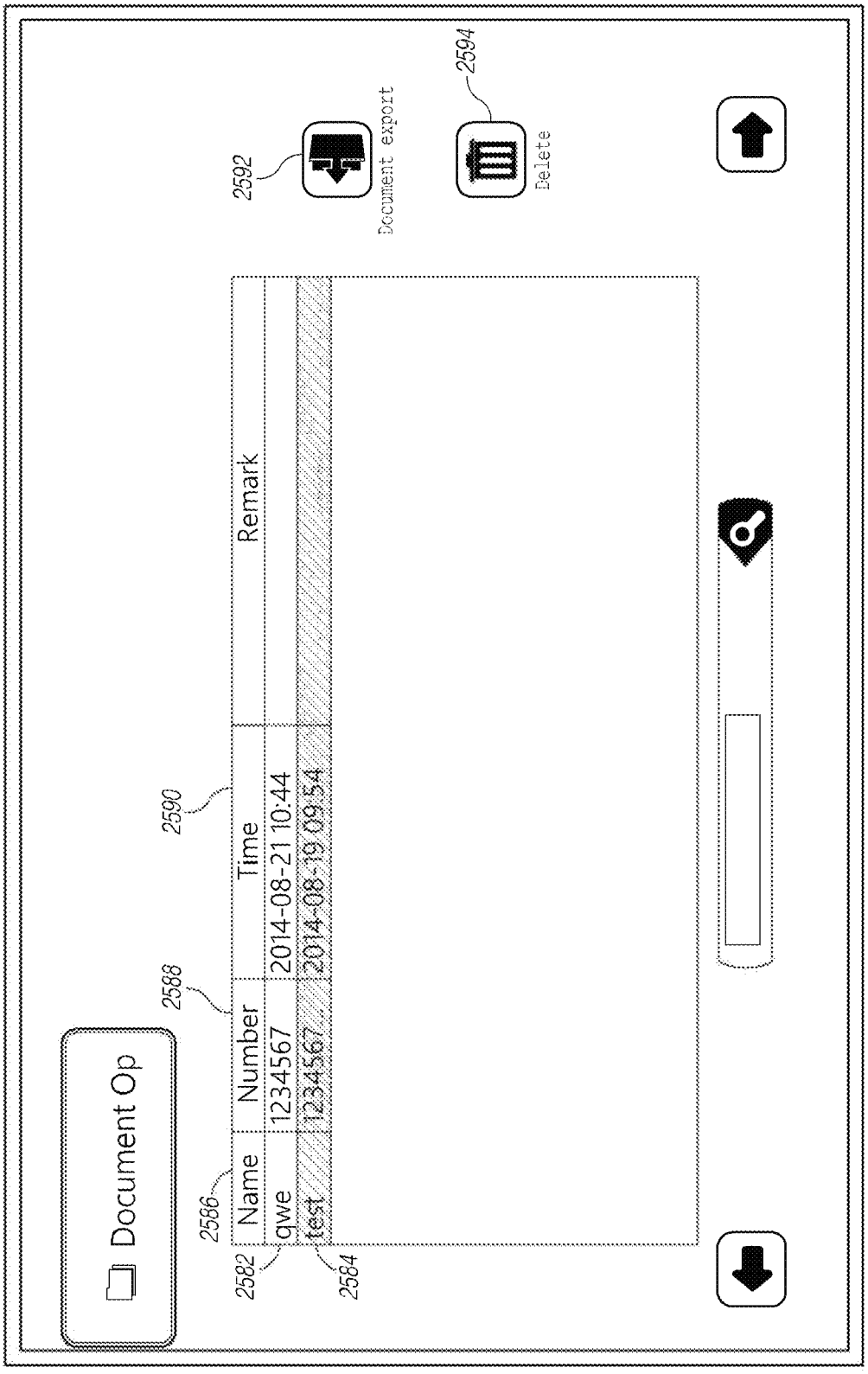
Document Op
2582
2584
2586
2588
2590
Name
Number
Time
Remark
qwe
1234567
2014-08-21 10:44
test
1234567
2014-08-19 09:54
2592
Document export
2594
Delete
2580

FIG. 25H

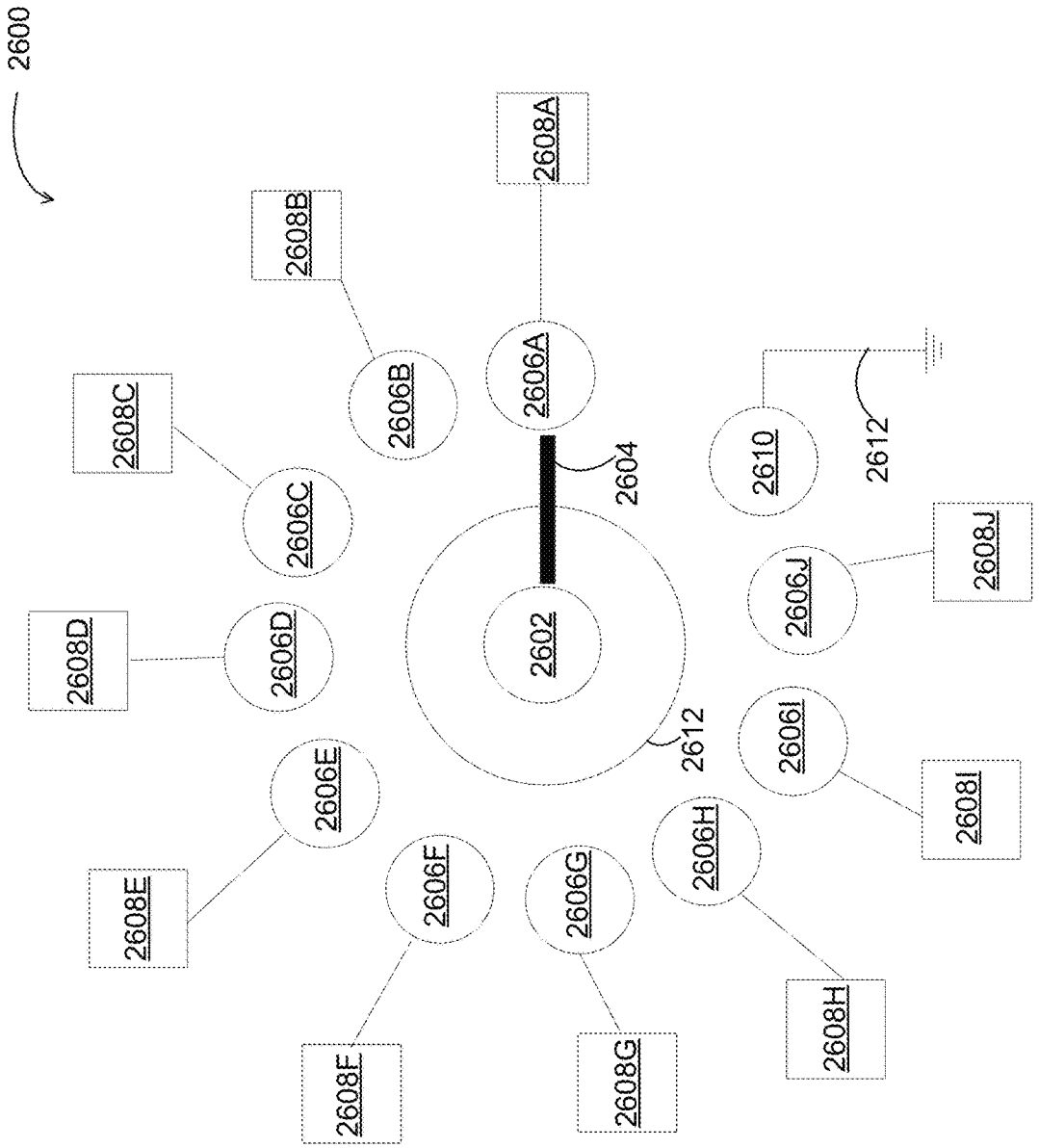
2600
2608A
2608B
2606A
2606B
2608C
2606C
2604
2610
2612
2608D
2606D
2602
2606J
2608J
2608E
2606E
2612
2606I
2606F
2606G
2606H
2608I
2608F
2608G
2608H

FIG. 26

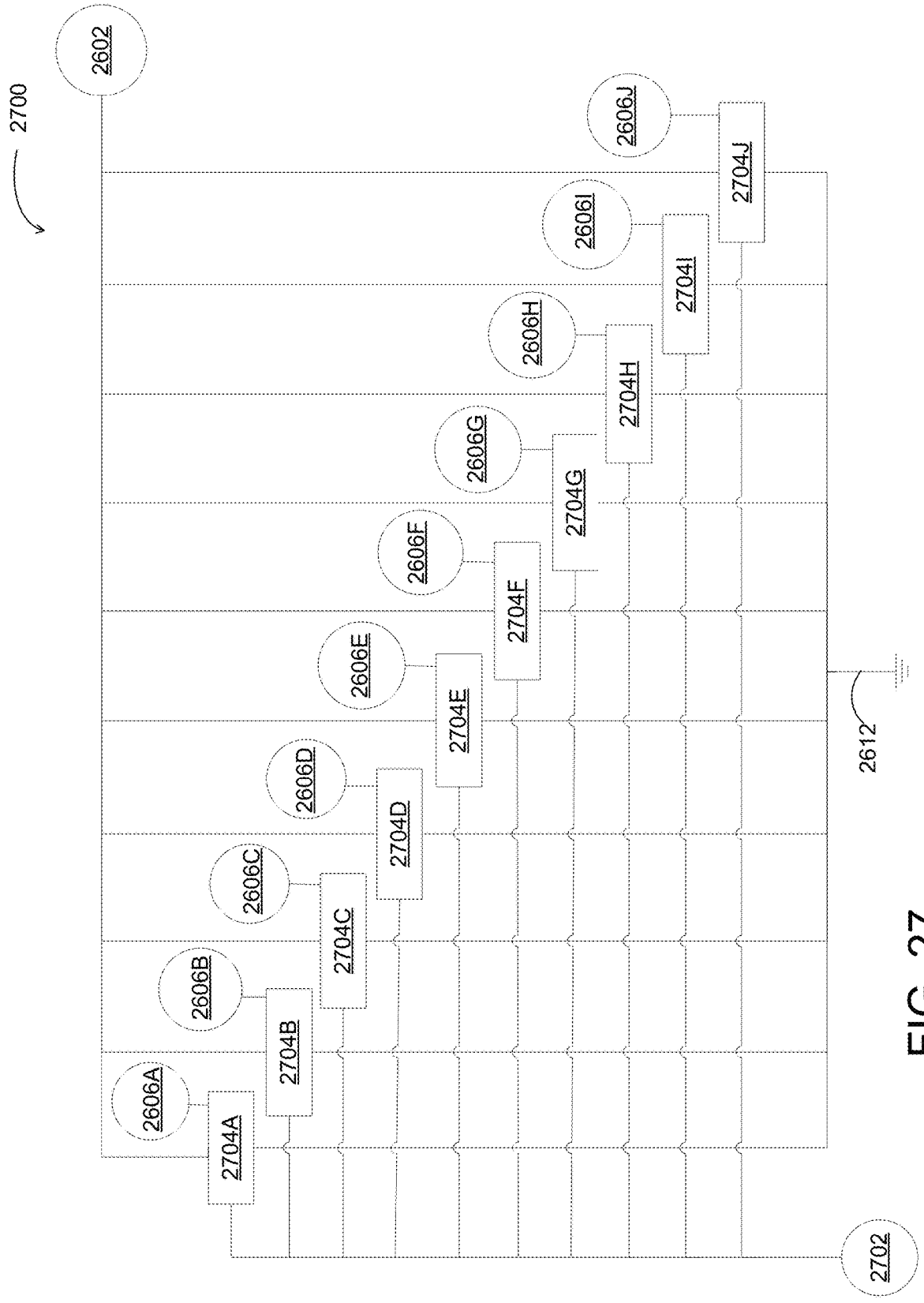
2700
2602
2606A
2606B
2606C
2606D
2606E
2606F
2606G
2606H
2606I
2606J
2704A
2704B
2704C
2704D
2704E
2704F
2704G
2704H
2704I
2704J
2612
2702

FIG. 27

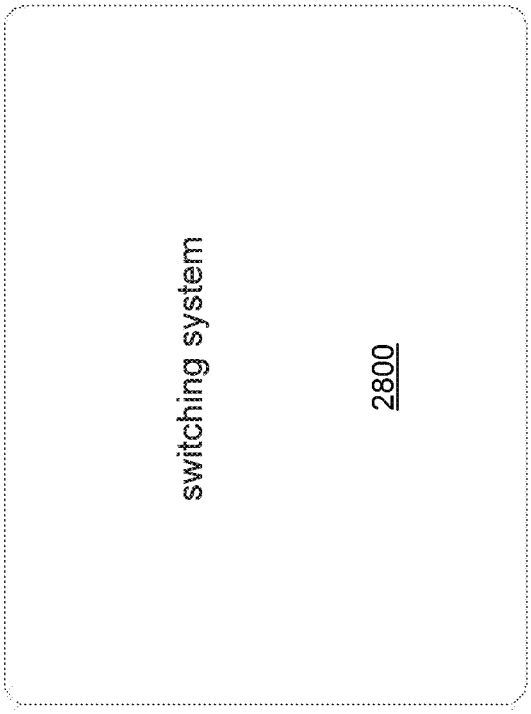

FIG. 28

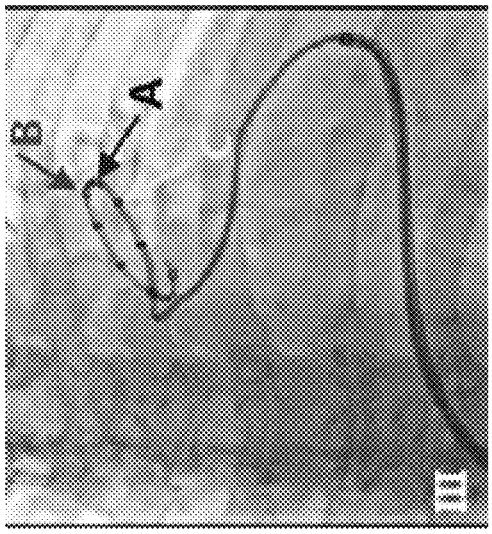

FIG. 29C

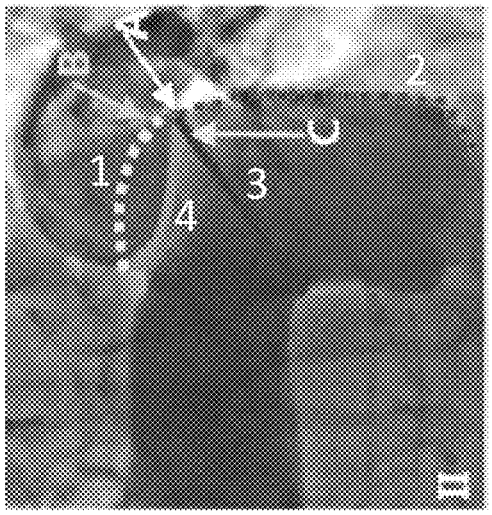

FIG. 29B

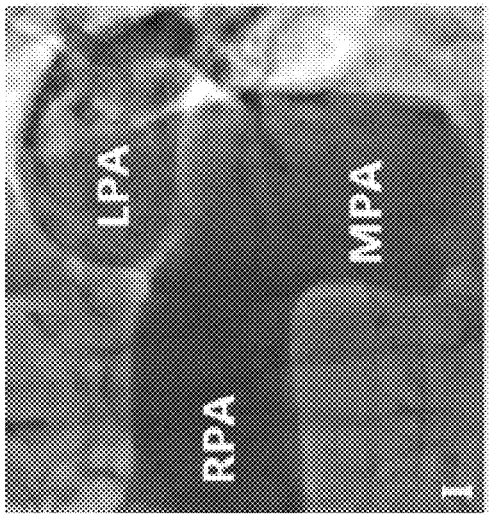

FIG. 29A

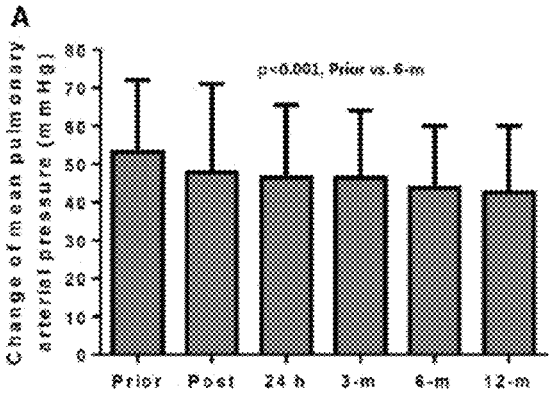

FIG. 30A

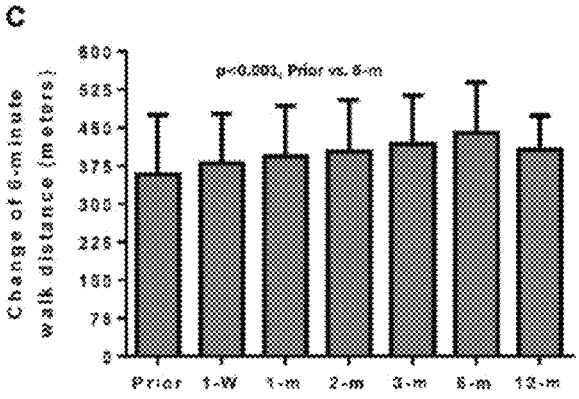

FIG. 30C

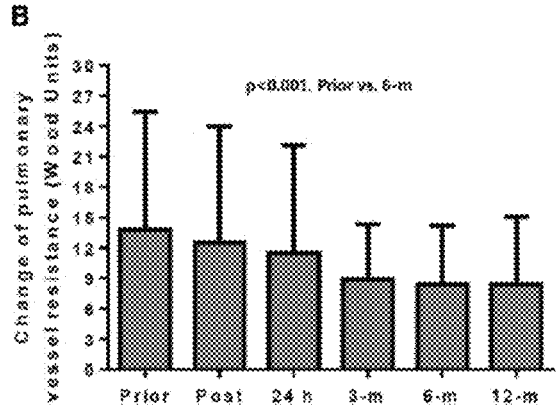

FIG. 30B

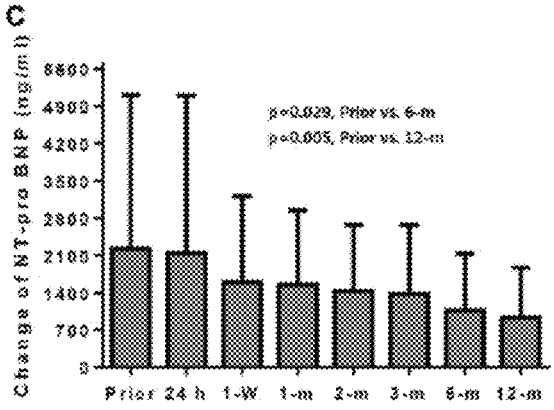

FIG. 30D

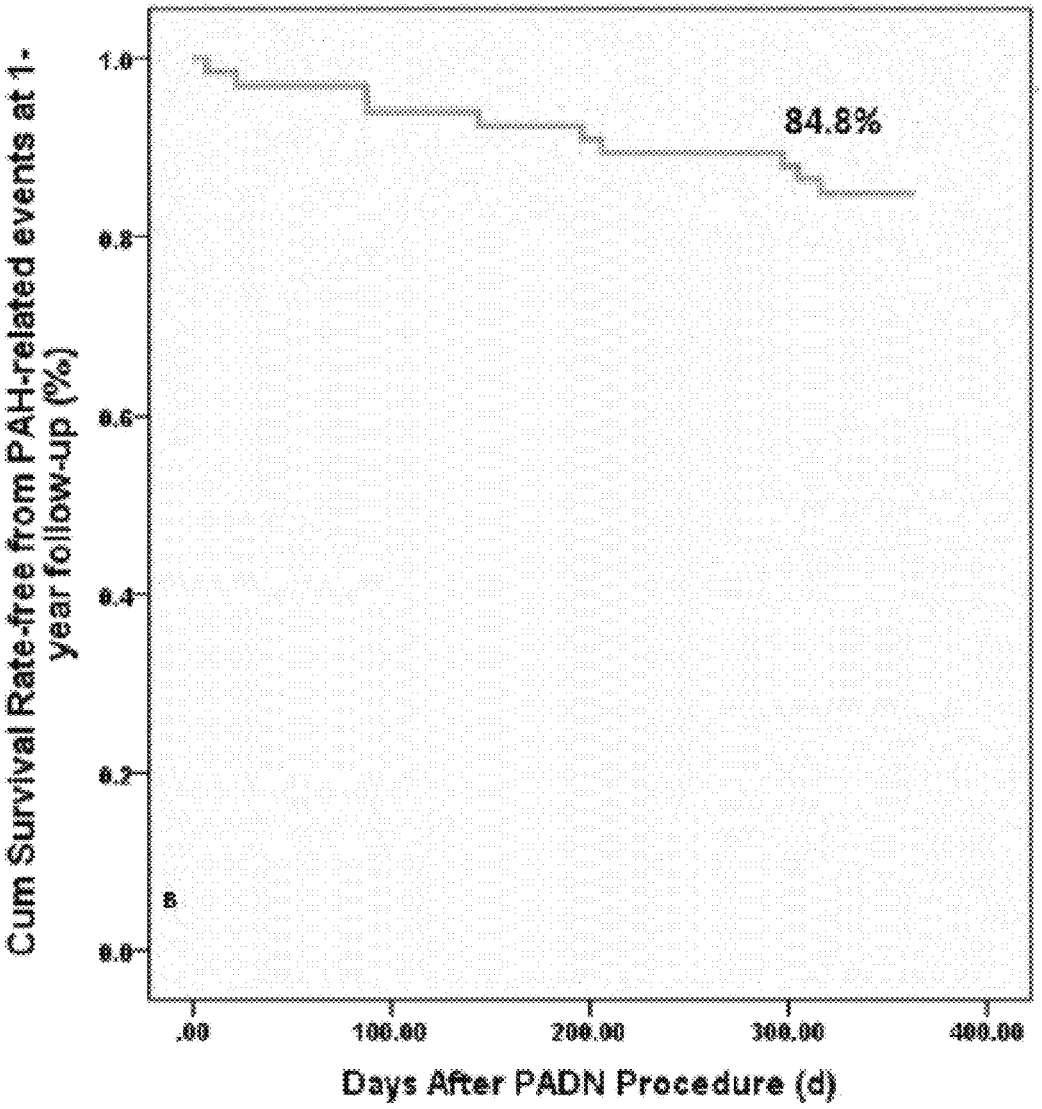
Cum Survival Rate-free from PAH-related events at 1-year follow-up (%)
1.0
0.8
0.6
0.4
0.2
0.0
84.8%
.00
100.00
200.00
300.00
400.00
Days After PADN Procedure (d)

FIG. 31

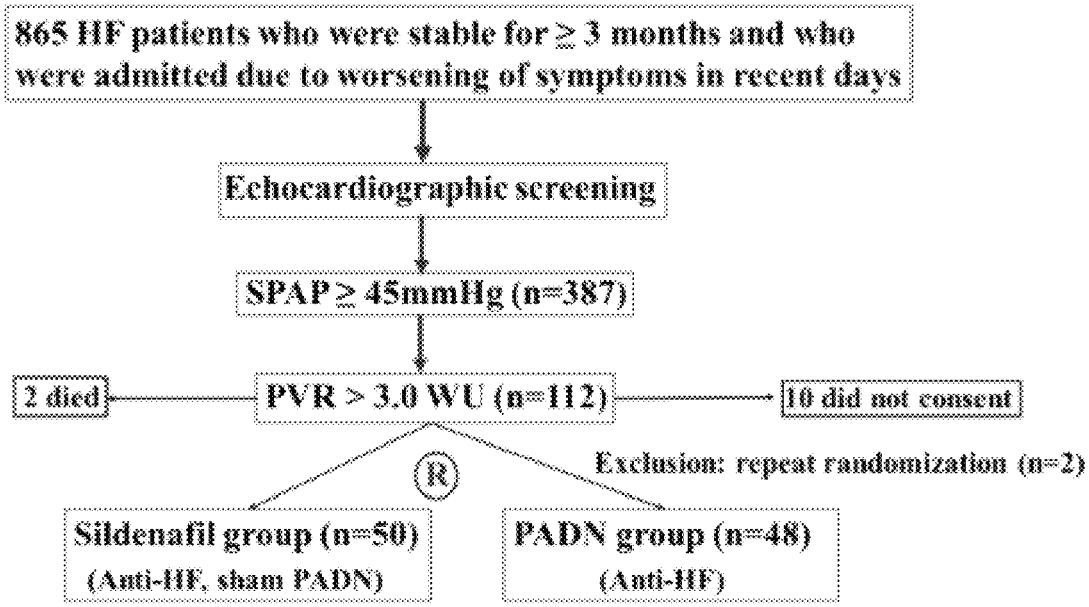
865 HF patients who were stable for ≥ 3 months and who were admitted due to worsening of symptoms in recent days
Echocardiographic screening
SPAP ≥ 45mmHg (n=387)
2 died
PVR > 3.0 WU (n=112)
10 did not consent
Exclusion: repeat randomization (n=2)
R
Sildenafil group (n=50)
(Anti-HF, sham PADN)
PADN group (n=48)
(Anti-HF)

FIG. 32

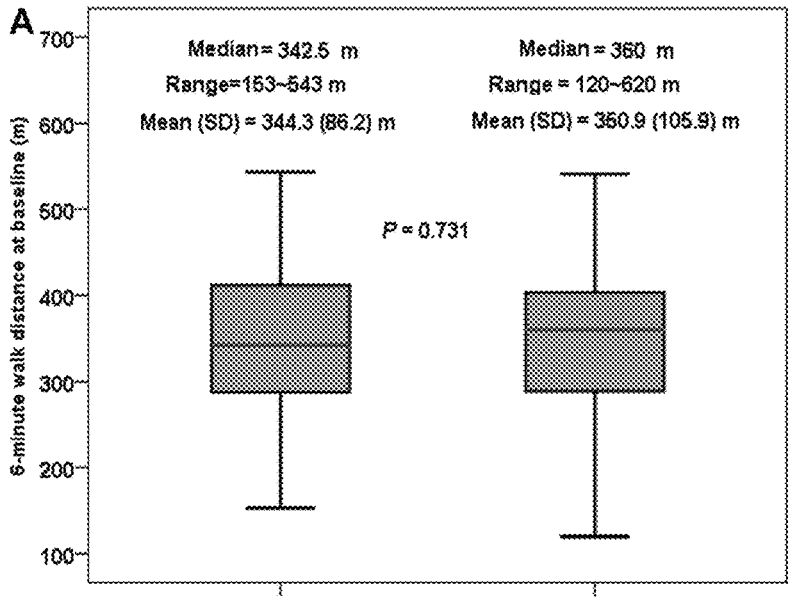

FIG. 33A

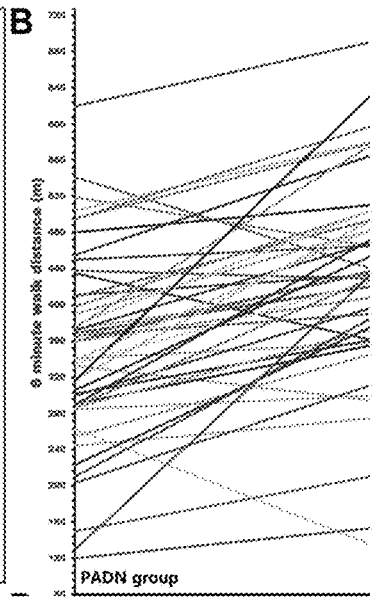

FIG. 33B

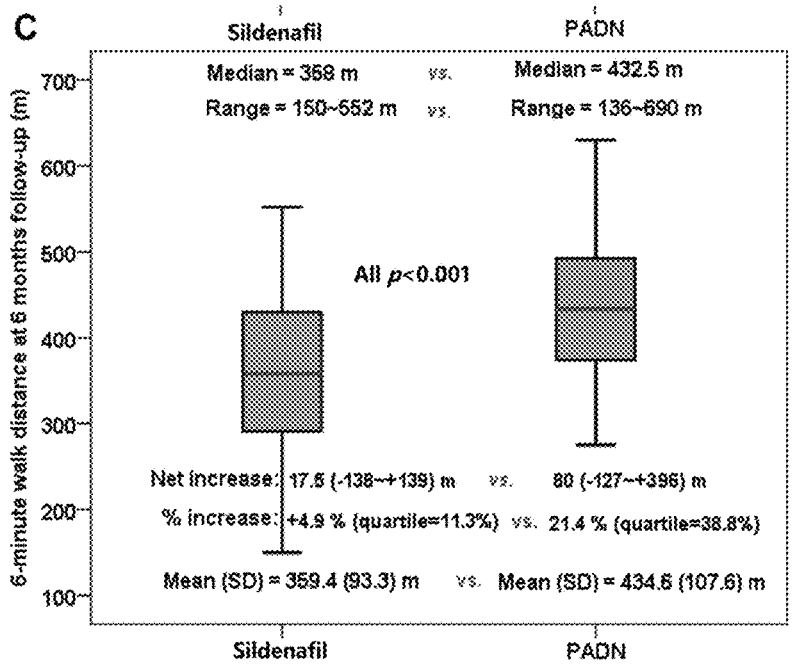

FIG. 33C

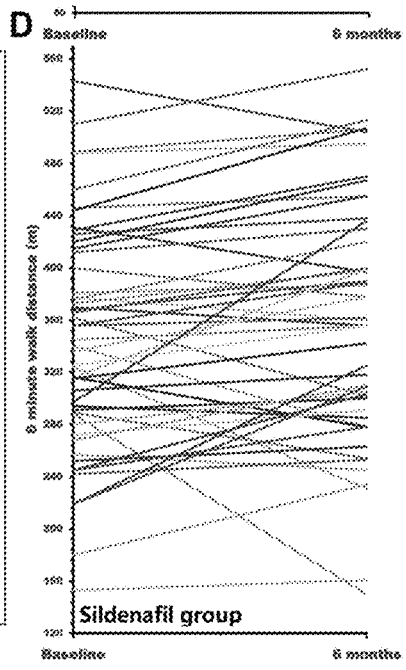

FIG. 33D

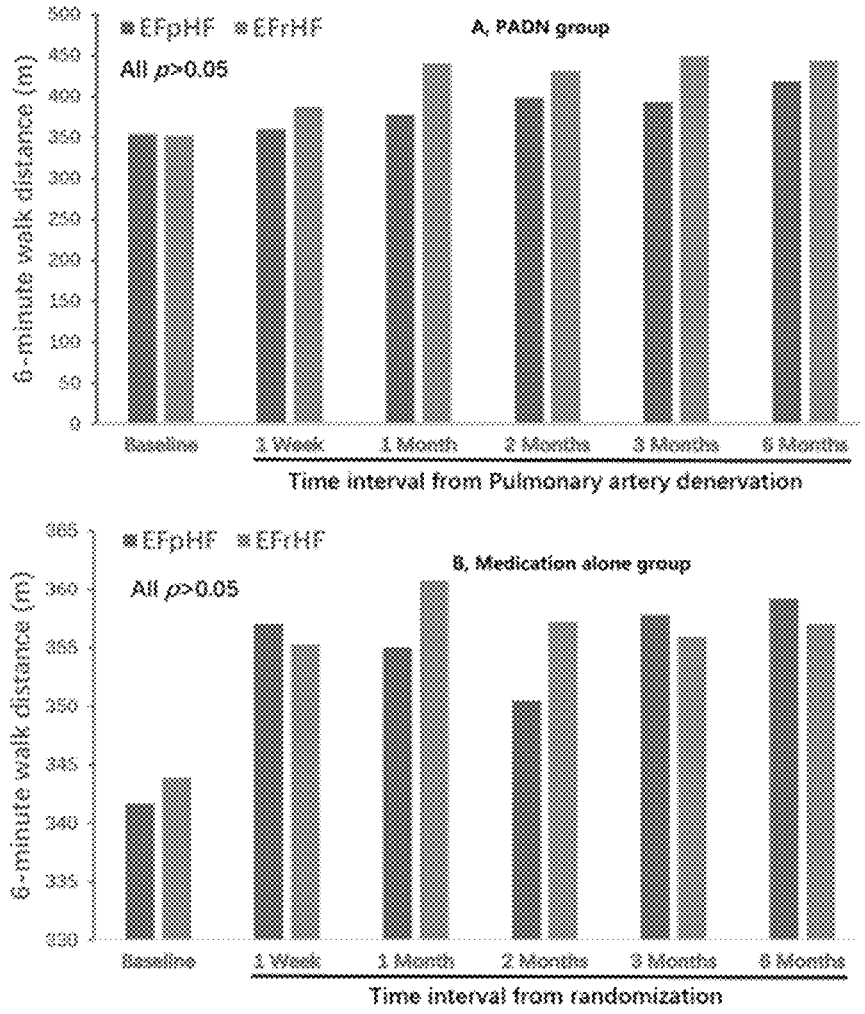
A, PADN group
EFpHF
EFrHF
All p>0.05
6-minute walk distance (m)
0
50
100
150
200
250
300
350
400
450
500
Baseline
1 Week
1 Month
2 Months
3 Months
6 Months
Time interval from Pulmonary artery denervation
B, Medication alone group
EFpHF
EFrHF
All p>0.05
6-minute walk distance (m)
330
335
340
345
350
355
360
365
Baseline
1 Week
1 Month
2 Months
3 Months
6 Months
Time interval from randomization

FIG. 34

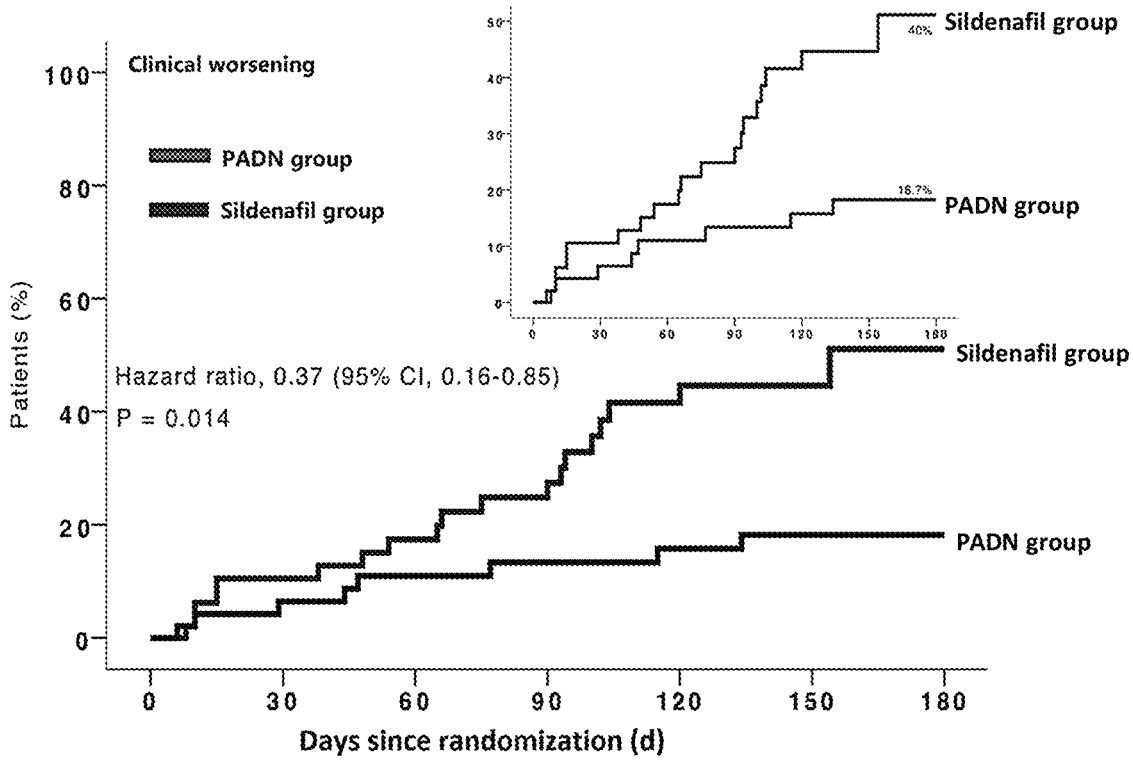
Clinical worsening
PADN group
Sildenafil group
Patients (%)
100
80
60
40
20
0
Hazard ratio, 0.37 (95% CI, 0.16-0.85)
P = 0.014
Sildenafil group
PADN group
0
30
60
90
120
150
180
Days since randomization (d)
40%
18.7%
No. at risk
PADN 48 45 43 42 41 40 40
Sildenafil 50 45 42 38 32 32 30

FIG. 35

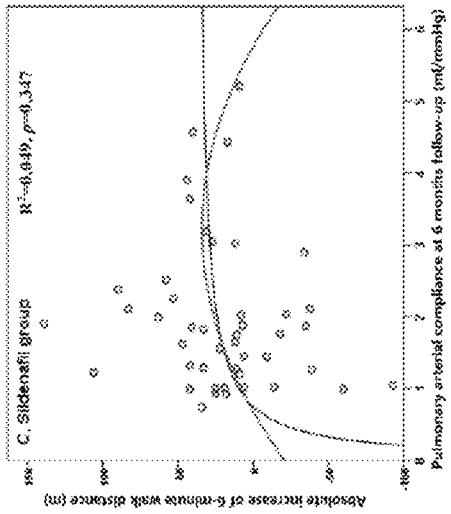

FIG. 36C

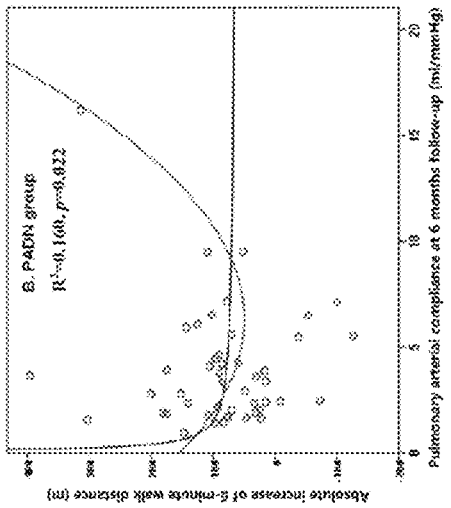

FIG. 36B

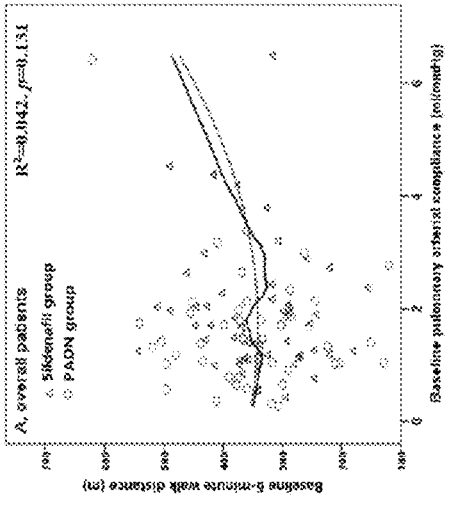

FIG. 36A

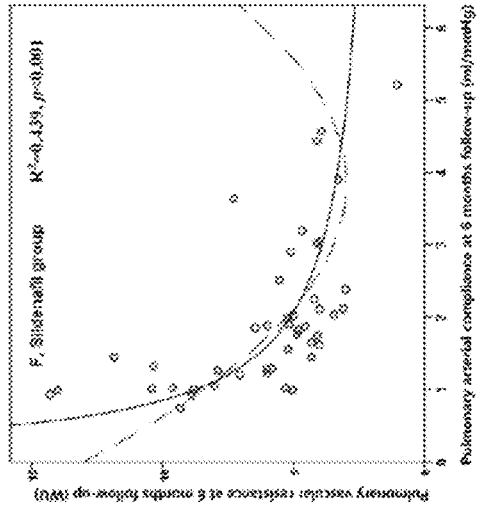

FIG. 36F

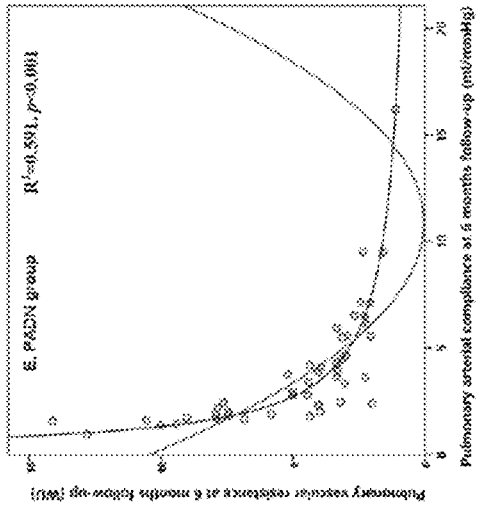

FIG. 36E

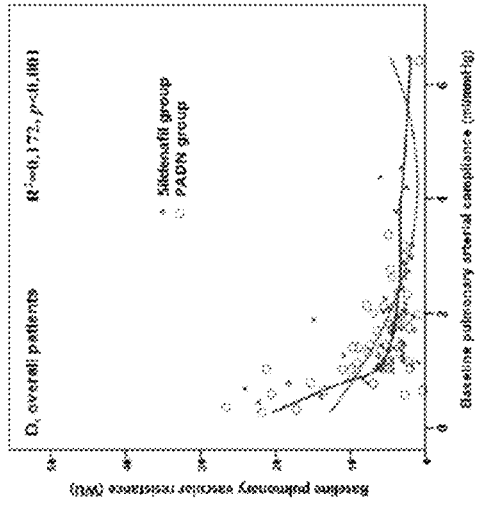

FIG. 36D

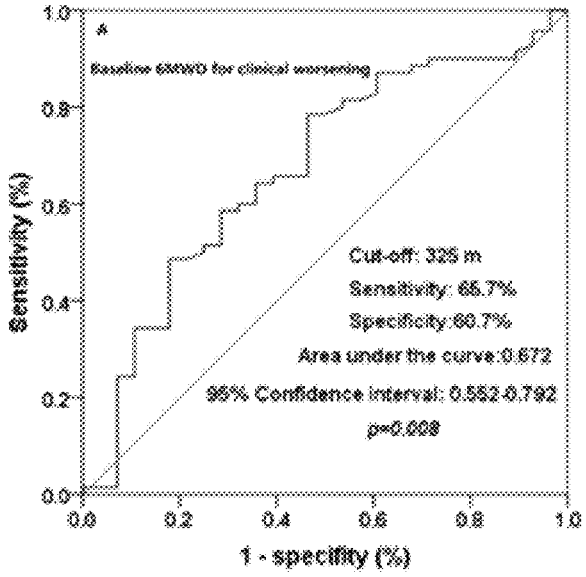

FIG. 37A

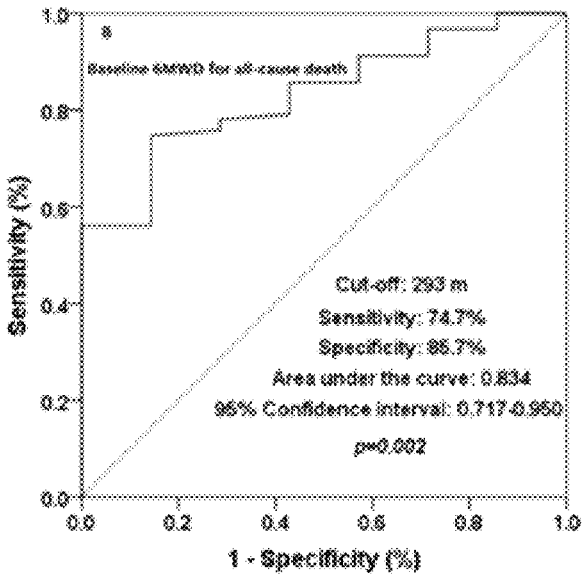

FIG. 37B

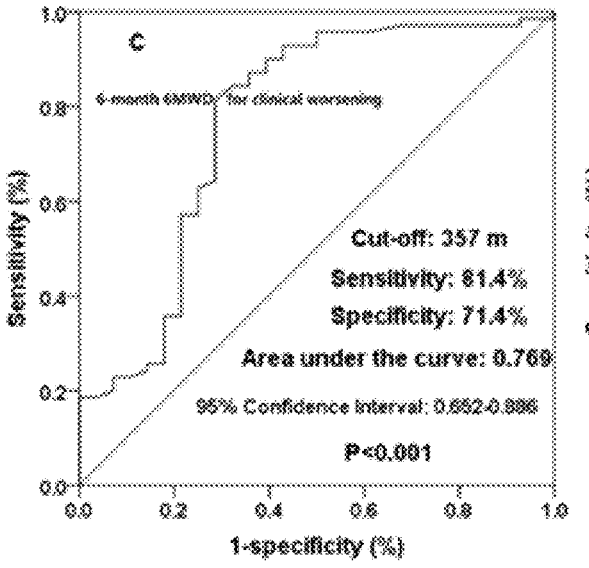

FIG. 37C

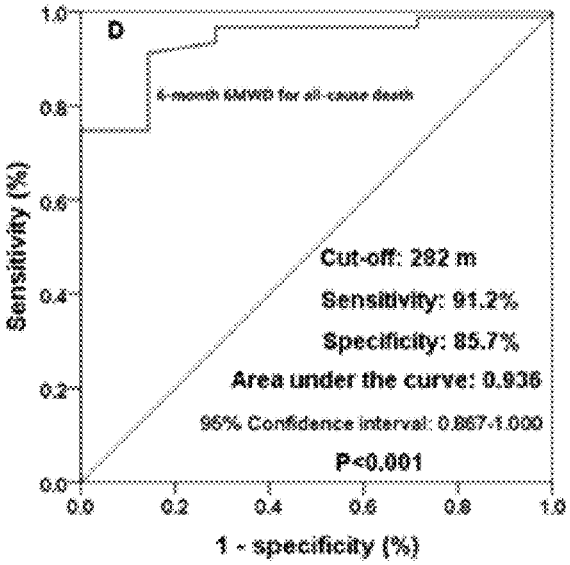

FIG. 37D

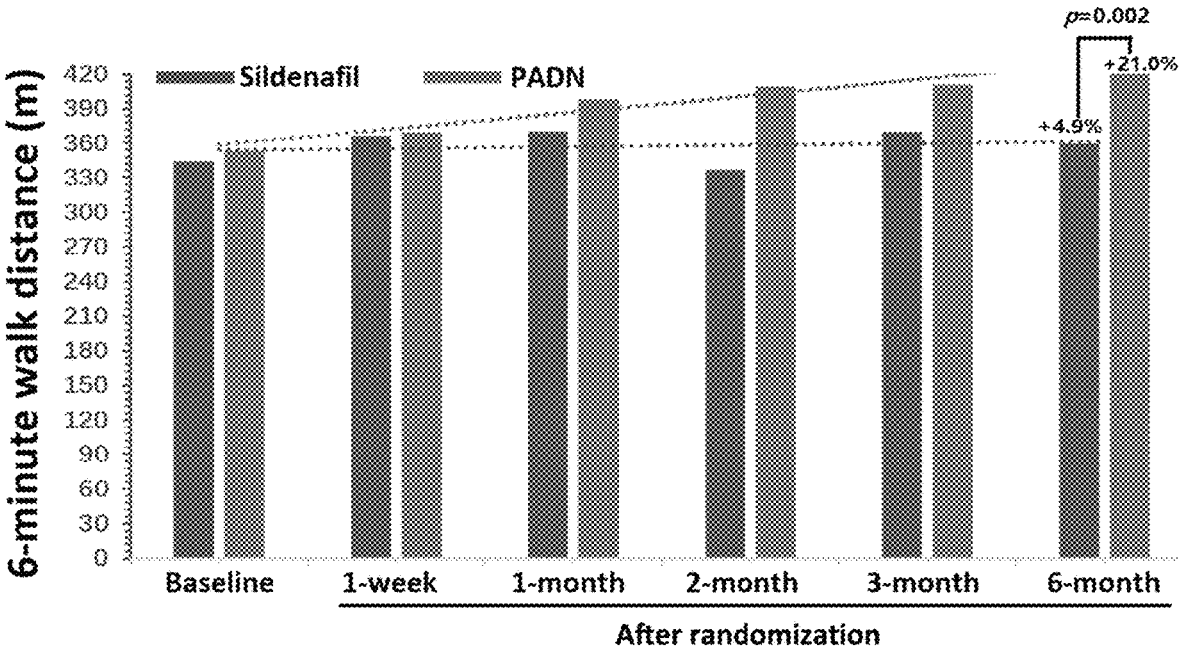
p=0.002
+21.0%
+4.9%
Sildenafil
PADN
6-minute walk distance (m)
420
390
360
330
300
270
240
210
180
150
120
90
60
30
0
Baseline
1-week
1-month
2-month
3-month
6-month
After randomization

FIG. 38

MULTI-POLE SYNCHRONOUS PULMONARY ARTERY RADIOFREQUENCY ABLATION CATHETER

CROSS-REFERENCE TO RELATED APPLICATIONS

The present application is a continuation-in-part of U.S. patent application Ser. No. 17/357,720, filed Jun. 24, 2021; which is a continuation of U.S. patent application Ser. No. 15/873,721, filed Jan. 17, 2018, now U.S. Pat. No. 11,241,267; which is a continuation of U.S. patent application Ser. No. 14/672,013, filed Mar. 27, 2015, now U.S. Pat. No. 9,918,776; which is a continuation of U.S. patent application Ser. No. 14/666,214, filed Mar. 23, 2015, now U.S. Pat. No. 9,827,036; which claims priority to U.S. Provisional Patent Application No. 62/023,781, filed on Jul. 11, 2014; the entire contents of each of which are hereby incorporated by reference; U.S. patent application Ser. No. 14/666,214 is also a continuation-in-part of U.S. patent application Ser. No. 14/530,588, filed on Oct. 31, 2014, and U.S. patent application Ser. No. 14/079,230, filed on Nov. 13, 2013; both of which claim priority to Chinese Patent Application No. 201210453470.4, filed on Nov. 13, 2012, and Chinese Patent Application No. 201310103141.1, filed on Mar. 27, 2013; the entire contents of each of which are hereby incorporated by reference.

BACKGROUND OF THE INVENTIONS

Field of the Inventions

The present inventions relate to medical devices for treatment of pulmonary hypertension in the pulmonary artery by de-sympathetic methods, for example, with multi-pole synchronous pulmonary artery radiofrequency ablation catheters, as well as methods for diagnosis and method of treating pulmonary hypertension.

Description of the Related Art

Pulmonary hypertension (PH) is understood to be an intractable disease in the cardiovascular, respiratory, connective tissue, immune and rheumatic systems. Currently available clinical treatments of pulmonary hypertension are limited and therapy efficacy thereof is poor. Incidence of primary pulmonary hypertension is low, but those secondary to pulmonary interstitial fibrosis, connective tissue disease, portal hypertension, chronic pulmonary artery embolism and left heart system disorder are common, with five-year mortality rate up to 30%. Therefore, prevention and treatment for pulmonary hypertension is of great significance.

In recent years, new targeted drugs have emerged based on the research into the pathogenesis of pulmonary hypertension. However, some of those drugs have serious limitations including many side effects, inappropriate dosage form, expensive cost and unreliable efficacy, and thus many have not been widely applied in clinical treatment.

SUMMARY OF THE INVENTIONS

An aspect of at least one of the inventions disclosed herein includes the realization, supported by experimental data which demonstrates, that pulmonary hypertension is associated with hyper sympathetic activity in pulmonary artery and hyperactive baroreceptor. Blocking the sympathetic nerves in the pulmonary artery or permanently damaging the baroreceptor structure and function thereof can decrease the pulmonary artery pressure, which can provide more successful treatments of pulmonary hypertension.

Some embodiments disclosed herein provide a multi-pole synchronous pulmonary artery radiofrequency ablation catheter or ablation device for treatment of pulmonary hypertension in the pulmonary artery by a de-sympathetic method.

In some embodiments, the catheter only heats the adherent tissue rather than the blood. Additionally, in some embodiments, the catheter can be configured to provide cold saline perfusion at or near the ablation site to protect the vascular intima. Some embodiments can also provide advantages of simple operation, short operation time and controllable, precise ablation.

In some embodiments, a multi-pole synchronous pulmonary artery radiofrequency ablation catheter can comprise a control handle, a catheter body and an annular ring. The control handle can be provided with an adjustment apparatus. The catheter body can be hollow and can include a cavity. One or a plurality of lead wires, one or more temperature sensing wires and one or more pull wires can be arranged in the cavity. One end of the catheter body can be flexible. The flexible end can be connected to an annular ring and the other end of the catheter body can be connected to the control handle. One end of the pull wire can be connected to the flexible end and the other end of the pull wire can be connected to the adjustment apparatus. Tension in the pull wire can be adjusted through the adjustment apparatus to achieve shape control, such as curvature control, of the flexible end. A shape memory wire can be arranged in the annular ring. One end of the shape memory wire can extend to the end of the annular ring and the other end of the shape memory wire can pass through the root of the annular ring and can be fixed on the flexible end of the catheter body. The annular ring can be provided with an electrode group with each electrode connected to the one or more lead wires and the one or more temperature sensing wires. The lead wire(s) and the temperature sensing wire(s) extend through the catheter body and are electrically connected to the control handle.

In some embodiments, the ablation catheter comprises an expandable ablation element.

An infusion tube can be arranged in the cavity of the catheter body and a through hole can be arranged on one or more of the electrodes. The infusion tube can be connected to the electrodes through the annular ring. The transfused fluid flows out from the through hole and thus can be used for cooling purposes during ablation as part of the percutaneous pulmonary denervation (PADN) procedure.

The electrodes on the annular ring can be made of material selected from a group consisting of platinum-iridium alloy, gold, stainless steel and nickel alloy, with the number in the range of 3-30 electrodes, a diameter in the range of 1.3-2.0 mm, a length in the range of 1.2-4 mm and an edge space between adjacent electrodes in the range of 0.5-10 mm.

The flexible end of the catheter body can be provided with a counterbore, an inner diameter of the counterbore can be sized to fit an outer diameter of the root of the annular ring, and thus the root of the annular ring can be inserted and fixed into the counterbore.

The flexible end of the catheter body is provided with a groove in which a connector is arranged, one end of the connector is connected to the pull wire and the other end of the connector is connected to the shape memory wire.

The material of the shape memory wire in the annular ring can be a shape memory alloy selected from a group con-

sisted of nickel-titanium alloy, stainless steel or titanium, with a diameter of 0.25-0.5 mm. The diameter of the annular ring can be 12-40 mm. For example, the annular ring can be configured so as to be biased toward a circumferential shape, having a desired diameter (e.g., in the range of 12-40 mm), for example, with the use of a memory shape material. Preferably, 10 electrodes are arranged on the annular ring. The width of naked section of the electrode is 0.75 mm, and the space therebetween is 5 mm.

The flexible end can be made of medical polymer materials with a length in the range of 30-80 mm. The connection can be achieved by a UV-curing adhesive. The joint between the flexible end and the annular ring can be sealed.

The pull wire is made of stainless steel or nickel-titanium alloy. The outside of pull wire is provided with a spring coil, and the outside of the spring coil is provided with a spring sleeve made of polyimide material.

In some embodiments, the catheter can be packaged into a kit including a plurality of different annular rings that are biased to different diameters. In some embodiments, where the annular rings, flexible bodies, and handles are permanently connected together, a kit can include a plurality of different catheters, each having handles and flexible bodies, but differently sized annular rings.

In some embodiments and/or methods of use, the catheter can heat, with radiofrequency energy, the tissue in direct contact with the electrode and avoid heating blood. Additionally, the catheter can provide advantages of simple operation, short operation time and controllable precise ablation. The catheter body can preferably be made of a polymer material, which is a poor heat conductor, so that it can avoid transmitting the heat when heating the electrodes to the flowing blood contacting the catheter body, thereby effectively avoid heating the blood.

Furthermore, the shape or curvature of the flexible end can be adjusted by operating the adjustment apparatus, which allows the operator to control the handle with one hand, so as to easily adjust the curvature of the flexible end for purposes of placement of the annular ring and the electrodes. As such, after achieving the desired placement, the electrodes on the annular ring can be pressed against the pulmonary artery and achieve ablation of pulmonary artery intima. During application of the radiofrequency current, the electrodes can produce high local temperature and cause severe damage on the vascular intima.

Thus, in some embodiments, the catheter can be configured to provide cold saline perfusion to cool down the local temperature. When the electrodes receive current, the saline is automatically and uniformly diffused through the through holes, which can provide beneficial cooling, for example, decreasing the local temperature to be below 60° C., thereby protecting the vascular intima.

In some embodiments, a multi-pole synchronous pulmonary artery radiofrequency ablation catheter may comprise a control handle, a catheter body and an annular ring. The control handle may include an adjustment apparatus. The catheter body may be hollow and comprise a cavity arranged in the catheter body. A lead wire, a temperature sensing wire and a pull wire may be arranged in the cavity. One end of the catheter body may be flexible, and the flexible end of the catheter body may be connected to the annular ring. The other end of the catheter body may be connected to the control handle. One end of the pull wire may be connected to the flexible end. The other end of the pull wire may be connected to the adjustment apparatus on the control handle. The adjustment apparatus may adjust the tension of the pull wire to change a curvature of the flexible end. A shape memory wire may be arranged in the annular ring. One end of the shape memory wire may extend to an end of the annular ring and the other end of the shape memory wire may pass through a root of the annular ring and be fixed on the flexible end of the catheter body. The annular ring may be provided with an electrode group. The electrode group may comprise a first electrode of a first length, a second electrode of a second length different than the first length, and a third electrode. Each electrode of the electrode group may be connected to the lead wire and temperature sensing wire. The lead wire and the temperature sensing wire may go through the catheter body and be electrically connected to the control handle.

The annular ring may extend from the root of the annular ring to the end of the annular ring and comprise a curve of less than 360 degrees. The annular ring may extend from the root of the annular ring to the end of the annular ring and comprise a curve of more than 270 degrees. The annular ring may comprise a first diameter and a second diameter different than the first diameter. The first diameter may be at least 25 mm and the second diameter may be at least 20 mm.

The electrodes of the electrode group may be substantially coplanar. The first length of the first electrode may be least 4 mm. The second length of the second electrode may be least 3 mm. The third electrode may comprise a third length different than the first length and different than the second length. The third length may be at least 2 mm.

In some embodiments, a catheter may comprise a catheter body and an annular ring. One end of the catheter body may be flexible and connected to the annular ring. The curve of the annular ring may be less than 360 degrees and greater than 270 degrees.

The annular ring may be provided with an electrode group comprising a first electrode of a first length, a second electrode of a second length different than the first length, and a third electrode of a third length different than the first length and different than the second length. The electrodes of the electrode group may be substantially coplanar and arranged along a curve of the annular ring that extends from a root of the annular ring to an end of the annular ring. The first length may be least 4 mm. The second length may be least 3 mm and may be less than the first length. The third length may be least 2 mm and may be less than the second length. The first length may be 4 mm. The electrode group may comprise less than four electrodes.

The first electrode may be separated from the second electrode and the third electrode by an equal distance. The equal distance may be 1 mm. The first electrode may be farther in distance from a root of the annular ring than the second electrode and the third electrode.

In some embodiments, a controller may comprise a housing, an electronic display, a battery, an electronic data store, and a computing device. The housing may comprise a catheter connection port disposed along a surface of the housing. The connection port may be configured to interface with a catheter. The catheter may comprise a first electrode of a first length, and a second electrode of a second length different than the first length. The housing may comprise an electronic display disposed along the surface of the housing. The housing may envelop a battery, an electronic data store and a computing device. The electronic display may be configured to present a user interface. The battery may be configured to store power at a level sufficient for ablation using the first electrode, or the second electrode. The electronic data store may comprise stored patient profiles characterizing a plurality of patients. The computing device may comprise one or more processors. The computing device

may be in communication with the electronic data store, the electronic display and the battery. The computing device may be configured to at least: receive a selection of a first patient profile of the stored patient profiles from the user interface, display information characterizing the first patient profile on the user interface, receive a selection of the first electrode from the user interface, direct power from the battery at the level sufficient for ablation using the first electrode to the first electrode, receive a selection of the second electrode from the user interface, and direct power from the battery at the level sufficient for ablation using the second electrode to the second electrode.

The computing device may be configured to direct power from the battery to the first electrode and direct power from the battery to the second electrode at a same time. The computing device may be configured to direct power from the battery to the first electrode and direct power from the battery to the second electrode at different times. The computing device may be configured to interrupt power directed from the battery to the first electrode and direct power from the battery to the second electrode after the power directed from the battery to the first electrode is interrupted. The computing device may be configured to direct power from the battery to the first electrode after the battery has finished charging. The computing device may be configured to display on the user interface first electrode ablation information captured by the first sensor while the first electrode receives power from the battery. The computing device may be configured to store the first electrode ablation information with the first patient profile. The computing device may be configured to display on the user interface first electrode ablation information captured by the first sensor while the first electrode receives power from the battery and second electrode ablation information captured by the second sensor while the second electrode receives power from the battery. The second electrode ablation information may be displayed on the user interface after the first electrode stops receiving power from the battery.

The housing may comprise a power connection port configured to receive power at a level sufficient to charge the battery.

The catheter may comprise a first sensor connected with the first electrode. The catheter may comprise a first sensor connected with the first electrode and a second sensor connected with the second electrode.

In some embodiments, a computer-implemented method, under control of one more computing devices executing specific computer executable instructions, may comprise receiving a selection of a first patient profile of a plurality of stored patient profiles from a user interface presented on an electronic display disposed across a surface of a housing. The method may comprise displaying information characterizing the first patient profile on the user interface. The method may comprise receiving a selection of the first electrode from the user interface. The method may comprise directing power from a battery at the level sufficient for ablation using the first electrode to the first electrode, the battery configured to store power at a level sufficient for ablation using the first electrode. The method may comprise receiving a selection of the second electrode from the user interface. The method may comprise directing power from the battery at the level sufficient for ablation using the second electrode to the second electrode. The battery may be configured to store power at a level sufficient for ablation using the second electrode. The housing may comprise a catheter connection port disposed along a surface of the housing. The connection port may be configured to interface with a catheter comprising a first electrode of a first length, and a second electrode of a second length different than the first length. The housing may envelop the battery, an electronic data store and the one or more computing devices executing specific computer executable instructions. The electronic data store may comprise the plurality of stored patient profiles characterizing a plurality of patients.

The first electrode and the second electrode may be configured to convert the power from the battery to radiofrequency (RF) energy for ablation of sympathetic nerve fibers. The first electrode and the second electrode may be configured to convert the power from the battery to ultrasonic energy for ablation of sympathetic nerve fibers. The first electrode and the second electrode are configured to convert the power from the battery to electroporation energy for ablation of sympathetic nerve fibers. The first electrode and the second electrode may be configured to convert the power from the battery to ionizing energy for ablation of sympathetic nerve fibers.

In some embodiments, a computer-readable, non-transitory storage medium storing computer executable instructions that, when executed by one or more computer systems, configure the one or more computer systems to perform operations comprising receiving a selection of a first patient profile of a plurality of stored patient profiles from a user interface presented on an electronic display disposed across a surface of a housing. The operations may comprise displaying information characterizing the first patient profile on the user interface. The operations may comprise receiving a selection of the first electrode from the user interface. The operations may comprise directing power from a battery at the level sufficient for ablation using the first electrode to the first electrode. The battery may be configured to store power at a level sufficient for ablation using the first electrode. The operations may comprise receiving a selection of the second electrode from the user interface. The operations may comprise directing power from the battery at the level sufficient for ablation using the second electrode to the second electrode. The battery may be configured to store power at a level sufficient for ablation using the second electrode.

The housing may comprise a catheter connection port disposed along a surface of the housing. The connection port may be configured to interface with a catheter comprising a first electrode of a first length, and a second electrode of a second length different than the first length. The housing may envelop the battery, an electronic data store and the one or more computer systems. The electronic data store may comprise the plurality of stored patient profiles characterizing a plurality of patients.

The directing power from the battery to the second electrode may be performed by switching power directed from the battery from the first electrode to the second electrode. The directing power from the battery to the second electrode may direct an amount of power greater than an amount of power directed from the battery to the first electrode.

In some embodiments, a multi-pole synchronous pulmonary artery radiofrequency ablation catheter comprises a control handle, a catheter body and an annular ring. The control handle may comprise an adjustment apparatus. The catheter body may be hollow and comprising a cavity arranged in the catheter body. One end of the catheter body may be flexible. The flexible end may be connected to the annular ring. The other end of the catheter body may be connected to the control handle. One end of the pull wire may be connected to the flexible end, and the other end of the pull wire may be connected to the adjustment apparatus

on the control handle. The adjustment apparatus may adjust the tension of the pull wire to change a curvature of the flexible end. A shape memory wire may be arranged in the annular ring. One end of the shape memory wire may extend to an end of the annular ring and the other end of the shape memory wire may pass through a root of the annular ring and be fixed on the flexible end of the catheter body. The annular ring may be shaped with an oval comprising a major axis and a minor axis. The major axis may comprise a first diameter along the major axis longer than a second diameter along the minor axis. The annular ring, extending from the root of the annular ring to the end of the annular ring, may comprise a curve of less than 360 degrees. The annular ring may comprise an electrode that straddles the apex of the major axis.

In some embodiments, a catheter comprises a catheter body and an annular ring. One end of the catheter body may be flexible and connected to the annular ring. The annular ring may be oval shaped.

The annular ring may comprise a major axis and a minor axis, the major axis comprising a first diameter along the major axis longer than a second diameter along the minor axis. The first diameter may be 5 mm longer than the second diameter. The major axis may be along a first axis of symmetry and the minor axis may be along a second axis of symmetry. The annular ring may comprise an electrode that straddles the apex of the major axis. The annular ring may be orthogonal to the end of the catheter body that is flexible. The annular ring may be planar. The annular ring may comprise a curve of less than 360 degrees. The annular ring may comprise a curve of less than 360 degrees and greater than 270 degrees.

The annular ring may comprise an electrode group comprising a first electrode of a first length, a second electrode of a second length different than the first length, and a third electrode of a third length different than the first length and different than the second length. The electrodes of the electrode group may be substantially coplanar. The first length may be least 4 mm. The second length may be least 3 mm and may be less than the first length. The third length may be least 2 mm and may be less than the second length. The first length may be 4 mm. The first electrode may be separated from the second electrode and the third electrode by an equal distance.

In some embodiments, a method of performing pulmonary denervation may comprise positioning an ablation device in a pulmonary artery trunk of a live animal. The pulmonary artery trunk may include a distal portion of a main pulmonary artery, a proximal portion of a left pulmonary artery, and a proximal portion of a right pulmonary artery. The method may comprise deploying an annular ring from the ablation device. The annular ring may comprise a major axis and a minor axis. The major axis may comprise a first diameter along the major axis longer than a second diameter along the minor axis. The method may comprise ablating at least one of the distal portion of the main pulmonary artery, the proximal portion of the left pulmonary artery and the proximal portion of the right pulmonary artery.

In some embodiments, a controller may comprise a housing, an electronic display, an electronic data store, and a computing device. The housing may comprise a connection port disposed along a surface of the housing. The connection port may be configured to interface with a catheter comprising a first electrode of a first length, and a second electrode of a second length different than the first length. The electronic display may be disposed along the surface of the housing. The housing may envelop the electronic data store and the computing device. The electronic display may be configured to present a user interface. The electronic data store may comprise stored patient profiles characterizing a plurality of patients. The computing device may comprise one or more processors. The computing device may be in communication with the electronic data store and the electronic display. The computing device may be configured to at least receive a selection of a first patient profile of the stored patient profiles from the user interface, display information characterizing the first patient profile on the user interface, and direct power at a first power level sufficient for ablation using the first electrode to the first electrode. The first power level may be based on the first patient profile. The power may be directed from a power source. The power source may be a battery. The power source may be a wall socket connected to a power grid.

The catheter may comprise a second electrode of a second length different than the first length. The computing device may be configured to direct power at a second power level sufficient for ablation using the second electrode to the second electrode. The second power level may be based on the first patient profile. The second power level may be different than the first power level.

The housing may envelop the battery. The battery may be configured to store power at the first power level sufficient for ablation using the first electrode. The computing device may be in communication with the battery and configured to direct power from the battery at the first power level sufficient for ablation using the first electrode to the first electrode. The housing may comprise a power connection port configured to receive power at a level sufficient to charge the battery. The computing device may be configured to direct power from the battery to the first electrode after the battery has finished charging. The computing device may be configured to direct power to the first electrode before the battery has finished charging.

The catheter may comprise a first sensor connected with the first electrode. The computing device may be further configured to display on the user interface first electrode ablation information captured by the first sensor while the first electrode receives power from the battery. The computing device may be further configured to store the first electrode ablation information with the first patient profile. The first electrode ablation information may comprise a temperature. The catheter may comprise an annular ring shaped with an oval comprising a major axis and a minor axis. The major axis may comprise a first diameter along the major axis longer than a second diameter along the minor axis. The first electrode may straddle the apex of the major axis.

In some embodiments, a computer-implemented method may be under control of one more computing devices executing specific computer executable instructions. The method may comprise receiving a selection of a first patient profile, displaying information characterizing the first patient profile on a user interface, receiving a selection of the first patient profile from the user interface, determining, from the first patient profile, a first power level sufficient for ablation using a first electrode, and directing power at the first power level to the first electrode.

The first patient profile may be part of a plurality of stored patient profiles from the user interface presented on an electronic display disposed across a surface of a housing. The housing may comprise a catheter connection port dis-

posed along a surface of the housing. The connection port may be configured to interface with a catheter comprising the first electrode.

The housing may envelop an electronic data store and the one or more computing devices executing specific computer executable instructions. The electronic data store may comprise the plurality of stored patient profiles characterizing a plurality of patients.

The first electrode may be configured to convert the power to radiofrequency (RF) energy for ablation of sympathetic nerve fibers. The first electrode may be configured to convert the power to ultrasonic energy for ablation of sympathetic nerve fibers. The first electrode may be configured to convert the power to electroporation energy for ablation of sympathetic nerve fibers. The first electrode may be configured to convert the power to ionizing energy for ablation of sympathetic nerve fibers.

In some embodiments, a computer-readable, non-transitory storage medium storing computer executable instructions that, when executed by one or more computer systems, configure the one or more computer systems to perform operations comprising receiving a selection of a first patient profile of a plurality of stored patient profiles from a user interface presented on an electronic display disposed across a surface of a housing, displaying information characterizing the first patient profile on the user interface, receiving a selection of the first patient profile from the user interface, determining, from the first patient profile, a first power level sufficient for ablation using the first electrode, determining, from the first patient profile, a second power level sufficient for ablation using the second electrode, directing power at the first power level to the first electrode, and directing power at the second power level to the second electrode.

The housing may comprise a catheter connection port disposed along a surface of the housing. The connection port may be configured to interface with a catheter comprising a first electrode of a first length, and a second electrode of a second length different than the first length. The housing may envelop an electronic data store and the one or more computer systems. The electronic data store may comprise the plurality of stored patient profiles characterizing a plurality of patients. The directing power to the second electrode may direct an amount of power greater than an amount of power directed to the first electrode.

In some embodiments, a controller may comprise a housing, a user interface, an electronic data store, and a computing device including one or more processors, the computing device in communication with the electronic data store, and the user interface. The housing may comprise a connection port disposed along the surface of the housing, a user interface disposed along the surface of the housing. The housing may envelop the electronic data store and the computing device. The connection port may be configured to interface with a catheter comprising a first electrode of a first length, and a second electrode of a second length different than the first length. The computing device may be configured to at least receive a selection of the first electrode from the user interface, direct power at a first power level sufficient for ablation using the first electrode to the first electrode, receive a selection of the second electrode from the user interface, and direct power at a second power level sufficient for ablation using the second electrode to the second electrode.

The computing device may be configured to direct power to the first electrode and direct power to the second electrode at a same time. The computing device may be configured to direct power to the first electrode and direct power to the second electrode at different times. The computing device may be is configured to interrupt power directed to the first electrode and direct power to the second electrode after the power directed from the battery to the first electrode is interrupted.

The catheter may comprise an annular ring shaped with an oval comprising a major axis and a minor axis. The major axis may comprise a first diameter along the major axis longer than a second diameter along the minor axis. The first electrode may straddle the apex of the major axis.

The controller may comprise a battery configured to store power at the first power level sufficient for ablation using the first electrode or the second power level sufficient for ablation using the second electrode. The housing may envelop the battery. The computing device may be in communication with the battery and configured to direct power from the battery at the first power level sufficient for ablation using the first electrode, and direct power from the battery at the second power level sufficient for ablation using the second electrode. The housing may comprise a power connection port configured to receive power at a level sufficient to charge the battery. The computing device may be configured to direct power from the battery to the first electrode after the battery has finished charging. The computing device may be configured to direct power from the battery to the second electrode after the battery has finished charging.

The catheter may comprise a first sensor connected with the first electrode. The computing device may be further configured to display on the user interface first electrode ablation information captured by the first sensor while the computing device directs power to the first electrode. The catheter may comprise a first sensor connected with the first electrode and a second sensor connected with the second electrode. The computing device may be configured to display on the user interface first electrode ablation information captured by the first sensor while the computing device directs power to the first electrode and second electrode ablation information captured by the second sensor while the computing device directs power to the second electrode. The second electrode ablation information may be displayed on the user interface after the computing device stops directing power to the first electrode.

In some embodiments, a computer-implemented method may, under control of one more computing devices executing specific computer-executable instructions, comprise receiving a selection of a first electrode on a user interface disposed across a surface of a housing, directing power at a first power level sufficient for ablation using the first electrode to the first electrode, receiving a selection of the second electrode from the user interface, and switching from directing power to the first electrode to directing power at a second power level sufficient for ablation using the second electrode to the second electrode. The housing may comprise a connection port disposed along a surface of the housing, the connection port configured to interface with a catheter comprising the first electrode (which may be of a first length), and the second electrode (which may be of a second length different than the first length). The housing may envelop an electronic data store and the one or more computing devices executing specific computer-executable instructions.

The switching may be performed using a mechanical switch that comprises at least one moving part. The user interface may be a rotatable knob. The switching may be performed using a switching system comprising a mechani-

cal switch that comprises at least one moving part, and a solid state switch that comprises no moving parts.

In some embodiments, a computer-readable, non-transitory storage medium storing computer executable instructions that, when executed by one or more computer systems, may configure the one or more computer systems to perform operations. The operations may comprise receiving a selection of a first electrode from a user interface presented on an electronic display disposed across a surface of a housing, directing power at a first power level sufficient for ablation using the first electrode to the first electrode, receiving a selection of the second electrode from the user interface, and switching from directing power to the first electrode to directing power at a second power level sufficient for ablation using the second electrode to the second electrode. The housing may comprise a connection port disposed along the surface of the housing. The connection port may be configured to interface with a catheter comprising the first electrode (of a first length), and the second electrode (of a second length different than the first length). The housing may envelop an electronic data store and the one or more computer systems. The switching may be performed by controlling a solid state switch that comprises no moving parts.

In some embodiments, the ablation device or method described herein can be used to treat heart failure. In some embodiment, symptoms and signs of heart failure include pulmonary arterial hypertension (PAH), heart failure with preserved LVEF (HFpEF), heart failure with reduced LVEF (HFrEF), mean pulmonary arterial pressure (mPAP) of 20 mmHg or greater, pulmonary vascular resistance (PVR) of 3 Wood units (WU) or greater, rest pulmonary capillary wedge pressure (PCWP) of 15 mmHg or greater, exercise PCWP of 25 mmHg or greater, or pulmonary artery systolic pressure of 35 mmHg or greater.

In some embodiments, the catheter or method described herein can be used to treat pulmonary hypertension associated with left heart failure.

Also described herein is a method of reducing appearance or worsening of signs of heart failure, the method comprising: position an ablation device in a pulmonary artery trunk of a patient, the pulmonary artery trunk including a distal portion of a main pulmonary artery, a proximal portion of a left pulmonary artery, and a proximal portion of a right pulmonary artery, and ablating target tissue in the pulmonary artery trunk under conditions effective to affect an increase in one or more of 6-minute walk distance (6MWD) or cardiac output at least 6 months after the ablating, wherein the target tissue comprises at least one of the distal portion of the main pulmonary artery, the proximal portion of the left pulmonary artery, or the proximal portion of the right pulmonary artery with the ablation device.

Also described herein is a method of reducing appearance or worsening of signs of heart failure, the method comprising: position an ablation device in a pulmonary artery trunk of a patient, the pulmonary artery trunk including a distal portion of a main pulmonary artery, a proximal portion of a left pulmonary artery, and a proximal portion of a right pulmonary artery, and ablating target tissue in the pulmonary artery trunk under conditions effective to affect a reduction in mean pulmonary artery pressure and reduce systolic pulmonary artery pressure, wherein the target tissue comprises at least one of the distal portion of the main pulmonary artery, the proximal portion of the left pulmonary artery, or the proximal portion of the right pulmonary artery with the ablation device.

Also described herein is a method of treating a heart disease, the method comprising: position an ablation device in a pulmonary artery trunk of a patient, the pulmonary artery trunk including a distal portion of a main pulmonary artery, a proximal portion of a left pulmonary artery, and a proximal portion of a right pulmonary artery, and ablating target tissue in the pulmonary artery trunk under conditions effective to affect an increase one or more of 6-minute walk distance (6MWD) or cardiac output at least 6 months after the ablating,

wherein the target tissue comprises at least one of the distal portion of the main pulmonary artery, the proximal portion of the left pulmonary artery, or the proximal portion of the right pulmonary artery with the ablation device.

Also described herein is a method of treating a heart disease, the method comprising: position an ablation device in a pulmonary artery trunk of a patient, the pulmonary artery trunk including a distal portion of a main pulmonary artery, a proximal portion of a left pulmonary artery, and a proximal portion of a right pulmonary artery, and ablating target tissue in the pulmonary artery trunk under conditions effective to affect a reduction mean pulmonary artery pressure and a reduction systolic pulmonary artery pressure,

wherein the target tissue comprises at least one of the distal portion of the main pulmonary artery, the proximal portion of the left pulmonary artery, or the proximal portion of the right pulmonary artery with the ablation device.

BRIEF DESCRIPTION OF THE DRAWINGS

FIG. **1** is a schematic structural diagram of an embodiment of a catheter in accordance with an embodiment.

FIG. **2** is a partially enlarged view of Part B identified in FIG. **1**.

FIG. **3** is schematic sectional view taken along line A-A' of FIG. **1**.

FIG. **4** is a schematic structural view of an optional outer surface of an electrode that can be used with the catheter of FIG. **1**.

FIG. **5** is a front elevational and partial sectional view of a human heart.

FIG. **6** is a schematic sectional diagram of a pulmonary artery trunk including a distal portion of a main pulmonary artery and the proximal portions of the left and right pulmonary arteries.

FIGS. **7**A and **7**B are diagrams of the inner surfaces of two canine pulmonary arteries that have been dissected and laid flat.

FIG. **8** is a schematic diagram of segmentations of dissected pulmonary arteries including the distal portion of the main pulmonary artery and the proximal portions of the left and right pulmonary arteries.

FIGS. **9**A-**9**C are diagrams of three of the segmentations identified in FIG. **8**.

FIGS. **10**A-**10**D are enlargements of microscopy slides corresponding to the portions identified as S**1**-S**4** of level A1 of the right pulmonary artery of FIG. **9**A.

FIG. **11** is a photograph of microscopy of the portion identified as S**6** of level A9 of the main pulmonary artery of FIG. **9**C.

FIG. **12** is a posterior and perspective view of a model of the left pulmonary artery of FIGS. **7**A and **7**B.

FIG. **13** is an anterior view of the left pulmonary artery of FIG. **12**.

FIG. **14**A is a diagram identifying the location corresponding to microscopy of six different locations on level A9 of the main pulmonary artery of FIG. **8**.

FIG. **14**B is a table showing reductions in pulmonary artery pressure (PAP) resulting from the use of different ablation operating parameters.

FIG. **15**A is a perspective view of a catheter that can be used to perform pulmonary denervation.

FIG. **15**B is an enlarged end view of a distal end of the catheter of FIG. **15**A with indicia indicating positions of ten (10) RF electrodes.

FIG. **15**C is a perspective view of a controller that can be used for controlling the catheter of FIG. **15**A during an ablation procedure.

FIG. **15**D is a top plan view of the controller of FIG. **15**C.

FIG. **15**E is a perspective view of the controller connected to the catheter of FIG. **15**A.

FIG. **16**A is a fluoroscope image of a sheath device inserted into the main pulmonary artery for guiding the catheter of FIG. **15**A into the main pulmonary artery.

FIGS. **16**B-**16**C are additional fluoroscope images of the catheter of FIG. **15**A having been inserted and expanded within the left pulmonary artery of a human patient.

FIG. **16**D illustrates a position used for ablation and arterial denervation of the left pulmonary artery of the patient.

FIG. **16**E illustrates the catheter of FIG. **15**A being positioned within the main pulmonary artery of the patient in a position used for ablation.

FIGS. **16**F and **16**G illustrate the catheter of FIG. **15**A being positioned in the proximal right pulmonary artery and being pushed (FIG. **16**F) and pulled (FIG. **16**G) to determine if the catheter is properly seated for purposes of ablation.

FIG. **16**H is a fluoroscope image of the catheter of FIG. **15**A in a position for performing ablation in a proximal portion of the right pulmonary artery.

FIG. **17**A is a schematic diagram of the trunk of a pulmonary artery and identifies locations for ablation in a distal portion of a main pulmonary artery.

FIG. **17**B is a schematic diagram of a pulmonary artery trunk and identifies locations for ablation in proximal portions of the left and right pulmonary arteries.

FIG. **18**A is a schematic diagram of a pulmonary artery trunk identifying a position for ablation in a portion of the left pulmonary artery proximal to a pulmonary artery duct.

FIG. **18**B is a schematic diagram of points of ablation in the anterior wall of the ablation position identified in FIG. **18**A.

FIG. **19**A is a schematic diagram of a pulmonary artery trunk identifying a position for ablation in a proximal portion of the right pulmonary artery for treatment of unilateral chronic thrombotic embolism.

FIG. **19**B is an enlarged schematic diagram of the portion identified in FIG. **19**A and indicates positions for ablation in the anterior wall of the proximal portion of the right pulmonary artery.

FIG. **20** is a schematic diagram of a pulmonary artery trunk including a distal portion of a main pulmonary artery and the proximal portions of the left and right pulmonary arteries.

FIG. **21** is a schematic diagram of optional points of ablation along "Level C" identified in FIG. **20**, proximate to a transition between a left lateral wall of the main pulmonary artery and a lower wall of a proximate portion of the left pulmonary artery.

FIG. **22**A is an enlarged perspective view of a further embodiment of the catheter of FIGS. **1** and **15**A with indicia indicating positions of five (5) RF electrodes.

FIG. **22**B is an enlarged perspective view of a further embodiment of the catheter of FIG. **22**A with three (3) electrodes.

FIGS. **23**A-**23**C are angiographs illustrating parts of the PADN procedure.

FIG. **24**A is a chart illustrating the 6-minute walk distance (6MWD) at the 6-month follow-up minus the baseline 6MWD in the Medication treatment and the PADN procedure.

FIG. **24**B is a chart illustrating how the 6MWD after the PADN procedure is correlated with a Medication treatment.

FIG. **24**C is a chart illustrating how improvements in hemodynamic and cardiac functions were sustained through a one-year follow-up after the PADN procedure.

FIGS. **25**A-**25**H are various perspective views and user interface screenshots of a digital ablation controller.

FIG. **26** is a schematic diagram illustrating a mechanical switching system that may be implemented in the controller of FIGS. **25**A-**25**H or the controller of FIGS. **15**C-**15**D.

FIG. **27** is a schematic diagram illustrating a solid state switching system that may be implemented in the controller of FIGS. **25**A-**25**H or the controller of FIGS. **15**C-**15**D.

FIG. **28** is a diagram illustrating a generic switching system that may be implemented in the controller of FIGS. **25**A-**25**H or the controller of FIGS. **15**C-**15**D.

FIG. **29**A-FIG. **29**C are pulmonary arterial angiography images illustrating position of electrodes and pulmonary artery denervation (PADN) procedure.

FIG. **30**A-FIG. **30**D illustrate dynamic changes in mean pulmonary arterial pressure, pulmonary vessel resistance, 6-minute walk distance, and N-terminal pro-brain natriuretic peptide (NT pro-BNP). All variables improved significantly at the 6-month follow-up, without any additional significant change between the 6-month and the 1-year follow-up.

FIG. **31** is a Kaplan-Meier survival analysis at 1-year follow-up after PADN.

FIG. **32** illustrates a PADN study flowchart. **100** heart failure (HF) patients with pulmonary vessel resistance (PVR)>3.0 Wood Unit (WU) were screened, and 50 patients were randomly assigned to medication alone group and 48 patients were randomly divided to pulmonary artery denervation (PADN) group (2 patients who were excluded because of repeat randomization). SPAP, systolic pulmonary arterial pressure.

FIG. **33**A-FIG. **33**D illustrate the increase of 6MWD. At baseline, the 6-min walk (6MWD) in the pulmonary artery denervation (PADN) group and the Sildenafil group were not significantly different (FIG. **33**A). At 6 months, improvement in 6MWD was significantly higher in the PADN group (FIG. **33**C). FIG. **33**B and FIG. **33**D illustrate the change in 6MWD in individual patients in the PADN and sildenafil groups, respectively. Gray lines in boxes in FIG. **33**A and FIG. **33**C indicated the median value of 6MWD.

FIG. **34** illustrates the dynamic change of 6-minute walk distance (6MWD).

FIG. **35** is a Kaplan-Meier survival analysis. Survival rate free from clinical worsening between the sildenafil and pulmonary artery denervation (PADN) groups. The inset represents the rate of clinical worsening. CI=confidence interval.

FIG. **36**A-FIG. **36**F illustrate the correlation of pulmonary arterial compliance with pulmonary vessel resistance and 6-minute walk distance.

FIG. **37**A-FIG. **37**D illustrate predictions of 6-minute walk distance (6MWD for clinical events.

FIG. **38** illustrates changes of 6-Min Walk Distance Over the Time in Both Sildenafil and PADN Groups.

DETAILED DESCRIPTION OF THE PREFERRED EMBODIMENTS

The following examples further illustrate embodiments of the present inventions, but should not be considered as to limit the present inventions. Without departing from the spirit and essence of the present inventions, modification or replacement of the method, steps or conditions of the embodiments disclosed below still falls in the scope of the present inventions.

If not otherwise specified, the technical means used in the embodiments are conventional means well known by a person skilled in the art.

Example 1

Through the example below and with reference to FIGS. **1-3**, some of the technical solutions that can be achieved by various embodiments are further described below.

In some embodiments, a multi-pole synchronous pulmonary artery radiofrequency ablation catheter for de-sympathetic ablation in the pulmonary artery can include a catheter body **1** that has a distal end and a proximal end. The distal end can be provided with a flexible end **3** and the proximal end can be provided with a control handle **2**. A pull wire can extend in the catheter body.

Preferably, the catheter body can be made of a polymer material, which is a poor heat conductor, so that it can avoid transmitting or reducing the amount of heat transferred from the electrodes to the blood flow contacting the catheter body, and thereby can better prevent the electrode from heating the blood flow.

The flexible end **3** can include a proximal end and a distal end. An annular ring **4** can be arranged on the distal end. The flexible end **3** can be soft relative to the rest of the catheter body. The annular ring **4** can be provided with a plurality of electrodes **5**, wherein each electrode **5** can be configured to sense or extract neural electrical signals, sense temperature and conduct ablation. Each of the electrodes can be connected to lead wires and temperature sensing wires, which extend through the catheter body to the control handle, thus is electrically connected to the control handle. One or more temperature sensing wires can be embedded under each electrode for precise monitoring of the temperature during ablation. Additionally, in some embodiments, the temperature sensing wires can be connected to a thermocouple connected to an inner facing side of the electrodes **5**, or can include integrated thermocouples. Other configurations can also be used.

In accordance with several embodiments, ablation may be performed by the electrodes **5** using radiofrequency (RF) energy to ablate sympathetic nerve fibers to cause neuromodulation or disruption of sympathetic communication. In some embodiments, the electrodes **5** may use ultrasonic energy to ablate sympathetic nerve fibers. In some embodiments, the electrodes **5** use ultrasound (e.g., high-intensity focused ultrasound or low-intensity focused ultrasound) energy to selectively ablate sympathetic nerve fibers. In other embodiments, the electrodes **5** use electroporation to modulate sympathetic nerve fibers.

However, the electrodes **5**, as used herein, shall not be limited to causing ablation, but also include devices that facilitate the modulation of nerves (e.g., partial or reversible ablation, blocking without ablation, or stimulation). In some embodiments, the catheter may use agents offloaded at the location of the electrodes **5** to nerve fibers to modulate the nerve fibers (e.g., via chemoablation). Chemical agents used with chemoablation (or some other form of chemically-mediated neuromodulation) may, for example, include phenol, alcohol, or any other chemical agents that cause chemoablation of nerve fibers. In some embodiments, cryotherapy is used. For example, the catheter may use agents offloaded at the location of the electrodes **5** for cryoablation to selectively modulate (e.g., ablate) sympathetic nerve fibers. In other embodiments, the catheter may use brachytherapy to modulate the nerve fibers. The catheter may further utilize any combination of RF energy, microwave energy, ultrasonic energy, focused ultrasound (e.g., HIFU, LIFU) energy, ionizing energy (such as X-ray, proton beam, gamma rays, electron beams, and alpha rays), electroporation, drug delivery, chemoablation, cryoablation, brachytherapy, or any other modality to cause disruption or neuromodulation (e.g., ablation, denervation, stimulation) of autonomic (e.g., sympathetic or parasympathetic) nerve fibers.

In accordance with some embodiments, the neuromodulation system is used to modulate or disrupt sympathetic nerve fibers at one or more locations or target sites. For example, the catheter may perform ablation in a circumferential or radial pattern (such as by using the annular ring **4**), and/or the catheter may perform ablation at a plurality of points linearly spaced apart along a vessel length. In other embodiments, the catheter performs ablation at one or more locations in any other pattern capable of causing disruption in the communication pathway of sympathetic nerve fibers (e.g., spiral patterns, zig-zag patterns, multiple linear patterns, etc.). The pattern can be continuous or non-continuous (e.g., intermittent). The ablation may be targeted at certain portions of the circumference of the vessels (e.g., half or portions less than half of the circumference).

A shape memory wire can be arranged in the annular ring **4**, and a distal end of the shape memory wire can extend to the distal end of the annular ring **4**. The proximal end of the shape memory wire can be fixed to the distal end of the flexible end **3**. The shape memory wire in the annular ring **4** can preferably be made of various shape memory alloys such as nickel-titanium alloy, stainless steel or titanium, with a diameter in the range of 0.25-0.5 mm.

The diameter of the annular ring **4** is in the range of 12-40 mm. For example, the shape memory wire can be configured to bias the annular ring **4** to a desired diameter, such as in the range of 12-40 mm. Additionally, in some embodiments, the pull wire can be used to change or adjust the diameter of the annular ring **4** through a range of diameters including 12-40 mm or other ranges.

The length of the flexible end **3** can be in the range of 30-80 mm and can be made of medical polymer materials such as fluorine, polyesters, polyurethane, polyamide and polyimide. A counterbore can be arranged on the distal end of the flexible end **3**, the proximal end of the annular ring can be fixed in the counterbore, wherein the proximal end of the annular ring is a ground thin end.

A pull wire can be embedded in the catheter body, and one end of the pull wire can be fixed to the control handle. The curvature of the flexible end **3** can be controlled by operating the control handle. For example, one end of the pull wire can be fixed to a control button on the handle and the curvature of the flexible end **3** can be controlled by operating the button. This allows the operator to control the handle with

one hand and adjust the curvature of the flexible end **3** easily, so that the electrodes **5** on the annular ring **4** can be pressed into contract with the pulmonary artery and achieve acceptable ablation of pulmonary artery intima.

Furthermore, a counterbore can be made on the distal end of the flexible end **3**, and its depth can be set according to actual needs, preferably with a depth in the range of 2-8 mm. The proximal end of the annular ring **4** can be a ground thin end, and an outer diameter of the ground thin end fits an inner diameter of the counterbore. The ground-thin end can be inserted into the flexible end **3** and can be fixed to the distal end of the flexible end **3** by bonding, welding or other suitable means, preferably by UV-curing adhesive. Excess glue may be used to seal the distal end of the flexible end **3** and the proximal end of the annular ring **4**.

FIG. **1** shows a schematic structural diagram of the multi-pole synchronous pulmonary artery radiofrequency ablation catheter. The annular ring **4** can be arranged at the distal end of the flexible end **3**. The annular ring **4** can be an annular structure, and the radius of the annular ring **4** can be effected with shape memory wire.

The annular ring **4** can be provided with a plurality of electrodes **5**. Each electrode **5** can be configured to extract or detect neural electrical signals, sense the temperature and conduct ablation. The number of electrodes **5** can vary from the range of 3 to 30, preferably 5 to 20. The electrodes **5** are made of platinum-iridium alloy, gold, stainless steel or nickel alloy. The electrode diameter can be generally 1.3-2.0 mm, and the length of the electrode **5** can be generally in the range of 1.2-4 mm, more suitably 2-3.5 mm. Edge space between the adjacent electrodes suitably can be in the range of 0.5-10 mm, more suitably 1-5 mm.

The pull wire **8** can preferably be made of stainless steel or nickel-titanium. As shown in FIG. **2** and FIG. **3**, the distal end of the pull wire **8** extends through a hollow cavity **9** to the proximal end of the annular ring **4**, and can be fixed to the distal end of the flexible end **3**. The method used for fixing the pull wire **8** to the distal end of the flexible end **3** can be any known method in the prior art.

Optionally, a groove can be arranged on the distal end of the flexible end **3**, and a connector **11** can be arranged in the groove. One end of the connector **11** can be connected to the pull wire **8** and the other end of the connector **11** can be connected to the shape memory wire **12**. The connector **3** can be fixed to the distal end of the flexible end **3** by injecting glue such as UV-curing adhesive into the groove.

A segment of pull wire **8** extends in the flexible end **3** and a segment of pull wire **8** extends in the catheter body **1**. The pull wire can preferably be jacketed with a coil spring **13**, and the coil spring **13** can be jacketed with a spring sleeve **14**. The spring sleeve **14** may be made of any suitable material, preferably a polyimide material.

The proximal end of the pull wire **8** can be fixed on or in the control handle **2**, which can be provided with an adjustment apparatus, and the adjustment apparatus can be configured to adjust the curvature or the diameter of the annular ring **4**.

Lead wire **6**, as shown in FIG. **2** and FIG. **3**, extends through the lead wire cavity **10** to the lead wire cavity of the annular ring **4**. The distal end of the lead wire **6** can be connected to electrode **5**. The distal end of the lead wire **6** can be fixed to electrode **5** by welding. In some embodiments, the catheter includes one lead wire **6** for each of the electrodes **5**.

The distal end of the temperature sensing wire **7** can be embedded under the electrode **5** and the distal end of the temperature sensing wire **7** can be fixed on electrode **5** by bonding, welding or other suitable means. The temperature sensing wire **7** can extend into the catheter body **1** in the lead wire cavity **10** of the flexible end **3** and then extend out from the control handle **2** and can be connected to a temperature control device. In some embodiments, the catheter includes one temperature sensing wire **7** for each of the electrodes **5**.

When using the catheter, the pull wire **8** can be operated through the control handle **2** in order to deflect the flexible end **3**, thereby providing enhanced control for the user when positioning the annular ring **4** in a desired location, such as an orifice of the pulmonary artery. At this time, the electrodes **5** can be energized for performing ablation on pulmonary artery intima.

The multi-electrode design according to some embodiments can improve the efficacy and safety of ablation, and achieve signal analysis and preferably simultaneous ablation by a plurality of electrodes. This can also improve target accuracy, achieve timely judgment of ablation effect and save operation time. For example, with the annular ring **4** in a desired location, the electrodes can be individually activated to perform ablation at selected sites. This can be a benefit because in some methods of treatment described below, ablation can be performed at selected sites, less than the entire circumferential surface of certain anatomy.

Example 2

A multi-pole synchronous pulmonary artery radiofrequency ablation catheter comprises a control handle **2**, a catheter body **1**, and an annular ring **4**. The control handle **2** can be provided with an adjustment apparatus, the catheter body **1** can be hollow, and a cavity can be arranged in the catheter body **1**. One or more lead wires **6**, temperature sensing wires **7**, and a pull wire **8** can be arranged in cavity.

One end of catheter body can be flexible, and the flexible end **3** can be connected to the annular ring **4**. The other end of the catheter body can be connected to the control handle **2**. One end of the pull wire **8** can be connected to the flexible end **3**, and the other end of the pull wire **8** can be connected to the adjustment apparatus of the control handle, and the adjustment apparatus adjusts the tension of the pull wire **3** to control the curvature of the flexible end. This allows the operator to control the handle with one hand and adjust the curvature of the flexible end **3** easily. Thereby the electrodes **5** of the annular ring **4** can be pressed against to better contact an inner surface of a desired anatomy, such as a pulmonary artery, so as to enhance ablation of pulmonary artery intima.

A shape memory wire **12** can be arranged in the annular ring **4**. One end of the shape memory wire **12** can extend to the end of the annular ring **4**, and the other end of the shape memory wire **12** goes through the root of the annular ring **4** and can be fixed on the flexible end **3** of the catheter body.

The annular ring **4** can also be provided with an electrode group. Each electrode **5** can be connected to a lead wire **6** and a temperature sensing wire **7** and can be configured to extract or detect the nerve electrical signals, sense the temperature and conduct ablation. The lead wires **6** and temperature sensing wires **7** can extend through the catheter body **1** and can be electrically connected to the control handle **2**. The control handle **2** can be connected to an external temperature control device.

The annular ring electrodes **5** can be made of a material selected from a group consisting of platinum-iridium alloy, gold, stainless steel and nickel alloy material, with the number in the range of 3-30, a diameter in the range of

1.3-2.0 mm, a length in the range of 1.2-4 mm and an edge space between adjacent electrodes in the range of 0.5-10 mm.

The flexible end **3** of the catheter body can have a counterbore **32**. An outer diameter of the root of the annular ring **4** can fit an inner diameter of the counterbore **32**. The root of the annular ring **4** can be inserted into the counterbore **32** and fixed.

The flexible end **3** of the catheter body can be provided with a groove. A connector **11** can be arranged in the groove. One end of the connector can be connected to the pull wire **8** and the other end of the connector can be connected to the shape memory wire **12**.

The shape memory wire **12** can be made of shape memory alloy such as nickel-titanium alloy, stainless steel or titanium, with a diameter in the range of 0.25-0.5 mm. The diameter of the annular ring **4** can be in the range of 12-40 mm. Preferably, 10 electrodes are arranged on the annular ring, and the width of naked (exposed) side of electrodes can be 0.75 mm, and the space there between can be 5 mm.

The flexible end **3** of the catheter body can be made of medical polymer materials such as fluorine, polyesters, polyurethane, polyamide and polyimide, with a length in the range of 30 mm to 80 mm.

The connection can be via UV-curing adhesive. The joint between the flexible end of the catheter body and the annular ring can be sealed. The pull wire **8** can be made of stainless steel or nickel-titanium alloy. The pull wire **8** can be jacketed with a coil spring **13**, and the coil spring **13** can be jacketed with a spring sleeve **14** made of polyimide material.

Example 3

Example 3 is similar to Example 1 and Example 2, and the differences can include an infusion tube **22** arranged in the catheter body, a group of evenly distributed through holes **15** (FIG. **4**) arranged on one or more of the electrodes **5**, with a bore diameter of 1 m. One end of the infusion tube **22** can be connected to the electrodes **5** through the annular ring **4** such that fluid diffuses out from the through holes **15** on each of the electrodes **5**. For example, the annular ring **4** can include or define at least one lumen **24** extending between a proximal end of the annular ring **4** and to the through holes **15** so as to form a closed fluidic connection. In such embodiments, a distal end of the infusion tube **22** can be connected to the proximal end of the lumen **24** in the annular ring **4**. The other end of the infusion tube **22** can be connected to a transfusion system, such as a constant-flux pump or other known pumps.

When electrodes **5** generate current, the liquid automatically diffuses from the through holes **15**. The transfused liquid can be saline. The cold saline (4° C.) perfusion can help decrease local temperature. When the electrode generates current, the saline can automatically diffuse from the through holes **15**, and thus can allow the local temperature to be controlled to a desired temperature, such as to below 60° C. and thereby protect the vascular intima.

FIG. **5** is a schematic diagram of a human heart and surrounding vasculature, which can be an environment in which the catheter of FIGS. **1-4** can be used to perform ablation treatments such as, for example, but without limitation, denervation of the pulmonary artery. In some methods of treatment, access to the inner walls of the main pulmonary artery **502** as well as the left pulmonary artery **504** and right pulmonary artery **506** can be achieved by passing a catheter, using well known techniques, into a femoral vein, upwardly into the inferior vena cava **508** (lower left hand corner of FIG. **5**). The catheter can then be pushed upwards into the right atrium **510**, down into the right ventricle **512**, then up through the pulmonary semilunar valve **514** into the trunk of the main pulmonary artery **502**. As used herein, the term main pulmonary artery (MPA) **502** includes the proximal end of the main pulmonary artery which is the furthest upstream end of the main pulmonary artery **502**, at the pulmonary semilunar valve **514**, up to the bifurcation of the main pulmonary artery. The distal portion of the MPA **502** includes the portions of the MPA **502** near the bifurcation of the MPA **502** into the left and right pulmonary arteries (LPA **504**, RPA **506**).

Similarly, the proximal ends of the RPA **506** and LPA **504** are those ends of the LPA **504** and RPA **506** which are adjacent and connected to the distal end of the MPA **502**. The distal direction along the LPA **504** and RPA **506** would be the downstream direction of blood flow through the LPA **504** and RPA **506** toward the left and right lungs, respectively.

Thus, using well known techniques, a catheter can be used to provide access to the proximal and distal portions of the MPA **502** as well as the proximal and distal portions of the LPA **504** and RPA **506**.

FIG. **6** is a schematic diagram of the "trunk" of the pulmonary artery. As used herein, the "trunk" of the MPA **502** is intended to include at least the distal portion of the MPA **502** and the proximal portions of the LPA **504** and RPA **506**. FIG. **6** also includes a schematic representation of a carina **602** at the branch of the LPA **504** and RPA **506** from the MPA **502**.

As described below, an aspect of at least some of the inventions disclosed herein includes the realization that the trunk of the pulmonary artery of certain animals, including canine and humans, can include concentrated bundles of sympathetic nerves extending from the MPA **502** into the LPA **504** and RPA **506**. For example, it has been discovered that there are higher concentrations of sympathetic nerves on the anterior sides of the MPA **502** and in particular, in the vicinity of the distal portion of the MPA **502**. Additionally, it has been discovered that the sympathetic nerves bifurcate from this area of higher concentration into the anterior side of the proximal portions of the LPA **504** and RPA **506**. In the area of these proximal portions, it has also been discovered that higher concentrations of the sympathetic nerves extend upwardly and toward the posterior side of the LPA **504** and RPA **506**.

Thus, in accordance with some of the inventions disclosed herein, ablation is performed in the distal portion of the MPA **502** and the proximal portions of the LPA **504** and RPA **506**. In some embodiments ablation is preferentially performed on the anterior side of the inner walls of these structures. In some embodiments, ablation is performed preferentially on the anterior side of the proximal portion of the MPA **502** and on the anterior side and an upper portion of the proximal portions of the LPA **504** and RPA **506**, such as at approximately the upper conjunctive site of the distal portion of the MPA **502** at the LPA **504** and RPA **506**. As such, high success rates of sympathetic nerve denervation can be achieved as well as high success rates of reduction or elimination of the symptoms of pulmonary hypertension.

It is widely accepted that all vascular walls are regulated by sympathetical and parasympathetical nervous systems. Particularly, pulmonary vessels are known to be innervated by sensory nerve fibers. Previous studies have demonstrated that sympathetic noradrenergic innervation density along the pulmonary artery is highest at its proximal segments and then decreases toward the periphery, a typical finding that is different than arteries in other organs where highest inner-

vation density is found at the level of the smallest arterioles. However, the conclusions of the above-noted study were based on procedures in which the identification of innervation in the pulmonary artery was mainly based on the stimulation of sympathetical nerves or equivalent methods, without direct evidence or other location of sympathetical nerve fibers. However, it has been discovered that some of the conclusions of the above-noted study are incorrect, through the use of techniques for identifying the presence and location of sympathetical nerves in the pulmonary artery using direct labeling techniques.

In particular, experimental procedures were approved by the Institutional Animal Care and Use Committees of the Nanjing Medical University and were performed in accordance with the National Guide for the Care and Use of Laboratory Animals. Mongolia dogs (n=6, weight 7.8±1.2 kg) were obtained from the Nanjing Experimental Center (Nanjing, China). All animals were housed in a single room at 24° C. on a 12 h-light/12 h-dark cycle with fresh food and water.

In this study, a dog was anesthetized with sodium pentobarbital (60 mg per kg, intraperitoneal injection). The chest was excised and opened carefully. The whole pulmonary artery was removed from the chest, with particular attention to avoid the injury of adventitia. In one dog, the pulmonary artery was longitudinally cut along the blood flow direction from the orifice of the main pulmonary artery (the proximal portion of the main pulmonary artery) toward the right and left branches. Then, a vernier focusing camera was used to take pictures in order to identify whether there is a visible difference in the surface of the pulmonary artery between different segments.

With regard to five other dogs, connective tissue was manually dissected away from the pulmonary artery using fine microdissection scissors, under the guidance of stereomicroscope. During this procedure, great care was taken to avoid stripping off the adventitia and possible damage to the perivascular nerves. Vessels were stored at −70° C. for further staining.

Frozen vessels were processed in paraffin wax and fixed in 4% paraformaldehyde for 30 minutes and then incubated at 0.5% Pontamine Sky Blue (Sigma-Aldrich, St. Louis, MO) in phosphate-buffered saline (PBS) for 30 minutes to reduce background fluorescence. This was followed by 1 hour at room temperature in a blocking solution of 4% normal goat serum/0.3% Triton X-100 in PBS, then overnight at 4° C. in blocking solution containing an affinity-purified polyclonal antibody against tyrosine hydroxylase (Temecula, CA). Vessel segments were then washed in PBS and incubated for 1 hour with secondary antibody (Invitrogen, Carlsbad, CA), washed again and positioned on a glass slide. Preparations remained immersed in PBS during image acquisition to maintain hydration and preserve vessel morphology.

Based on previous studies, the sympathetical nerves were thought to be mainly localized at the proximal segment of the pulmonary artery. Thus the distal segment (5 mm in length) of the main pulmonary artery and proximal 5 mm segments of the right and left branches were selected for investigation in the present study. FIG. **6** schematically illustrates, not to scale, a 5 mm segment of the distal portion of the MPA and 5 mm long proximal portions of the LPA and RPA.

Multiple transverse slices (2 μm of thickness) of the vessels were cut at 1.6 mm intervals and are identified in the description set forth below in accordance with the labels of FIG. **8** (A**1**, A**2**, A**3**, A**4**, A**5**, A**6**, A**7**, A**8**, A**9**, A**10**, A**11**, A**12**). FIG. **14**A is a diagram identifying the location corresponding to microscopy of six different locations on level A9 of the main pulmonary artery of FIG. **8** showing a posterior section **1006**, adventitia **1003**, and media **1004**. Care was taken to keep the luminal morphology of slices consistent with the vessel contour, in order to precisely position the location of nerves. The slices were examined by a pathologist.

Images of each slice were recorded (magnification 40× to 200×) using stereomicroscope (Olympus), and the numbers of total sympathetical nerves bundles (SPNDs) per level were manually calculated. Then all images were input to Image Analysis Software (Image-proplus 5.0), to calculate the minor radius (μm), major radius (μm) and total surface area (TSA, $\mu m^2 \times 10^3$) area of axons.

After the pulmonary artery was removed from the chest of the dog, the pulmonary artery was repeatedly cleaned with saline to clean away all blood on the surface of the vessel. Then the whole vessel was cut along the direction from the proximal portion of the main pulmonary artery up through the trunk and into the right and left branches. The above-noted diagrams (FIGS. **7**A, **7**B) showed that in the anterior wall of the main pulmonary artery, there was an obvious ridgy cystica **702** close to the orifice of the left pulmonary artery. The site of the ridgy cystica **702** felt rigid to the touch, compared to other areas of the pulmonary artery.

In the vicinity of the bifurcation portion of the pulmonary artery, segments 5 mm in length of the distal main pulmonary artery and the proximal portions of the right and left pulmonary arteries were studied. Four transverse slices (thickness 2 μm, 1.6 mm intervals) from each segment were prepared for analysis. Each slice ("level") was divided into 4 subsegments in the right and left pulmonary arteries (S**1**, S**2**, S**3**, S**4** in FIGS. **9**A-**9**C)_and 6 subsegments in the main pulmonary artery along the counterclockwise direction (S**1**, S**2**, S**3**, S**4**, S**5**, S**6** in FIGS. **9**A-**9**C). FIG. **9**A further shows an anterior wall **1009** and a posterior wall **1010**. FIG. **9**B further shows a posterior wall **1008** and an anterior wall **1007**. FIG. **9**C further shows a posterior wall **1011** and a anterior wall **1012**. FIG. **10**A-**10**D are enlargements of microscopy slides corresponding to the portions identified as S**1**-S**4**, respectively, of level A1 of the right pulmonary artery of FIGS. **9**A-**9**C. FIGS. **10**A-**10**D show adventitia **1003**, media **1004**, and a lumen **1005**.

Upon inspection of these samples, it was observed that more SPNDs **1002** were identified in the posterior wall in both the left and right pulmonary arteries (FIG. **10**A). However, the number of SPNDs **1002** was 1.6±0.2 in the S1 subsegment of the A5 level in the left pulmonary artery branch, significantly different from 1.2±0.2 in the S1 subsegment of level A1 in the right pulmonary artery (p=0.033). In contrast, more SPNDs **1002** were labeled in the anterior wall (S6) of the main pulmonary artery (FIG. **11**) and decreased gradually from the levels A9 to A12.

The minor and major radii of sympathetical axons in the main pulmonary artery were 85±2 μm and 175±14 μm, compared to 65±3 μm and 105±12 μm in the left pulmonary artery or 51±2 μm and 86±8 μm in the right pulmonary artery, respectively, resulting in significant differences in surface area of axons between the main pulmonary artery and the LPA and RPA (FIGS. **9**A-**9**C).

Based on the results of the above-described observations, it has been determined that in canines, sympathetical nerves are distributed in higher concentrations along the anterior wall of the main pulmonary artery, then extend into the left and right pulmonary arteries, then extend upwardly and then

toward the posterior walls of the left and right pulmonary arteries, as schematically represented in FIG. **12** and FIG. **13**.

Further, inspection of subsegment S6 in level A9 (FIG. **11**) of the MPA (magnification 200×) revealed that a bundle or main bundle of sympathetical nerves originate from approximately the middle of the anterior wall of the distal portion of the main pulmonary artery and that this main bundle is bifurcated to the left and right pulmonary arteries.

This discovery provides a basis for more effective denervation of the pulmonary artery. For example, by selectively ablating only portions of the main pulmonary artery and the left and right pulmonary arteries, a higher success rate of denervation can be achieved with less unnecessary tissue damage. Such denervation can provide significant benefits in the treatment of diseases such as pulmonary hypertension, as described below.

With regard to the disease of pulmonary hypertension, it is well known that the lung receives axons from principal sympathetic neurons residing in the middle and inferior cervical and the first five thoracic ganglia (including the stellate ganglion), and the vasculature is the major sympathetic target in the lung. Sympathetic nerve stimulation increases pulmonary vascular resistance and decreases compliance, which is mediated by noradrenaline via a-adrenoreceptors, primarily of the al-subtype.

Previous studies have confirmed the multiplicity of transmitters released from one nerve ending which might explain why pharmacological blockade of the "classical" transmitter alone does not effectively abolish the effects elicited by nerve stimulation. The present study explained above supports the concept that more successful sympathetical denervation along the pulmonary trunk can be enhanced at the proximal segments of the left and right pulmonary arteries rather than at the distal basal trunks. Further, the percutaneous pulmonary denervation (PADN) procedure has potential for decreasing pulmonary pressure and resistance induced by unilateral balloon occlusion in the interlobar artery. However, until now, there was a lack of data showing the distribution of sympathetical nerves in the pulmonary trunk. Thus, the accurate identification of the position of sympathetical nerves is important for performing a successful PADN procedure. In the present study, significantly larger bundles of sympathetical nerves were identified in the mid-anterior wall of the distal portion of the main pulmonary artery, which is bifurcated into the posterior wall of the left and right pulmonary arteries. These results imply that one or more ablation procedures, for example, by the PADN procedure, especially around the distal portion of the main pulmonary bifurcation and the proximal portions of the LPA and RPA are more likely to provide enhanced results and more successful denervation, as was suggested in the animal study noted above.

It is noted that sympathetic noradrenergic innervation density is highest at the large extra-pulmonary and hilar blood vessels, both arteries and veins, and then decreases toward the periphery. This is in marked contrast to many other organs, in which the highest innervation density is found at the level of the smallest arterioles. Such distribution varies from species to species with regard to the extent to which the sympathetic noradrenergic axons reach into the lung. In guinea pigs, rabbits, sheep, cats, dogs, and humans, small arteries down to 50 μm in diameter are innervated, whereas in rats, mice, hedgehogs, and badgers, noradrenergic innervation stops close to the lung.

An extensive network of noradrenergic and NPY-containing fibers has been noted around pulmonary arteries of several species, but only a few studies used double-labeling techniques to evaluate the extent of colocalization. In the guinea pig, principally all noradrenergic fibers innervating pulmonary arteries and veins contain NPY and, in addition, dynorphin, a neuropeptide of the opioid family. In this aspect, pulmonary vascular innervation differs markedly from that of skin arteries in the same species, wherein three different combinations of noradrenaline, NPY, and dynorphin are used by sympathetic axons. Each of these populations is restricted to a specific segment of the arterial tree in the skin. Still, noradrenergic and NPY-containing fibers do not match 1:1 in the lung either, as there is a minor population of axons innervating guinea pig pulmonary arteries and veins that contains NPY plus vasoactive intestinal peptide (VIP) but not noradrenaline. It remains to be clarified whether this less-frequent fiber population represents the non-noradrenergic neurons projecting to the guinea pig lung or originates from other systems.

The present study explained above, which relied on the serial slicing at various levels through the pulmonary artery trunk, demonstrates that larger bundles of nerves are more localized in the anterior wall of the main pulmonary artery and then bifurcate into the left and right pulmonary arteries along the posterior walls of the LPA and RPA. The above study was performed on canine anatomy.

One of the diseases that can be treated with the present methods and devices is idiopathic pulmonary arterial hypertension (IPAH). IPAH is characterized by elevations of mean pulmonary artery pressure (PAP) and pulmonary vascular resistance (PVR). The pathogenesis of IPAH was believed to be due to imbalance between locally produced vasodilators and vasoconstrictors. Recent studies have demonstrated that vascular wall remodeling also contributed to elevated PVR. The role of neural reflex in the mediation and development of IPAH has not been specifically investigated. The present animal study described above demonstrates that the PADN procedure can reduce or completely abolish elevations of PAP induced by balloon occlusion at interlobar segments, but not at the basal trunk.

In a further phase of the present study, a human study was conducted. Prior to enrollment, all 21 patients received a diuretic (hydrochlorothiazide at a dose of 12.5 mg to 25 mg, once daily, and/or spironolactone at a dose of 20 mg to 40 mg, once daily) and beraprost (120 mg, 4 times daily) (Table 1), with either sildenafil (20 mg, 3 times a day) or bosentan (120 mg, twice daily) or digoxin (0.125 mg, once daily). Functional capacity of the patients was determined by a 6-minute walk test (6MWT), followed by an assessment of dyspnea using the Borg scale. The 6MWT was performed at 1 week, 1 month, 2 months, and 3 months following the PADN procedure. The WHO classification at rest and during exercise was recorded by a physician who was blinded to the study design.

Echocardiography was performed at 1 week, 1 month, 2 months, and 3 months following the procedure. Echocardiographic studies were done using a Vivid 7 ultrasound system with a standard imaging transducer (General Electric Co., Easton Turnpike, CT, US).

All of the echocardiograms were performed and interpreted in the Medical University Echocardiographic Laboratory. All of the measurements were performed following the recommendations of the American Society of Echocardiography. Digital echocardiographic data that contained a minimum of 3 consecutive beats (or 5 beats in cases of atrial fibrillation) were acquired and stored. RV systolic pressure is equal to systolic PAP in the absence of pulmonary stenosis. Systolic PAP is equal to the sum of right atrial (RA)

pressure and the RV to RA pressure gradient during systole. RA pressure was estimated based on the echocardiographic features of the inferior vena cava and assigned a standard value. The RV to RA pressure gradient was calculated as 4 v_t^2 using the modified Bernoulli equation, where v_t is the velocity of the tricuspid regurgitation jet in m/s. The mean PAP was estimated according to the velocity of the pulmonary regurgitation jet in m/s. The tricuspid excursion index (TEI) is defined as (A−B)/B, where A is the time interval between the end and the onset of tricuspid annular diastolic velocity, and B is the duration of tricuspid annular systolic velocity (or the RV ejection time). PA compliance for patients was calculated as stroke volume divided by pulse pressure (systolic PAP minus diastolic PAP).

Hemodynamic measurements and blood oxygen pressure/saturation determinations from the RA, RV, and PA were done prior to and immediately after the PADN procedure. These measurements were repeated at 24 hours and 3 months.

A 7F flow-directed Swan-Ganz catheter (131HF7, Baxter Healthcare Corp., Irvine, CA) was inserted into an internal jugular or subclavian vein. Measurements of resting RA pressure, RV pressure, systolic/diastolic/mean PAP, pulmonary artery occlusive pressure (PAOP), cardiac output (CO) (using thermodilution method), and mixed venous oxygen saturation were recorded. The PVR [=(mean PAP-PAOP)/CO] and trans-pulmonary gradient (TPG=mean PAP-PAOP) were then calculated. All of the measurements were recorded at the end of expiration. Five criteria were used to evaluate if a PAOP measurement was valid: (1) the PAOP was less than the diastolic PAP; (2) the tracing was comparable to the atrial pressure waveform; (3) the fluoroscopic image exhibited a stationary catheter following inflation; (4) free flow was present within the catheter (flush test); and (5) highly oxygenated blood (capillary) was obtained from the distal portion in the occlusion position. If the PAOP measurement was unreliable, the left ventricular end-diastolic pressure was then measured and used rather than the PAOP. The blood samples from the SVC and pulmonary artery were obtained for the measurements of oxygen pressure and saturation. Particularly significant reductions in systolic and mean PAP were achieved using temperatures above 50° C., drawing an electrical load of 8-10 W for a duration of 60-120 s, for example as shown in FIG. **14**B.

The PADN procedure was performed with a dedicated 7.5F multiple-function (temperature-sensor and ablation) catheter which comprised two parts, a catheter shaft **3** and handle **2** (FIG. **15**A) which is an embodiment of the catheter illustrated in FIGS. **1-4**. The catheter of FIG. **15**A had a tapered (to 5F) annular ring **4** with 10 pre-mounted electrodes **5** (E**1**-E**10**) each separated by 2 mm, however, other spacings can also be used. For purposes of the description set forth below, the electrodes **5** have been numbered, as shown in FIG. **15**B, with the distal-most electrode **5** identified as electrode E**1** and the proximal-most electrode **5** identified as electrode E**10**.

As described above with reference to FIGS. **1-4**, the annular ring **4** or ("circular tip") can be constructed so as to be biased into an annular/circular shape, such as the circular shape illustrated in FIG. **15**B and FIG. **1** to have any desired outer diameter. For example, in various embodiments, the annular ring **4** can be configured to be biased into a circular shape having an outer diameter of 20 mm, 25 mm, 30 mm, 35 mm, 40 mm, 45 mm, or other diameters. Additionally, a kit containing the catheter of FIG. **1** can include a plurality of different annular rings **4** configured to be biased to a plurality of different outer diameters, such as those noted above, or other diameters.

A controller or "connect box" can be connected to the handle **2** of the catheter for providing ablation energy. For example, an ablation controller **100** can be configured to provide ablation energy to each of the electrodes E**1**-E**10**. Thus, in some embodiments, the controller **100** includes a selector knob **102** configured to allow a user to select activation of all the electrodes E**1**-E**10**, or selective actuation of individual ones of the electrodes E**1**-E**10**, one at a time.

Thus, in some embodiments, as illustrated in FIG. **15**D, the selector knob **102** includes a position indicator **104** which, by rotating the knob **102** can be aligned with indicia corresponding to the electrodes E**1**-E**10**. In the illustrated embodiment, the indicia on the controller **100** includes the numbers 1-10 as well as a position identified as "OFF" and a position identified as "NULL." In some embodiments, the connect cable **106** can include a plurality of wires, for example, ten wires which correspond to the lead wire **6** described above with reference to FIGS. **1-4**, each one of which is individually connected to respective electrodes E**1**-E**10**.

The controller **100** can include a physical switch for creating an electrical connection between a source of RF energy and a desired one of the electrodes E**1**-E**10**. An electrode can be directly connected to the knob **102** with additional contacts disposed around the electrode at approximately the positions identified as 1 through 10 on the controller **100**. Thus, rotation of the knob **102** will connect an internal electrode with the contacts aligned with each one of the positions **1-10**.

The controller **100** can be configured to provide the desired amount of ablation energy when a circuit is created by the alignment of the position indicator **104** with the corresponding position (1 through 10) on the controller **100** thereby delivering electrical energy to the selected one of the electrodes E**1**-E**10** causing electrical energy to pass through the selected electrode **5** into any conductive material in contact with that selected electrode.

For example, during the PADN procedure, the electrodes E**1**-E**10** can be in contact with an inner wall of the pulmonary artery trunk thereby allowing electrical energy from one of the electrodes E**1**-E**10** to flow through the tissue of the inner wall of the pulmonary artery, described in greater detail below.

In some embodiments, with continued reference to FIG. **15**D, the controller **100** can include a plurality of ports. For example, the controller **100** can include a catheter port **120**, which can be configured for creating a fluidic connection to the annular ring for purposes of providing a flow of saline to the annular ring **4**. The controller **100** can also include an RF port **122** configured to connect to any known radiofrequency generator used with regard to ablation procedures.

Additionally, the controller **100** can include an "ECG" port **124** configured for connection with standard ECG monitoring equipment. Thus, in some embodiments, the connect cable **106** can also include wires or conduits for transmitting data through the RF port **124**.

Thus, in some configurations, the RF port **122** can be connected to a source of RF energy (not shown). One or more wires (not shown) can connect the port **122** to a contact on the end of an electrode connected to the selector knob **102**. Additionally, the ten wires (not shown) can be configured to deliver RF electrical energy to the electrodes E**1**-E**10** each of which can be connected to contacts (not shown)

associated with the selector positions **1**-**10** disposed around the periphery of the selector knob **102**.

Thus, the electrode connected to the rotating selector knob **102** can be moved into contact with the electrical contacts associated with each of the positions **1**-**10** thereby creating a circuit connecting the electrical energy entering the controller **100** through the port **122** with the associated lead wire **6** for conducting electrical energy to the desired electrode E**1**-E**10**.

Thus, specifically, when the selector knob **102** is turned such that the position indicator **104** is aligned with position **1** on the controller **100**, electrical energy from the RF port **122** is conducted through an associated lead wire **6** to the electrode E**1**. Aligning the indicator **104** with the other positions on the controller **100** would conduct electrical energy to the other electrodes associated with those other positions.

In some embodiments, a method for treating pulmonary hypertension can include a step of identifying the position of the pulmonary trunk of the patient using angiography. For example, baseline pulmonary artery angiography can be performed to identify the position of the pulmonary artery bifurcation from the main pulmonary artery into the left and right pulmonary arteries.

Additionally, the baseline pulmonary artery angiography can be used to determine the diameter of the portions of the pulmonary artery trunk upon which ablation is desired. As such, the appropriate diameter of the annular ring **4** can be determined based on the determined diameters of the pulmonary artery trunk noted above. For example, in some embodiments, an annular ring **4** having a biased diameter slightly larger than the diameters of the targeted anatomy can be used so as to enhance the contact between the electrodes **5** and the inner surface of the targeted anatomy. As such, for example, when the annular ring **4** is moved out of a sheath **1602** and allowed to expand into its biased circumferential configuration which has an outer diameter slightly larger than the inner diameter of the targeted portions of the pulmonary artery trunk, the bias of the annular ring **4** will assist in pressing the electrodes **5** into contact with the targeted tissue.

In some embodiments, with reference to FIGS. **16**A-**16**H, a method can include a step of positioning a catheter in a pulmonary artery trunk. For example, the sheath **1602** can be inserted through the femoral vein and advanced to the main pulmonary artery, as shown in FIG. **16**A. A catheter, such as the catheter illustrated in FIG. **1** and FIGS. **15**A-**15**E can be advanced along the sheath **1602** shown in FIG. **16**A to the location of the pulmonary artery trunk.

With the distal end of the catheter maintained in place, the sheath **1602** can be withdrawn. It may be necessary to push on the catheter to maintain its position with the portion of the catheter forming the annular ring **4** held within the pulmonary artery trunk.

As the annular ring **4** is released from the sheath **1602**, as illustrated in FIG. **16**B, the annular ring **4** can adopt the shape and diameter to which it is biased.

By slightly rotating and pushing the handle **2** in a clockwise direction, the annular ring **4** can be positioned at the proximal portion of the left pulmonary artery, such as at the ostium. In some embodiments, this initial position can be within a range of approximately 5 mm from the orifice of the left pulmonary artery or within a range of 2 mm, as illustrated in FIG. **16**D.

By observing the orientation of the annular ring **4**, the desired one or plurality of the electrodes E**1**-E**10** can be selectively energized so as to perform ablation at the desired location on the interior surface of the left pulmonary artery. For example, in some embodiments, it may be more effective to selectively ablate the posterior wall of the left pulmonary artery, so as to achieve at least some sympathetic denervation of the left pulmonary artery and the proximal portion thereof, such as within 2 mm or 5 mm of the ostium of the left pulmonary artery.

The annular ring **4** can then be rotated, such as in the counterclockwise direction, by rotating and withdrawing the handle **2** in order to reposition the annular ring **4** into the distal portion of the main pulmonary artery such as at the bifurcation area. For example, in some embodiments, as illustrated in FIG. **16**E, the annular ring **4** can be positioned within about 5 mm of the bifurcation in the pulmonary artery trunk. Ablation can then be performed using the desired one or plurality of the electrodes E**1**-E**10**.

For example, positioned as such, the selected one or plurality of electrodes E**1**-E**10** can be energized to achieve the desired sympathetic denervation of the distal portion of the main pulmonary artery. In some embodiments, it may be desirable to perform ablation preferentially on the anterior wall of the distal portion of the main pulmonary artery.

Additionally, further rotating and pushing the handle **2** can be performed until the annular ring **4** is positioned in the proximal portion of the right pulmonary artery, such as at the ostium. In some embodiments, this position can be within 5 mm of the ostium of the right pulmonary artery. Further, in some embodiments, this position can be within 2 mm of the ostium of the right pulmonary artery.

With the annular ring **4** positioned as such, the desired one or plurality of electrodes E**1**-E**10** can be energized so as to achieve at least some sympathetic denervation in the proximal portion of the right pulmonary artery. For example, in some embodiments, it may be beneficial to focus on the posterior wall of the right pulmonary artery.

In some embodiments, a method for treating pulmonary hypertension can also include a step of confirming the appropriate contact between the electrodes E**1**-E**10** and the endovascular surface corresponding to the three positions noted above. For example, in some embodiments, such confirmation can be performed by determining if there is strong manual resistance when attempting to rotate the handle **2**. Additionally, it can be determined if the annular ring **4** cannot be advanced distally, resulting in the deformation of the catheter as illustrated in FIG. **16**G or if there is ease in withdrawing proximally, resulting in the deformation of the catheter illustrated in FIG. **16**H. Additionally, confirmation can be performed using angiographic confirmation.

After the annular ring **4** is positioned as desired, such as in the positions illustrated in FIG. **16**D, FIG. **16**E and FIG. **16**F, at least one of the electrodes E**1**-E**10** can be energized so as to perform ablation. For example, in some embodiments, a method for treating pulmonary hypertension can include the sequential energization of each of the electrodes E**1**-E**10**.

Additionally, in some embodiments, a method for treating pulmonary hypertension or for performing pulmonary denervation can include the step of repositioning the annular ring **4** so as to shift the location of the electrodes E**1**-E**10** and then repeating energization of all of the electrodes E**1**-E**10**. As such, a more complete denervation of the entire inner surface of the associated vessel can be achieved.

In some embodiments, any desired energy levels or temperatures can be used for performing ablation using the electrodes E**1**-E**10** noted above. For example, in some embodiments, ablation can be performed at temperatures

above 50° C., drawing an electrical load of 8-10 W for a duration of 60-120 s. Additionally, in some embodiments, the method of treatment of pulmonary hypertension or the method of sympathetic denervation of the pulmonary artery can be performed with a patient anesthetized but conscious. Thus, any ablation procedure can be stopped if the patient complained of intolerable chest pain.

In some embodiments, EKG and hemodynamic pressure can be monitored and continuously recorded throughout the method. In a study performed in accordance with the description noted above, success was defined as a reduction in the mean PAP>10 mmHg (as measured by the Swan-Ganz catheter). During the study, there were no complications. Additionally, the patients were monitored in the Coronary Care Unit (CCU) for at least 24 hours after the PADN procedure was performed.

For example, in some embodiments of methods disclosed herein, a dedicated 7.5 F triple-function catheter (A) can be used, which can include a tapered annular ring **4** with 10 electrodes **5** (each has 0.75 mm electrode-width and is separated by 2 mm, pre-mounted. Electrodes are connected with a connect-cable **106** and a connect-box/controller **100**. There are 10 positions of the knob **102** (FIG. **15**D) on the surface of controller **100**, and each is associated with one of the electrodes E**1**-E**10** on the annular ring **4** of the ablation catheter. Sequential ablation can be performed by turning the knob **102** as desired after the whole system is set up. In certain embodiments, ablation is interrupted while switching ablation from one electrode to another.

In some embodiments of methods for performing pulmonary artery denervation or methods for treating primary PAH ablation of the distal portion of the main pulmonary artery can be performed preferentially on the anterior side thereof. For example, in some embodiments, as shown in FIG. **17**A, ablation can be performed at the positions identified as M**1**, M**2**, M**3**, M**4**, and M**5**.

With a continued reference to FIG. **17**A, the position identified as M**1** is at the "6 o'clock" position in the distal portion of the main pulmonary artery. The positions identified as M**3** and M**5** are the sites where the anterior wall of the main pulmonary artery connects to the left and right pulmonary arteries, respectively. The positions identified as M**2** and M**4** correspond to the "5 o'clock" and the "7 o'clock" positions on the anterior side of the distal portion of the main pulmonary artery.

In some embodiments, with reference to FIG. **17**B, sympathetic denervation in the left and right pulmonary arteries can be performed, preferentially, at approximately the middle of the anterior wall of the proximal portion of the left pulmonary artery (L**1**) and at approximately the upper conjunctive site of the distal portion of the main pulmonary artery in the left pulmonary artery (L**2**).

Similarly, during a method of performing pulmonary denervation of the right pulmonary artery, ablation can be preferentially performed at a point approximately at the middle anterior wall of the proximal portion of the right pulmonary artery (L**3**) and at approximately the upper conjunctive site of the distal portion of the main pulmonary artery and the right pulmonary artery (L**4**).

In some embodiments, sympathetic denervation can be performed, for example, for treatment of pulmonary hypertension associated with a pulmonary duct artery (PDA) **1802**. For example, a pulmonary duct artery usually connects the descending aorta with the left pulmonary artery **504**, as shown in FIG. **5**. With this anatomy, the left pulmonary artery can be significantly larger than the right pulmonary artery.

Thus, in some embodiments, ablation can be performed at a position proximal to connection between the left pulmonary artery and the pulmonary duct artery, identified by line **18**A-**18**A in FIG. **18**A and referred to as "Level A". Thus, using the technique described above with reference to FIGS. **16**A-**16**H, the annular ring **4** can be positioned at a position corresponding to "Level A" of FIG. **18**B. Ablation can then be performed around part or all of the interior wall of the left pulmonary artery at that location.

In some embodiments, ablation can be preferentially performed on the anterior wall of the left pulmonary artery proximal to the proximal end of the pulmonary duct artery. For example, ablation can be performed at four or more sites, such as those identified as sites L**11**, L**12**, L**13**, L**14**. As illustrated in FIG. **18**B, which shows an anterior wall **1007** and a posterior wall **1008**, position L**11** corresponds to "12 o'clock", position L**12** corresponds to "2 o'clock", position L**13** corresponds to "3 o'clock", and position L**14** corresponds to "6 o'clock." Other positions can also be used.

Additionally, in some embodiments, ablation can also be performed at positions M**1**-M**5** illustrated in FIG. **17**A and positions L**1**-L**4** of FIG. **17**B.

In some embodiments, a method for sympathetic denervation can be used for treating pulmonary hypertension resulting from unilateral chronic thrombotic embolism. For example, a patient suffering from unilateral CTEH can have an occluded right pulmonary artery. For example, in some patients, the RPA can be significantly enlarged as illustrated on the left side of FIG. **19**A. Similar to the method described above with reference to FIG. **18**B, ablation can be performed at the position identified by line **19**A-**19**A in FIG. **19**A and referred to as "Level B". Ablation can be performed at one or a plurality of locations along the inner surface of the right pulmonary artery at the position of Level B, or other positions. Additionally, ablation can be preferentially performed on a plurality of points along the anterior wall of the right pulmonary artery at the position of Level B.

For example, the positions identified in FIG. **19**B can be considered such as position L**21** corresponding to "12 o'clock", position L**22** corresponding to "2 o'clock", position L**23** corresponding to "3 o'clock", and position L**24** corresponding to "6 o'clock." Additionally, in some embodiments, ablation can also be performed at positions M**1**-M**5** illustrated in FIG. **17**A and positions L**1** and L**2** illustrated in FIG. **17**B.

With reference to FIG. **20**, further embodiments of treatments for pulmonary hypertension can include selected ablation of portions of the pulmonary artery trunk, at fewer ablation sites than some of the embodiments described above. For example, FIG. **20** identifies "Level C", indicated as **20**C, for reference with regard to the ablation sites identified in FIG. **21**.

With reference to FIG. **21**, an enlarged schematic diagram of "Level C" identified in FIG. **20** identifies a plurality of that ablation sites, b_1, b_2, b_3 which are grouped in a portion of the pulmonary artery trunk proximal to a left side lateral wall at the upper end of the main pulmonary artery and proximal to a lower wall of the proximal portion of the left pulmonary artery, where those portions meet. For example, as illustrated in FIG. **21**, the ablation site b_1 is disposed at approximately a left lateral apex of the distal end of the main pulmonary artery, which connects with a lower wall of the proximal end of the left pulmonary artery.

Additionally, the ablation sites b_2, b_3 are disposed, along or substantially along the "Level C" identified in FIG. **20**, on the anterior and posterior sides, respectively, of the ablation site b_1. These ablation sites b_1, b_2, and b_3 may be targeted to

ablate a particular bundled cluster of sympathetical nerves on the left lateral side of the distal end of the main pulmonary artery. These bundled clusters may be approximately 5 mm above the pulmonary valve **514** (FIG. **5**) but under the carina **602** (FIG. **6**).

FIG. **22**A illustrates a further embodiment of the annular ring **4** illustrated and described above with reference to FIG. **1** and FIG. **15**B. The embodiment of the annular ring **4** illustrated in FIG. **22**A is identified with the reference **204**. The annular ring **204** illustrated in FIG. **22**A can be constructed in accordance with the description set forth above with regard to the annular ring **4** and can be used with the handheld device **1** (FIG. **1**), except with regard to the differences described below.

As shown in FIG. **22**A, the annular ring **204** can have a fewer number of electrodes than that included in the annular ring **4** described above. In the illustrated embodiment, the annular ring **204** includes five electrodes, **200**, **205**, **206**, **208**, **210**. Additionally, the annular ring **204** is provided with and configured to conform to (or be biased to) an oval shape, when in its deployed/relaxed state. In its deployed/relaxed state, the annular ring **204** may be substantially planar. Also, in its deployed/relaxed state, the annular ring **204** may be substantially orthogonal, and optionally perpendicular, to a portion of the flexible end **3** of the catheter body connected with the annular ring **204**. As illustrated in FIG. **22**A, in its deployed state, the annular ring **204** can have a diameter D_1 along its major axis. The diameter D_1 is larger than the second diameter D_2 along the minor axis of the annular ring **204**. Such a configuration provides the angular ring **204** with an oval shape, when in its deployed state. The electrodes **200**, **205**, **206**, **208**, **210** of the annular ring **204** can be sized in space with the dimensions identified in FIG. **22**A, or other dimensions. Also, in certain embodiments, the annular ring **204** may be elliptical and optionally substantially planar. Optionally, such an elliptical ring can be less than a complete loop. For example, the distal end of the annular ring **204** may not curve 360 degrees back to the proximal end of the annular ring but may curve around by an angle of less than 360 degrees (for example by curving at an angle of 270 degrees to 359 degrees). In certain embodiments, the proximal end of the annular ring may be separated by a distance of 3 mm as illustrated in FIG. **22**A due to not curving 360 degrees back to the proximal end of the annular ring **204**.

With continued reference to FIG. **22**A, the electrodes **206**, **205**, **208** can be arranged and sized to provide for selective ablation of a pulmonary artery corresponding to the ablation sites b_1, b_2, b_3 described above with reference to FIG. **21**. Further, the electrodes **206**, **205**, **208** can have different sizes. In some embodiments, the electrode **206**, configured and sized to accommodate denervation of the site b_1 can be larger than the electrodes **205**, **208**. Further, in some embodiments, the electrode **205** can be larger than the electrode **208**. For example, the electrode **206** for ablation at b_1 may be 4 mm long while the electrode **205** for ablation at b_2 may be 3 mm long and the electrode **208** for ablation at b_3 may be 2 mm long. Other arrangements, configurations, and sizes can also be used. The electrode **206**, for ablation at b_1, may be located at an end of diameter D_1 and/or straddle an apex of the major axis of annular ring **204**.

With continued reference to FIG. **22**A, the annular ring **204** can be constructed with several sizes. For example, FIG. **22**A includes examples of diameters D_1, D_2 that can be used for five different sizes of the annular ring **204**. The diameters D_1, D_2 for those five different sizes can be combined in the following listed pairs of diameters (in millimeters), which are listed in the format (D_1, D_2): (25, 20), (30, 25), (35, 30), (40, 35), and (50, 45). Thus, in some embodiments, the diameter D_1 is 5 mm larger than the diameter D_2. Other sizes and proportions can also be used.

It has been noted that in at least some patients, the sympathetic enervation of the pulmonary arteries (PAs) is concentrated mostly about the left proximal PA. There can be relatively less sympathetic enervation of the right PA. The vagus nerve can travel deep (from the PA perspective) to the sympathetic nerves.

In some embodiments, as noted above, effective reduction of PA hypertension (PAH) can be achieved by ablating at 3 sites in the left side only, such as approximately at the locations b_1, b_2, b_3 identified above with reference to FIG. **21**. Additional ablations can be omitted. Thus, in some embodiments, ablations can be carried out at or in the vicinity of the ablations locations b_1, b_2, b_3 and further ablations be avoided or omitted.

FIG. **22**B illustrates a further embodiment of the annular ring **204** illustrated and described above with reference to FIG. **22**A. The embodiment of the annular ring **204** illustrated in FIG. **22**B is identified with the reference **220**.

As illustrated in FIG. **22**B, in its deployed state, the annular ring **220** can have a diameter D_3 along its major axis. The diameter D_3 is larger than the second diameter D_4 along the minor axis of the annular ring **220**. Such a configuration provides the angular ring **220** with an oval shape, when in its deployed state. For example, FIG. **22**B includes examples of diameters D_3, D_4 that can be used for five different sizes of the annular ring **220**. The diameters D_3, D_4 for those five different sizes can be combined in the following listed pairs of diameters (in millimeters), which are listed in the format (D_3, D_4): (25, 20), (30, 25), (35, 30), (40, 35), and (50, 45). Thus, in some embodiments, the diameter D_3 is 5 mm larger than the diameter D_4. Other sizes and proportions can also be used.

The annular ring **220** may be configured for the ablation of three sites with electrodes **206**, **205**, and **208** at approximately at the locations b_1, b_2, b_3 identified above with reference to FIG. **21** and FIG. **22**A. The electrode **206**, for ablation at b_1, may be located at an end of diameter D_3 and/or straddle an apex of the major axis of annular ring **220**. The electrodes **208**, **206**, and **205** of the annular ring **220** can be sized in space with the dimensions identified in FIG. **22**A, or other dimensions.

In some embodiments, the tissue temperature is raised to 50° C., (range 48°-52°), for example, by applying RF energy to each of the 3 sites b_1, b_2, b_3 for 2 minutes each. As noted above, optionally, additional ablations can be omitted.

The generator can be configured to, and can be operated to, deliver 3-15 watts of RF energy. In some embodiments, it has been observed that an immediate decrease in PA blood pressure of at least about 10% can be achieved by ablating the three sites b_1, b_2, b_3 as described above. Such a physiological change can serve as immediate feedback and can be used to further guide treatment.

In some animals, visualization of the sympathetic nerves shows thinning of the axons following RF ablation. In humans with PAH and in animals (treated with MCHT to produce PAH experimentally), there is evidence of vascular remodeling 3 months post treatment, with some resolution of HTN induced wall thickening. For some patients, 1-2 years after treatment, the initial improvement in PAH note above persists for those intervals following treatment.

The efficacy of the PADN procedure versus standard pharmacotherapy for the treatment of PAH with different etiologies was investigated in an additional study. In the additional study, 28 patients with PAH were assigned to

standard medication and the PADN procedure sequentially. The PADN procedure was associated with significant improvements in 6-minute walk distance (6MWD) and hemodynamics six months following the PADN procedure. Also, the PADN procedure had less frequent PAH-related events after 6- to 12-month following the PADN procedure.

The additional study included a total of 28 patients (11 males and 17 females, with an average age of 49 years). As described in Table, 1, there were 8 patients with IPAH, 9 with PH from LHD, 4 with connective tissue disease, 3 with chronic thrombolitic PH and 4 with congenital heart disease after surgical repairing. The mean time interval from the diagnosis of PAH/PH to the present study was 4.24 years. During wash-out period, there was 1 patient with LHD having the worsening of symptom needed diuretic treatment.

TABLE 1

Baseline characteristics

Variables	Results
Patient number, n	28
Male, n (%)	11 (39.3)
Age, yr	49 ± 17
Etiology, n (%)	
IPAH	11 (39.3)
LHD	8 (28.6)
CTD	2 (7.1)
CTEPH	3 (10.7)
CHDSR	4 (14.3)
Time from diagnosis to enrolling, yr	4.24 ± 7.13
Presentation, n (%)	
Chest pain	8 (28.6)
Syncope	4 (14.3)
Fatigue	27 (96.4)
Dyspnea	27 (96.4)
Medication at screening, n (%)	
Diuretics	23 (82.1)
Calcium-channel antagonist	4 (14.3)
Beta-blocker	8 (28.6)
Prostacyclin	23 (82.1)
5'-PDE	10 (35.7)
ET receptor antagonist	5 (17.9)
Digoxin	13 (46.4)

IPAH, idiopathic pulmonary hypertension;
LHD, left heart disease;
CTD, connective tissue disease;
CTEPH, chronic thrombolytic pulmonary hypertension;
CHDSR, congenital heart disease after surgical repair;
5'-PDE, phosphodiesterase type 5 inhibitor

CTD, connective tissue disease;
CTEPH, chronic thrombolytic pulmonary hypertension;
CHDSR, congenital heart disease after surgical repair;
5'-PDE, phosphodiesterase type 5 inhibitor

Patients with a resting mean PAP (mPAP)>25 mmHg with WHO functional class II-IV PAH were included in the additional study. Particularly, for the patients with pulmonary hypertension (PH) secondary from left heart disease (LHD), additional requirements included a pulmonary vessel resistance (PVR)>2.5 woods unit and a pulmonary arterial obstructive pressure (PAOP)>15 mmHg at rest. None of the patients had active inflammation or cancer. Also, none of the patients had PH secondary from portable hypertension and drug or toxin exposure. The study protocol was approved by the Institute Research Board (Nanjing Medical University).

A wash-out consisting of 5 half-lives was performed for all the patients. All the patients who met the above inclusion and exclusion criteria were included and entered into the first wash-out period (defined as stopping all medications for at least 5 half-lives, with the exception of warfarin) as right heart catheterization and adenosine test for all patients were not performed before study. Warfarin was continuously prescribed. Otherwise, aspirin (100 mg/d) and Plavix (75 mg/d) were prescribed instead of warfarin for the patients who were intolerable to warfarin. Immediately after the PADN procedure, the standard medication for PAH were stopped for all the patients.

If the patients were taking multiple drugs, the longest half-lives of any drug was selected. For example, for a patient who was taking bosentan (half-time<5 h) and digoxin (half-time=33 h), then the wash-out period would be 5×33 h=165 h (7 days). After the wash-out period, the drugs were prescribed again and continued for 6 months (Medication treatment). The selection of drugs was left to the physician's discretion based on comprehensive analysis. After 6 months, the patients underwent a second wash-out period of 5 half-lives in order to establish the PADN procedure as a standard alone therapy.

For the PADN procedure, a 7F flow-directed Swan-Ganz catheter (Edwards, USA) was inserted percutaneously in the patients who were under local anesthesia into an internal jugular vein for the measurements of the resting RAP, sRVP, sPAP, mPAP, PAOP, and cardiac output (CO) values. The PVR [=(mPAP-PAOP)/CO] was then calculated. All the measurements were performed at the end of expiration. If the PAOP measurement was unreliable, the left ventricular end-diastolic pressure was measured and used rather than the PAOP measurement. Two blood samples from the RA, RV and PA were obtained for the measurements of oxygen pressure and saturation. If the difference between the oxygen pressure or saturation measurement of these two samples was >7%, further sampling was performed to identify the location of the left-to-right shunt.

The PADN procedure was performed at three sites around the conjunctional area between the distal main trunk and the ostial left branch. FIG. **23**A illustrates an anterior-posterior and cranial (20°) view of pulmonary arterial angiograph **2300**. Specifically, the angiograph **2300** illustrates the RPA **2302**, MPA **2306** and LPA **2304** of a heart of one of the patients. FIG. **23**B illustrates the angiograph of FIG. **23**A with a line representing the lateral wall of MPA **2320**, a line **2318** representing the anterior wall of the LPA. The crossing site by these two lines **2312** and **2316** is the point **2310**. The crossing site by a line **2314** representing the posterior wall of LPA and the line **2320** representing a wall of the MPA is the point **2308** which is 1-2 mm posteriori to the point **2310**. The line **2316** starts from the inferior wall of RPA and ends at the point **2310**, the point **2312** localizes at this level and 1-2 mm anteriorly to the point **2310**. FIG. **23**C illustrates the angiograph of FIG. **23**A with a catheter with 10 electrodes is positioned at the distal MPA. In FIG. **23**C, electrode **2332** matches with point **2310**, electrode **2330** matches with point **2308** and electrode **2334** matches with point **2312**. The following ablation parameters were programmed at each point: a temperature of 45° C.-50° C., energy≤15 W, and a time of 120 s. The procedure would cease for 10 seconds if the patient felt intolerable chest pain during the procedure. The EKG and pressure lines (including cardiac output) were monitored and continuously recorded throughout the PADN procedure.

The patients were monitored in the CCU for at least 24 hours. All measurements were repeated post-procedure, at 24 hours, at 3 months, at 6 months, and at 12 months. Magnet resonance image (MRI) and CT scanning of the

pulmonary artery were performed before the PADN procedure and at 6 months after the PADN procedure.

The success of a PADN procedure was defined as the reduction of sPAP or mPAP immediately after the procedure or at 24 hour>10% compared to the baseline values, without intra-procedural complications. The primary endpoint of the additional study was the difference in 6MWD after the 6 months between the medication and PADN procedure. The secondary endpoints included composite and individual PAH-related events including the worsening of PAH, the initiation of treatment with the intravenous or subcutaneous injection of drugs, lung transplantation, atrial septostomy or all-cause death. Repeat hospitalization also served as a secondary endpoint.

For assessing the 6MWD, baseline blood samples were obtained for the analysis of N-terminal brain natriuretic peptide (NT-pro BNP) levels prior to administering the 6MWD. The 6MWD, the Borg scale and the WHO functional class at rest and during exercise were estimated and recorded by a physician who was blinded to the study design. The 6MWD has been selected as an endpoint in previous studies of PAH patients. Notably, the 6MWD in patients without PAH-related events was higher than that in patients with PAH-related events, which suggests that a 15% reduction in the 6MWD may be clinically meaningful. This result supports the use of a 15% reduction in the 6MWD as a criterion for PAH worsening in clinical studies. Also, PAP, RAP and PVR are useful parameters correlated with the prognosis of the PAH patients. A sPAP between 50-70 mmHg and RAP>8 mmHg were markers indicating the severity of PAH disease. The 6MWD improvement after the PADN procedure was paralleled by an improvement in RAP, sPAP and mPAP. However, a correlation between the PA hemodynamics at baseline or post-medication with 6MWD was not established, most likely because the improvement of skeletal blood flow without a change in PA hemodynamics may also account for the improvement of 6MWD.

For the echocardiographic measurements, all echocardiograms were performed (Vivid 7, General Electric Co., Easton Turnpike, CT, US) and interpreted in the Nanjing Echocardiographic Laboratory following the recommendations of the American Society of Echocardiography. Digital echocardiographic data that contained a minimum of 3 consecutive beats (or 5 beats in cases of atrial fibrillation) were acquired and stored. RV systolic pressure (sRVP) is equal to systolic PAP (sPAP) in the absence of pulmonary stenosis. sPAP is equal to the sum of right atrial (RA) pressure (RAP) and the RV to RA pressure gradient during systole. RAP was estimated based on the echocardiographic features of the inferior vena cava and was assigned a standard value. The RV to RA pressure gradient was calculated as $4\,v_t^2$ using the modified Bernoulli equation in which v_t is the velocity of the tricuspid regurgitation jet in m/s. mPAP was estimated according to the velocity of the pulmonary regurgitation jet in m/s. The tricuspid excursion index (Tei) is defined as (A−B)/B in which A is the time interval between the end and the onset of tricuspid annular diastolic velocity, and B is the duration of tricuspid annular systolic velocity (or the RV ejection time).

Table 2 provides data indicating how the 6MWD increased from 361±112 m to 373±111 m (p=0.009) after 6-month Medication treatment and from 358±115 m to 423±98 m (p<0.001) 6-month after PADN procedure, in line with the significant reduction of the NT-pro BNP and WHO functional class.

TABLE 2

Comparison of measurements before and after treatment

	Medication (n = 28)			PADN (n = 28)		
	Prior-to	6-month	p	Prior-to	6-month	p
NT-pro BNP, pg/ml	2293 ± 2741	1732 ± 1878	0.007	2669 ± 3178	1296 ± 947	0.015
WHO class, point	2.75 ± 0.52	2.46 ± 0.58	0.009	2.75 ± 0.52	2.21 ± 0.63	<0.001
6MWD, mm	361 ± 112	373 ± 111	0.009	358 ± 115	423 ± 98	<0.001
Cardiac output RHC	3.2 ± 0.94	3.26 ± 0.89	0.221	3.25 ± 1.05	3.91 ± 1.08	0.002
SPAP, mmHg	91.9 ± 33.0	91.5 ± 33.4	0.485	91.9 ± 33.3	78.2 ± 29.4	<0.001
mPAP, mmHg	56.1 ± 21.1	55.9 ± 21.2	0.762	56.7 ± 21.8	48.9 ± 19.2	<0.001
PCWP, mmHg	13 ± 7.7	13.8 ± 6.9	0.365	12.5 ± 8.6	12.9 ± 6.3	0.788
mRAP, mmHg	11.5 ± 4.2	11.8 ± 4.6	0.442	11.4 ± 4.7	8.8 ± 3.4	0.001
sRVP, mmHg	89.3 ± 31.2	91.3 ± 32.1	0.255	89.3 ± 31.6	83.0 ± 34.7	0.147
PVR, woods unit	13.8 ± 7.6	13.6 ± 6.9	0.721	14.3 ± 8.6	9.7 ± 6.8	0.002
Cardiac echo						
mPAP, mmHg	47.9 ± 24.2	45.6 ± 23.2	<0.001	47.4 ± 24.8	38.1 ± 16.5	0.002
mRAP, mmHg	11.8 ± 3.1	11.1 ± 2.8	0.043	11.8 ± 3.1	8.9 ± 3.1	<0.001
sRVP, mmHg	96.0 ± 87.9	87.9 ± 26.9	<0.001	96.1 ± 31.7	78.6 ± 23.3	<0.001
SPAP, mmHg	98.1 ± 29.5	87.2 ± 25.2	<0.001	98.2 ± 32.2	79.9 ± 24.6	<0.001
Pericardial fluid, mm	1.11 ± 1.64	1.43 ± 1.93	0.059	1.96 ± 2.89	0.85 ± 0.89	0.002
RV Tei, %	0.59 ± 0.17	0.55 ± 0.16	0.029	0.69 ± 0.09	0.36 ± 0.09	<0.001

PADN, pulmonary artery denervation;
NT-pro BNP, N terminal-pro brain natriuretic peptide;
6MWD, 6-minute walk distance;
RHC, right heart catheterization;
sPAP, systolic pulmonary arterial pressure;
mPAP, mean pulmonary arterial pressure;
mRAP, mean right atrial pressure;
sRVP, systolic right ventricular pressure;
PVR, pulmonary vessel resistance;

There was a significant difference in the increase in 6MWD at the 6-month follow-up between the Medication (13±24 m) and the PADN procedure (65±85 m) (95% CI: −21.34~-3.49, p=0.002), coupled with the significant improvement of hemodynamic after PADN procedure. The PADN procedure was associated with less frequent PAH-related events at the 6-month (10.8%) and 12-month (17.9%) follow-up, compared to 42.9% after 6-month Medication treatment (all p<0.05). As illustrated in Table 3 and FIG. **24**A, the Δ6MWD (defined as the 6MWD at the 6-month follow-up minus the baseline 6MWD) was +13±24 m (+3.9% increase) in the Medication treatment, which was significantly different to the +65±85 m (+23.9% increase, 95% CI: −21.34~-3.49, p=0.002) at the 6-month and +95±61 m (+34.9% increase) at one-year after the PADN procedure.

TABLE 3

Comparison of the differences in measurements after 6-month treatments

	Medication (n = 28)	PADN (n = 28)	95% CI	p
NT-pro BNP, pg/ml	−562 ± 1009	−1373 ± 2792	−42.84~1665.44	0.062
WHO functional class	−0.36 ± 0.49	−0.54 ± 0.58	−0.10~0.46	0.202
6MWD, m	13 ± 24	65 ± 85	−21.34~−3.49	0.002
% of increase	+3.9%	23.9%	−0.31~−0.09	0.001
Cardiac output RHC	0.06 ± 0.24	0.67 ± 1.05	−0.10~−0.20	0.005
sPAP, mmHg	−0.46 ± 3.47	−13.75 ± 14.1	8.38~18.19	<0.001
mPAP, mmHg	−0.14 ± 2.48	−7.86 ± 6.10	5.26~10.18	<0.001
PCWP, mmHg	0.82 ± 4.72	0.36 ± 6.96	−1.63~2.56	0.653
mRAP, mmHg	−0.21 ± 2.62	−2.53 ± 3.75	0.70~3.93	0.007
sRVP, mmHg	1.96 ± 8.93	−6.22 ± 22.07	1.76~14.62	0.014
PVR, woods unit	−0.17 ± 2.56	−4.59 ± 7.06	1.99~6.83	0.001
Cardiac echo				
mPAP, mmHg	−2.36 ± 2.78	−9.28 ± 13.93	1.98~11.86	0.008
mRAP, mmHg	−0.54 ± 1.57	−2.86 ± 2.86	1.20~3.44	<0.001
sRVP, mmHg	−8.07 ± 9.73	−17.54 ± 16.97	4.78~14.15	<0.001
sPAP, mmHg	−10.89 ± 11.87	−18.25 ± 16.73	3.13~11.58	0.001
Pericardial fluid, mm	0.11 ± 0.93	−0.74 ± 2.63	−1.04~2.47	0.036
RV Tei, %	−0.04 ± 0.09	−0.34 ± 0.11	0.24~0.35	<0.001

CI, confidence interval;
PADN, pulmonary artery denervation;
NT-pro BNP, N terminal-pro brain natriuretic peptide;
6MWD, 6-minute walk distance;
RHC, right heart catheterization;
sPAP, systolic pulmonary arterial pressure;
mPAP, mean pulmonary arterial pressure;
mRAP, mean right atrial pressure;
sRVP, systolic right ventricular pressure;
PVR, pulmonary vessel resistance;

In the Medication treatment, there were 9 patients (32%) whose 6MWD decreased (range from −6 m to −47 m) after the 6-month treatment. Of those 9 patients, 5 patients had an average 6MWD increase of 45 m 6-month after the PADN procedure, whereas no change was observed in 4 patients. Among those 4 patients, there was still no change 6MWD in 1 patient at one-year after the PADN procedure. Finally, there were 2 patients who had no change in 6MWD at one-year follow-up after PADN procedure. As illustrated in FIG. **24**B, the 6MWD after the PADN procedure rather than Medication treatment was negatively correlated with mPAP (r=−0.416, p=0.028) and sPAP (r=−0.401, p=0.034).

The study also demonstrated improvement of hemodynamic and cardiac function. The Δ mPAP and ΔCO at 6-month after the PADN procedure were greater than those in the Medication treatment (−7.86±6.10 mmHg vs. −0.14±2.48 mmHg, P<0.001; 0.67±1.05 L/min/1.73 m^2 vs. 0.06±0.24 L/min/1.73 m^2, p=0.005, Table 3), with resultant significant differences in the reduction of the pericardial fluid amount (−0.74±2.63 mm vs.+0.11±0.93 mm, p=0.036) and Tei (−0.34±0.11 points vs. −0.04±0.09 points, p<0.001). As illustrated in FIG. **24**C, these improvements were sustained through one-year follow-up after PADN procedure.

Table 4 illustrates how, after the 6-month treatment, a PAH-related event was observed in 12 patients (42.9%) in the Medication treatment and 3 patients (10.8%) in the PADN procedure (p=0.002). These events were mainly driven by the worsening of PAH.

TABLE 4

Clinical follow-up after the 6-month treatments

	Medication (n = 28)	PADN (n = 28)	p
PAH-event, n (%)	12 (42.9)	3 (10.8)	0.002
All-cause death	0	0	
Atrial septostomy	0	0	
Lung transplantation	0	0	
Needing IV & IS	2 (7.2)	0	
Worsening of PAH	10 (36.0)	3 (10.8)	
Re-hospitalization, n (%)	12 (38.3)	4 (14.4)	0.018
Cost, ×10,000 USD/per pt	3.5 ± 1.2	0.6 ± 0.7	<0.001
Any-cause Death, n (%)	0	0	

TABLE 4-continued

Clinical follow-up after the 6-month treatments

	Medication (n = 28)	PADN (n = 28)	p
Access site hematoma, n (%)	0	0	
Aneurysm, n (%)	0	0	
Thrombus, n (%)	0	0	

PADN, pulmonary artery denervation;
PAH, pulmonary arterial hypertension;
pt, patient;

The mean time from treatment to clinical worsening was 125 days (range of 22 to 166 days) in the Medication treatment, which was significantly shorter than the 166 days (range from 47 to 172 days) reported in the PADN procedure (p=0.01). Re-hospitalization was required in 42.9% of the patients in the Medication compared to 14.4% of the patients in the PADN procedure (as described when p=0.018 in Table 4). There were no access hematomas, aneurysms, thrombus formations or any-cause deaths after the 6-month treatment.

The Δ6MWD was approximately +60 m after PADN procedure and +15 m after the medication treatment. A total of 28 patients were required to achieve significance (2-sided p-value, 80% power). The difference in each variable (at the 6-month period minus the baseline) for each treatment was calculated and compared between the two treatments. The continuous variables were expressed as the mean±SD. A normality test for all the continuous variables was performed using the Kolmogorov-Smirnov and Shapiro-Wilk tests. The differences in the continuous variables between the two treatments were analyzed using a paired t-test or the Mann-Whitney U test when appropriate. The categorical variables were compared using Fisher's exact test. The event-free survival rate was generated using the Kaplan-Meier method and was analyzed with the log-rank test. Statistical significance was defined as a two-sided P value <0.05. All the analyses were performed using the statistical program SPSS 19.0 (SPSS Institute Inc., Chicago, Ill., USA).

For the additional study, a worsening of PAH was defined as the occurrence of all three of the following measurements: a decrease in the 6MWD of at least 15% from baseline, confirmed by a second 6MWD performed on a different day within 14 days of the first measurement; a worsening of the symptoms of PAH; and the need for additional treatment for PAH. A worsening of the symptoms of PAH was defined as any of the following measurements: a change from baseline to a higher WHO functional class (or no change in patients who were in WHO functional class IV at baseline) and the appearance or worsening of signs of right heart failure, which did not respond to oral diuretic therapy. An independent clinical event committee adjudicated, in a blind fashion, all the events related to PAH and all the deaths that were reported up to the end of the treatment.

At the one-year follow-up, there were 5 (17.9%) PAH-related events (2 new events, including 2 sudden deaths). The 6MWD in patients without PAH-related events was 467±100 m, which was higher than the 393±42 m reported in patients who had experienced an event (p=0.018). Accordingly, patients with 6MWD<400 m had higher rate of PAH-related event (44.4%) at one-year after the PADN procedure, compared 5.3% in patients with 6MWD≥400 m (p=0.010).

Therefore, the additional study indicated that the PADN procedure was associated with a significant improvements in 6MWD and hemodynamics at 6-month, with resultant less PAH-related events. For example, the PADN procedure led to a greater improvement of pulmonary arterial hemodynamics with subsequently less frequent PAH-related events and re-hospitalizations.

FIGS. **25**A-**25**H are various views of a digital ablation controller **2500** that can be used in lieu of the controller **100** illustrated in FIGS. **15**C-**15**D. Similar to the controller **100**, the digital ablation controller **2500** can be connected to the handle **2** of the catheter for providing ablation energy. For example, the digital ablation controller **2500** can be configured to provide ablation energy and control the electrodes E**1**-E**10** of FIG. **15**B.

Generally described, the digital ablation controller **2500** provides for a single, portable housing for both control and feedback during performance of the PADN procedure. The digital ablation controller **2500** may control the amount of power provided to the electrodes **5** from a power source (such as a battery or a power grid) such that the amount of power is within nominal limits for ablation. Also, the digital ablation controller **2500** may enable the storage and retrieval of various patient profiles that may include different configuration settings for catheter configuration and/or provision of power to the electrodes of the catheter.

For example, different patient profiles may include different settings for which the PADN procedure is to be performed with different settings for different electrodes. Also, the digital ablation controller **2500** may include a user interface from which a user or operator of the digital ablation controller may provide manual control and/or enter or retrieve information from the patient profiles.

For example, the user interface may include information on the operational characteristics of the electrodes (such as ablation temperature and time captured by the catheter's sensors) and the user or operator of the digital ablation controller may perform the PADN procedure based upon the operational characteristics of the electrodes. Also, the user or operator of the digital ablation controller may directly select a particular electrode (or electrodes) to activate for ablation from the user interface. Thereby, the digital ablation controller would direct power (such as power from the battery) to the appropriate electrode(s) selected via the user interface.

In certain embodiments, the digital ablation controller may provide automatic control of the PADN procedure based upon feedback from sensors on the catheter. For example, the operational characteristics of the electrodes may be captured by the catheter's sensors and used to regulate aspects of the PADN procedure (such as the amount of time ablation is performed at a particular location based upon the temperature at the location of ablation).

In certain embodiments, the digital ablation controller includes a battery configured to store power at a level sufficient for ablation using one or more electrodes **5** of the multi-pole synchronous pulmonary artery radiofrequency ablation catheter. By directly using the battery, the provision of power to the electrodes is contingent upon stored power rather than power provided ad hoc to the electrodes, such as from power provided by a local power grid. Thereby, the availability of power is not contingent upon power being readily available to the digital ablation controller but rather the digital ablation controller may function independent of the local power grid so long as the battery is sufficiently charged.

FIG. **25**A illustrates a top perspective view of the digital ablation controller **2500** in a closed position. The top perspective view illustrates the power cord **2504** connected to the digital ablation controller **2500**. As illustrated, the digital

ablation controller **2500** may be a single housing configured to provide an interface for control and power for the multi-pole synchronous pulmonary artery radiofrequency ablation catheter. For example, the digital ablation controller **2500** may receive and store power such that the PADN procedure may be performed using the stored (battery) power in the digital ablation controller **2500**. Also, the digital ablation controller **2500** may provide precise regulation of power by digitally controlling different aspects of the PADN procedure, such as the particular electrode(s) used for ablation, the power at any particular electrode and the time for ablation. The digital ablation controller **2500** may also provide real time feedback from sensors (such as temperature sensors and/or impedance sensors) disposed at various points on the multi-pole synchronous pulmonary artery radiofrequency ablation catheter (such as at the locations of the electrodes), as discussed in FIGS. **1**-**4**.

FIG. **25**B illustrates a top perspective view of the digital ablation controller **2500** in an open position. The user interface **2512** is visible and usable in the open position of the digital ablation controller **2500**. Also, a carrying handle **2510** is illustrated on the digital ablation controller **2500**. FIG. **25**C illustrates a back perspective view of the digital ablation controller **2500** in the open position.

FIG. **25**D is a screen shot of an initial user interface **2526** of the digital ablation controller **2500**. The initial user interface includes buttons that may be selected to interact with the digital ablation controller **2500**. For example, the initial user interface **2526** illustrates a button **2520** for changing a language setting of the user interface **2520**, a button **2522** to access data stored in the digital ablation controller **2500** and a button **2524** to begin operation of the digital ablation controller **2500**.

FIG. **25**E is a screen shot of the user interface **2530** presenting options for entering patient information for performance of the PADN procedure. The user interface includes a button **2532** to begin browsing existing patient profiles stored in the digital ablation controller **2500**. The user interface also includes sections **2534** for inputting information for a new patient profile, such as a patient's name, identification number, age, sex and the selection of various preset operational settings for the digital ablation controller **2500**. The user interface also includes a section **2536** to input remarks concerning the patient for the patient profile.

FIG. **25**F is a screen shot of a user interface **2540** of the digital ablation controller **2500** at the initiation of the PADN procedure. The user interface **2540** includes information concerning the power level **2542**, time **2544**, temperature **2546** and impedance **2548** of the electrodes of the catheter. The user interface also includes buttons from which a particular electrode **5** on the annular ring **4** may be selected for activation.

FIG. **25**G is a screen shot of a user interface **2550** of the digital ablation controller **2500** during operation. Ablation may be initiated by selecting a button for a particular electrode, such as a button **2570** associated with electrode **2572** designated with the number "2" highlighted on the user interface. The operational relationship of the electrode **2572** between impedance, power and temperature over time is displayed on a graph **2552**. Although a single electrode is selected in the user interface and used for ablation in the illustrated embodiment, certain embodiments provide for multiple electrodes selected and used at once for ablation. Also, ablation may be interrupted while switching between electrodes used for ablation. The switching between different electrodes for ablation may be implemented in any manner that allows for energy used for ablation to be guided to different electrodes of the multi-pole synchronous pulmonary artery radiofrequency ablation catheter, such as via digital or analog/solid state switching.

FIG. **25**H is a screen shot **2580** of a user interface of the digital ablation controller **2500** presenting information on stored patient profiles. The user interface indicates that there are two patient profiles **2582**, **2584** that may be selected. The patient profiles are presented with a name **2586**, patent identification number **2588** and time **2590** of last access of the stored patient profile. The user interface also includes buttons **2592** for exporting the various patient profiles and an option button **2594** to delete a selected patient profile.

FIG. **26** is a schematic diagram illustrating a mechanical switching system **2600** that may be implemented in the controller **2500** of FIGS. **25**A-**25**H or the controller **100** of FIGS. **15**C-**15**D. The mechanical switching system **2600** includes a source contact **2602**, a mechanical switch **2604**, electrode contacts **2606**A-J, and a ground contact **2610**. The source contact **2602** may be connected with a source of RF energy at a level sufficient for ablation. The electrode contacts **2606**A-J may be each connected with a different electrode **2608**A-J that may be used for ablation. The ground contact **2610** may be connected to ground **2612**. The electrodes **2608**A-J may be located at the distal end of the catheter. The mechanical switch **2604** may be actuated as part of a dial or knob **2612** that may be physically moved such that the mechanical switch **2604** connects the source contact **2602** with a particular electrode contact **2606**A-J or the ground contact **2610**. For example, the mechanical switch **2604** may be actuated by being physically moved in a clockwise or a counter clockwise direction. In the illustrated embodiment, the switch **2604** is positioned to connect the source contact **2602** to the electrode contact **2606**A.

FIG. **27** is a schematic diagram illustrating a solid state switching system **2700** that may be implemented in the controller **2500** of FIGS. **25**A-**25**H or the controller **100** of FIGS. **15**C-**15**D. In contrast with the mechanical switching system **2600** of FIG. **26**, the solid state switching system **2700** is actuated without use of any physically moving parts. The solid state switching system **2700** may include the source contact **2602**, a selector contact **2702** connected with a signal source, solid state switches **2704**A-J, the electrode contacts **2606**A-J, and ground **2612**. The electrode contacts **2606**A-J are each connected with the different electrodes **2608**A-J that may be used for ablation. The source contact **2602** may be connected with the source of RF energy at a level sufficient for ablation. The solid state switching system may set the selector contact **2702** to a particular signal (such as to a particular voltage level) that causes a particular solid state switch **2704**A-J to connect the source contact **2602** with a particular electrode contact **2606**A-J. For example, the solid state switching system may set the selector contact **2702** to a voltage level which activates solid state switch **2704**J to connect the source contact **2602** with the electrode contact **2606**J, thereby providing RF energy at a level sufficient for ablation to the electrode associated with the electrode contact **2606**J. Also, the other solid state switches **2604**A-I may maintain a connection between their associated electrode contacts **2606**A-I and ground **2612** while the solid state switch **2604**J connects the source contact **2602** to the electrode contact **2606**J. The solid state switches may be implemented using any type of solid state device, including MOSFETs, IGBTs, bipolar transistors, and thyristors.

FIG. **28** is a diagram illustrating a generic switching system **2800** that may be implemented in the controller **2500** of FIGS. **25**A-**25**H or the controller **100** of FIGS. **15**C-**15**D.

The generic switching system **2800** may implement any type of switching system to connect the source contact **2602** to a particular electrode contact **2606**A-J. For example, the generic switching system may be implemented using mechanical switches, solid state switches, or a combination of mechanical and solid state switches.

Example 4

The mechanisms underlying pulmonary arterial hypertension (PAH) are multifactorial. An additional study was conducted to analyze the hemodynamic, functional, and clinical responses to PADN in patients with PAH of different causes.

66 consecutive patients with a resting mean pulmonary arterial pressure ≥25 mm Hg treated with PADN were prospectively followed up. Target drugs were discontinued after the PADN procedure. Hemodynamic response and 6-minute walk distance were repeatedly measured within the 1 year post PADN follow-up. The clinical end point was the occurrence of PAH-related events at the 1-year follow-up. There were no PADN related complications. Hemodynamic success (defined as the reduction in mean pulmonary arterial pressure by a minimal 10% post PADN) was achieved in 94% of all patients, with a mean absolute reduction in systolic pulmonary arterial pressure and mean pulmonary arterial pressure within 24 hours of −10 mm Hg and −7 mm Hg, respectively. The average increment in 6-minute walk distance after PADN was 94 m. Worse PAH-related events occurred in 10 patients (15%), mostly driven by the worsening of PAH (12%). There were 8 (12%) all-cause deaths, with 6 (9%) PAH-related deaths.

Patients with a resting mean PAP (mPAP) >25 mm Hg, as measured by right heart catheterization, were included in the study, although they were receiving PAH expert-based standard medical treatment. In patients with pulmonary hypertension (PH) caused by left ventricular (LV) dysfunction, an additional requirement was pulmonary vascular resistance (PVR)>3 Wood units. An adenosine vasodilator test was performed during right heart catheterization in all patients. Exclusion criteria included active infection, cancer, toxin- or anorexia-induced PH, portal hypertension, chronic thromboembolic PH without surgical treatment, intolerance to the PADN procedure (caused by the use of an 8-F-long sheath that occludes blood flow in the orifice of the tricuspid and pulmonary valves, resulting in severe dyspnea), and inability to provide consent.

The study was approved by the Institutional Review Board and Ethics Committee of the Nanjing First Hospital (Nanjing, China), and all patients provided written inform consent.

Resting right atrial (RA) pressure, right ventricular (RV) pressure, PAP, pulmonary artery occlusion pressure (PAOP), and thermodilution cardiac output were obtained with a 7-F flow-directed Swan-Ganz catheter. PVR ([mPAP-PAOP]/cardiac output) and transpulmonary gradient (mPAP-PAOP) were then derived. All measurements were taken at end expiration. If the PAOP measurement was unreliable, the LV end-diastolic pressure was used rather than the PAOP. Blood samples from the RA, RV, and PA were obtained, and if the oxygen saturation measurements varied by >7% between chambers, further sampling was performed to identify the location of the left-to-right shunt.

PA ablation was performed using a dedicated 7-F temperature-sensing ablation catheter. The details of the device and the PADN procedure have been previously described.7,8 Briefly, PADN was thereafter performed only in the periconjunctional area between the distal main trunk and the ostial left branch (points A, B, and C in FIG. **29**B and FIG. **29**C).

FIG. **29**A-FIG. **29**C illustrate Pulmonary arterial angiography, position of electrodes, and pulmonary artery denervation (PADN) procedure. FIG. **29**A illustrates anterior-posterior and cranial (**200**) view of the pulmonary arterial angiograph. In FIG. **29**B, the dotted line **2** represents the lateral wall of the main pulmonary artery (MPA), the solid line **3** represents the anterior wall of the left pulmonary artery (LPA), and the point where the 2 lines intersect is point A; the intersection of the dotted line **1** (posterior wall of the LPA) and dotted line **2** is point B, which is 1 to 2 mm posterior to point A; the solid line **4** starts from the inferior wall of the right pulmonary artery (RPA) and ends at point A, and point C localizes at this level and 1 to 2 mm anterior to point A. (III) A pulmonary artery denervation catheter with 10 electrodes is positioned at the distal MPA, with electrodes A, B, and C at points A, B, and C, respectively.

The following ablation parameters were programmed at each point: temperature >45° C., energy ≤20 W, and time 120 s (for point C) or 240 s (for points A and B). The procedure was interrupted for 10 s if the patient reported severe chest pain. Electrocardiography and hemodynamic function were monitored and recorded continuously throughout the procedure.

A 5000-U heparin bolus was administered after the insertion of the venous sheath. Additional 2000- to 3000-U heparin boluses were administered if the procedural time was >1 hour. After the procedure, oral warfarin was prescribed and adjusted to an international normalized ratio of 1.5 to 2.5 for all patients. Aspirin (100 mg per day) and clopidogrel (75 mg per day) were indefinitely prescribed in the presence of contraindications for warfarin. Immediately after the PADN procedure, all target drugs (endothelial-receptor antagonists, phosphodiesterase type-5 inhibitors, and prostacyclin analogs) were discontinued. Diuretics were prescribed at a dosage less than or equal to that at baseline. Oxygen therapy was used according to patients' symptoms, as assessed by a physician.

Functional capacity was determined using a standard 6MWD protocol before PADN and at 1 week, 1 month, 2 months, 3 months, 6 months, and 1 year after the procedure. Dyspnea was assessed by using the Borg scale. The World Health Organization (WHO) classification of dyspnea at rest and during exercise was recorded by a physician blinded to the study design. Baseline blood samples were obtained to measure N-terminal pro-brain natriuretic peptide levels before each exercise test.

Transthoracic echocardiography (Vivid 7, General Electric Co, Easton Turnpike, CT) was performed immediately after the procedure and at 24 hours, 1 week, 1 month, 2 months, 3 months, 6 months, and 1 year and was analyzed at the Nanjing Medical University Echocardiographic Laboratory. Digital echocardiographic data that contained a minimum of 3 consecutive beats (or 5 beats in cases of atrial fibrillation) were acquired and stored. RV systolic pressure was set equal to systolic PAP (sPAP) in the absence of pulmonary stenosis. sPAP was calculated as the sum of RA pressure and the RV to RA pressure gradient during systole. RA pressure was estimated based on the echocardiographic features of the inferior vena cava and assigned a standard value. The RV to RA pressure gradient was calculated as 4 vt2 using the modified Bernoulli equation, where v_t is the velocity of the tricuspid regurgitation jet in m/s. The mPAP was estimated according to the velocity of the pulmonary regurgitation jet in m/s. The tricuspid excursion index is

defined as (A−B)/B, where A is the time interval between the end and the onset of tricuspid annular diastolic velocity and B is the duration of tricuspid annular systolic velocity (or the RV ejection time).

Patients were monitored in the critical care unit for at least 24 hours post procedure. Hemodynamic measurements, 6MWD, and echocardiographic measurements were repeated at 24 hours, 1 month, 2 months, 3 months, 6 months, and 12 months. Clinical follow-up was extended to 1 year. Magnetic resonance imaging and computed tomographic imaging of the pulmonary artery were performed before the PADN procedure and at 6 months.

The primary end points were changes in hemodynamic, functional, and clinical responses within the 1-year follow-up. PAH-related clinical events were defined as those caused by worsening of PAH, initiation of treatment with intravenous or subcutaneous prostanoids, lung transplantation, atrial septostomy, or all-cause mortality. Worsening of PAH was defined as the occurrence of all 3 of the following: >15% decrease in 6MWD from baseline, confirmed by a second 6MWD performed on a different day within 14 days; worsening PAH symptoms; and the need for additional treatment for PAH. Worsening PAH symptoms were defined as a change from baseline to a higher WHO functional class (or no change in WHO functional class IV from that at baseline) plus the appearance or worsening signs of right heart failure not responsive to oral diuretic therapy. An independent clinical event committee adjudicated all deaths and reported events with respect to their relationship with PAH. Additional secondary end points included changes in 6MWD, WHO functional class, N-terminal pro-brain natriuretic peptide levels, PAH-related or all-cause mortality, echocardiographic measurements, and rehospitalization rates for PAH in the long term. The prespecified definition of PADN procedural hemodynamic success was reduction in mPAP immediately after PADN by >10, without the occurrence of any intraprocedural complications.

Continuous variables are expressed as mean±SD. Normality was examined using the Kolmogorov-Smirnov and Shapiro-Wilk tests. Data having unequal variances at different times were transferred to log data. Differences in continuous variables between 2 different timing points (baseline versus 6 months or 6 months versus 1 year) were analyzed with paired t tests. Categorical variables between group I, group II, and chronic thromboembolic PH groups or between 2 different timing points were compared by using Fisher exact or McNemar test, as appropriate. Event-free survival rate at 1 year was estimated by using the Kaplan-Meier method. Statistical significance was defined as a 2-sided P value of <0.05. All analyses were performed with SPSS 16.0 (SPSS Institute Inc, Chicago, IL).

In all, 70 patients with qualifying PAH/PH were screened during the study period. Four patients were excluded: 2 patients with IPAH could not lie flat for 20 minutes, 1 with WHO group II PAH died in the ward after consent while waiting for the procedure, and 1 with WHO group IV PAH died of temporary pacing catheter-induced RV perforation before the PADN procedure. Thus, the study population consisted of 66 patients in whom PADN was attempted.

Among the 66 patients, 39 (59.1%) had WHO group I PAH (IPAH in 20 patients; 11 had PH secondary to connective tissue disorders; and 8 had PH secondary to congenital heart disease after surgical repair), 18 (27.3%) had group II PAH (PH secondary to LV dysfunction), and 9 (13.6%) had chronic thromboembolic PH after surgery. Of the 11 connective tissue disorders patients, 7 had systemic lupus erythematosus, 2 had mixed connective tissue disease, and 2 had primary Sjogren syndrome; of the 8 congenital heart disease after surgical repair patients, 5 had an atrial septal defect and 3 had patent ductus arteriosus. Of the patients with group II PAH, 15 had a previous myocardial infarction, and 3 had dilated cardiomyopathy.

Table 5 illustrates baseline clinical characteristics are shown. The average time from diagnosis of PAH to the PADN procedure was 3.8 years. A combination of drugs was required for 89.1% of patients. Most patients (90.9%) had WHO function classes II and III. In all, 55 patients (83.3%) were administered oxygen therapy. In all, 37 (56.1%) had pericardial effusion (Table 6).

TABLE 6

Echocardiographic Measurements at Baseline and 1 Year After PADN

	Baseline (n = 66)	6 m (n = 65)	1 y (n = 56)	P Value*
Left atrial diameter-s, mm	40.9 ± 8.8	41.5 ± 9.2	41.8 ± 8.9	0.75
Left ventricular diameter-d, mm	45.8 ± 13.1	47.4 ± 12.9	47.2 ± 11.2	0.024
Left ventricular diameter-s, mm	31.7 ± 14.4	29.4 ± 14.5	29.6 ± 14.1	0.041
Left ventricular EF, %	61.6 ± 13.2	63.9 ± 13.2	64.8 ± 12.6	0.001
Systolic PAP, mm Hg	93.3 ± 30.9	80.6 ± 25.4	79.1 ± 22.7	<0.001
Mean PAP, mm Hg	41.4 ± 12.8	36.1 ± 12.8	35.7 ± 12.6	<0.001
Right atrial pressure, mm Hg	11.2 ± 2.7	8.9 ± 2.5	8.2 ± 2.4	<0.001
Systolic RVP, mm Hg	91.5 ± 30.6	81.2 ± 26.3	78.3 ± 22.4	<0.001
Right atrial diameter, mm				
Long axis	58.5 ± 11.2	55.8 ± 12.1	56.4 ± 10.7	<0.001
Short axis	49.4 ± 10.5	48.7 ± 11.4	49.0 ± 10.0	0.39
Right ventricular diameter, mm	47.5 ± 10.6	45.2 ± 10.3	45.0 ± 10.1	0.046
Pericardial effusion, mm†	3.4 ± 4.5	1.5 ± 1.7	1.2 ± 1.6	0.039
Any, n (%)	37 (56.1)	24 (43.5)	22 (40.0)	0.17
Tei, %	0.63 ± 0.15	0.42 ± 0.17	0.39 ± 0.11	<0.001

EF indicates ejection fraction; PAP, pulmonary arterial pressure; RVP, right ventricular pressure; and Tei, tricuspid excursion index.
*Indicates the comparison of baseline vs 6 month; all variables were nonsignificantly different between 6 mo vs 1 y.
†Data were transferred to log data for analysis.

The median (interquartile range) duration of ablation at 2.8±0.3 sites during the PADN procedure was 22 (11-38) minutes. During the procedure, 47 patients (71.2%) complained of chest pain (including 3 patients [4.5%] with severe chest pain), and 15 patients (22.7%) complained of a

vague chest discomfort. All patients tolerated these symptoms without the need for additional sedative or analgesic agents. One patient developed sinus bradycardia from 88 to 43 bpm during the first ablation; the patient recovered after 3 minutes. A second PADN was attempted in 3 patients 2 to 4 days after the first attempt, during which patients were intolerable to dyspnea.

The mean absolute reduction in mPAP was −5 mm Hg (12.8±9.2% reduction) immediately post PADN procedure and −6.6 mm Hg (12.2±2.6%) at 24 hours after PADN. Hemodynamic success was achieved in 62 patients (93.9%). On the basis of univariable analysis, the predictors of hemodynamic failure were sPAP (P=0.022), mPAP (P=0.011), and pericardial effusion (P=0.036) (FIG. **30**A).

During the 6-month follow-up, there were significant reductions in sPAP, mPAP, diastolic PAP, RA pressure, and RV systolic pressure; and increment in cardiac output (all P<0.05) measured by either echocardiography (Table 6) or right heart catheterization (Table 3) all of which led to a significant decrease in PVR (Table 3; FIG. **30**B). However, there were no further improvements in values at 1-year follow-up compared with values at the 6-month follow-up (Table 7).

TABLE 7

Right Heart Catheterization Measurements at Baseline and 6-Month and 1-Year Follow-Up

	Baseline (n = 66)	6 mo (n = 65)	1 y (n = 56)	P Value*
Systolic PAP, mm Hg	86.6 ± 28.9	71.6 ± 25.8	70.1 ± 27.6	<0.001
Mean PAP, mm Hg	53.1 ± 19.1	44.8 ± 16.4	44.6 ± 17.6	<0.001
Diastolic PAP, mm Hg	34.8 ± 15.1	29.9 ± 14.2	28.4 ± 13.9	<0.001
Right atrial pressure, mm Hg	12.4 ± 7.3	10.6 ± 5.8	10.3 ± 5.4	0.005
Systolic RVP, mm Hg	85.1 ± 28.4	75.3 ± 29.7	72.9 ± 29.7	<0.001
PAOP, mm Hg†	14.7 ± 11.7	12.4 ± 5.3	11.8 ± 5.2	0.075
Cardiac output, L/min	3.3 ± 1.2	4.0 ± 1.1	4.1 ± 1.0	<0.001
PVR, Wood units	13.2 ± 6.9	8.4 ± 5.8	8.3 ± 6.6	<0.001

PAOP indicates pulmonary occlusion pressure; PAP, pulmonary arterial pressure; PVR, pulmmonary vessel resistance; and RVP, right ventricular pressure.
*Inidcated the comparison of baseline vs 6 mo; all variables were nonsignificantly different between 6 mo vs 1 y.
†Data were transferred to log data for analysis.

The 6MWD increased by a mean of 94±73 m (FIG. **30**C). The N-terminal pro-brain natriuretic peptide value decreased from 2229±2922 ng/mL at baseline to 917±947 ng/mL at the 1-year follow-up (P<0.001; FIG. **30**D; Table 8). During the 6-month follow-up, the WHO functional class improved in 42 patients (63.6%); among 56 patients who survived for 1 year, the mean paired WHO class was 2.7±0.6 at baseline and 1.9±0.7 at the last follow-up (P<0.001).

Table 6 illustrates the average reduction in RA (the long axis but not the short axis) and RV diameter at the 6-month follow-up, and these were 1.98 and 2.21 mm, respectively, with simultaneously significant absorption of pericardial effusion and reduction of tricuspid excursion index. Notably, left ventricular end-diastolic dimension and LV ejection fraction increased from 45.8±13.1 mm and 61.6±13.2% at baseline to 47.4±12.9 mm (P=0.024) and 63.9±13.2% (P=0.001) at 6-month follow-up, respectively. In contrast, left ventricular end-systolic dimension decreased from 31.7±14.4 mm at baseline to 29.4±14.5 mm at the 6-month follow-up (P=0.041). Similar to changes in hemodynamics, no further improvements in right heat size and cardiac function were noted at the 1-year follow-up compared with values at the 6-month follow-up.

During the follow-up, PAH target drugs were prescribed in 9 patients (3 in group I, 5 in group II, and 1 chronic thromboembolic PH) according to patients' expectation because of a slight nonsignificant increase in PVR after 6 months, and these drugs were then stopped after an average of 2.6 months since prescription.

TABLE 8

Clinical Outcomes at the 1-Year Follow-Up in 66 Patients

	1 mo	6 mo	12 mo
PAH-related events, n (%)	1 (1.5)	5 (7.6)	10 (15)
Death	0	1 (5.6)	6 (9)
Atrial septostomy	0	0	0
Wait listed for lung transplant	0	0	2 (3)
Requiring IV or SQ drugs	0	2 (3)	6 (9)
Worsening of PAH	1 (1.5)	2 (3)	6 (9)
15% decrease in 6MWD	2 (3)	3 (16.7)	8 (12)
Worsening of symptoms	1 (1.5)	2 (3)	6 (9)
Additional treatments	1 (1.5)	3 (16.7)	14 (21)
All-cause mortality	1 (1.5)	1 (5.6)	8 (12)
Rehospitalization	1 (1.5)	4 (22)	13 (19.7)
ANT pro-BNP, ng/ml	−673 ± 896*	−1189 ± 2551	−1291 ± 2662

A indicates 6-mo minus baseline; 6MWD, 6-minute walk distance; BNP, brain natriuretic peptide; IQR, interquartile range; IV, intravenous; NT, N terminal; and SQ, subcutaneous. Compared with 6 mo (P=0.029) and 1 y (P=0.005) after transferred to log data.

There were no PA perforations or other major cardiac or vascular complications. On the magnetic resonance imaging and computed tomography at the 6-month follow-up in 58 patients, no signs of thrombus or aneurysm formation were observed.

The 1-month and 6-month PAH-related event rates were 1.5% and 7.6%, respectively (Table 8). The median (interquartile range) follow-up was 652 (279-1130) days. As shown in FIG. **31**, PAH-related adverse events occurred in 10 patients during the 1-year follow-up (1-year 15.2% Kaplan-Meier estimated rate; FIG. **37**; Table 8). All-cause mortality occurred in 8 patients (1-year 12.1% Kaplan-Meier estimated rate) during the follow-up. Of the 8 deaths, 7 patients with group I PAH died after PADN: 1 with IPAH died of septic shock at 87 days, 2 with IPAH died of RV failure at 378 or 406 days, 1 with connective tissue disorders died of cerebral hemorrhage at 7 days, 2 with connective tissue disorders died of RV failure at 392 or 437 days, and 1 with congenital heart disease after surgical repair died of a traffic accident at 206 days. One patient with group II PAH died of RV failure at 433 days after the indexed procedure.

Univariable analysis showed that patients without an event at the 1-year follow-up had a slower resting heart rate (P=0.043), lower PAP values (based on either right heart catheterization or echocardiography), less pericardial effu-

sion (P=0.010), and higher 6MWD values (P=0.041) than the patients with events at the 1-year follow-up.

The PADN procedure was associated with favorable 1-year outcomes, as evidenced by improvements in WHO functional class, 6MWD, N-terminal pro-brain natriuretic peptide levels, and a low rate of PAH-related events.

Neurohumoral activation in PAH is evidenced by increased circulating catecholamine levels, abnormally high muscle sympathetic nerve activity, and impaired heart rate variability, which forms the theoretical basis of using β-blockers and PADN to treat PAH. As a result, the success of PAH therapies has been measured in terms of reduction in PAP and PVR. The hemodynamic response to medication using target drugs within 4 weeks to 6 months varies widely with a mean reduction in mPAP to <3 mm Hg. PADN resulted in an immediate reduction in PAP. post-PADN reductions in sPAP (−8 mm Hg) and mPAP (−5 mm Hg) were sustained throughout the follow-up period. No further reduction in PAP or further improvement in 6MWD was found after the 6-month follow-up, which might indicate that significant improvement in PA remodeling was achieved within 6 months after PADN treatment. Repeated PADN combined with target drugs can be more beneficial in patients with PAH.

Improvement in 6MWD was used as the primary end point on PAH therapeutics, and a 15% reduction in 6MWD is one criterion of PAH worsening. Previous studies have reported a mean increase of +34 m in the 6MWD at a median 14.5-week follow-up, which is lower than that in our study (+94 m). In addition to improvements in hemodynamic function, WHO functional class, and cardiac function, our results demonstrated that PADN resulted in improvement in PA remodeling and exercise capacity. Importantly, there was no additional increase in 6MWD after the 6-month follow-up, as already discussed. Nonetheless, obtaining similar results from other centers and results from randomized trials may further support that patients with PH could benefit from PADN.

Example 5

To assess the benefits of pulmonary artery denervation (PADN) among combined pre- and post-capillary pulmonary hypertension (CpcPH) patients, a prospective, randomized, sham-controlled trial was conducted.

Ninety-eight CpcPH patients, defined as mean pulmonary arterial pressure >25 mm Hg, pulmonary capillary wedge pressure >15 mm Hg, and pulmonary vascular resistance (PVR) >3.0 Wood units (WU), were randomly assigned to PADN or sildenafil plus sham PADN. Standard medical therapy for heart failure was administered to all patients in both groups. The primary endpoint was the increase in the 6-min walk distance at the 6-month follow-up. The secondary endpoint was change in PVR. Clinical worsening was assessed in a post hoc analysis. The main safety endpoint was occurrence of pulmonary embolism.

At 6 months, the mean increases in the 6-min walk distance were 83 m in the PADN group and 15 m in the sildenafil group (least square mean difference 66 m, 95% confidence interval: 38.2 to 98.8 m; p<0.001). PADN treatment was associated with a significantly lower PVR than in the sildenafil group (4.2±1.5 WU vs. 6.1±2.9 WU; p=0.001). Clinical worsening was less frequent in the PADN group compared with the sildenafil group (16.7% vs. 40%; p=0.014). At the end of the study, there were 7 all-cause deaths and 2 cases of pulmonary embolism.

In patients with heart failure (HF), the backward transmission of increased left ventricular filling pressure results in elevated pulmonary venous pressure, a status known as passive or isolated post-capillary (Ipc) pulmonary hypertension (PH), without an elevation of pulmonary vascular resistance (PVR) or diastolic pressure gradient (DPG). PH is associated with global pulmonary vascular remodeling, leading to reactive or combined pre-capillary and post-capillary PH (CpcPH), which is defined as a DPG of ≥7 mm Hg, a PVR of >3 Wood units (WU), or both.

Patients who were admitted to the hospital with the diagnosis of HF (recent onset of dyspnea and physical activity limitation) were eligible for enrollment. A diagnosis of HF was independently adjudicated by 2 general cardiologists on the basis of the current guidelines. All patients were screened via a preliminary echocardiographic examination after they were stable for at least 3 days since the initial treatment on admission. Patients who had a systolic pulmonary arterial pressure (PAP) >45 mm Hg (FIG. **32**) were referred for right heart catheterization (RHC) 12 to 24 h after ultrasound measurements.

Eligible patients were randomly assigned in a 1:1 ratio to PADN or sildenafil plus sham PADN groups using a central interactive web-based computerized system. Patients were included if they were older than 18 years, had a mean PAP (mPAP) >25 mm Hg, a pulmonary capillary wedge pressure (PCWP) >15 mm Hg, and a PVR >3.0 WU; volunteered for all follow-up assessments; and had not received any medications targeting PAH in the 3 months before admission. By contrast, patients were excluded if they had World Health Organization-defined PAH groups I, III, IV, and V; severe renal dysfunction (creatinine clearance <30 ml/min); a blood platelet count <100,000/1; an expected life span <12 months based on the DEALE method; systematic inflammation; malignancy, tricuspid, or pulmonary valvular stenosis; or were allergic to any of the studied drugs or various metals. Women who were pregnant were also excluded.

Standard anti-HF medicines, including calcium channel blockers, β-adrenergic receptor blockers, digoxin, diuretics, angiotensin-converting enzyme inhibitors, or angiotensin receptor blockers, were administered. The dosage of anti-HF medications could be titrated if patients showed deterioration in any HF symptoms. A combination of diuretics (primarily chlorthalidone 25 to 50 mg/day with spironolactone 40 to 80 mg/day or furosemide 40 mg/day) was prescribed at the referring cardiologist's discretion. A nurse who was unaware of the study design recorded the dosage of each drug every day.

Sildenafil, initially given at 20 mg 3 times daily, was the only primarily prescribed target drug in the sildenafil group. Patients were titrated to 40 mg 3 times daily after 1 week. A dose reduction was allowed if patients were intolerable to titration. The selection and dosage of other target drugs were left at the discretion of the referring physician. This part of the study was not blinded (i.e., patients in the sham PADN group were given open-label sildenafil).

Transthoracic echocardiography (Vivid 7, General Electric Co., Easton Turnpike, Connecticut) was performed by 2 registered cardiac sonographers based on a standard protocol and read/measured by an expert echocardiographer who was unaware of the study design and treatment allocation. The following parameters were measured: right ventricular systolic pressure, systolic PAP, right atrial pressure, the tricuspid excursion index, wall thickness, chamber dimension, the left ventricular ejection fraction (LVEF), mitral inflow velocity, septal annulus relaxation velocity (E'), the E/E' ratio, and tricuspid annular plane systolic excursion.

Hemodynamic measurements were performed before and immediately after the PADN procedure using a 7.5-F flow-directed Swan-Ganz catheter (774P75, Edwards Lifesciences, Irvine, California). These measurements were repeated at 6 months, with patients in a fasting state and in the supine position just 12 to 24 h after the measurement of the 6-min walk distance (6MWD). A continuous cardiac output (CO) and mixed venous oxygen saturation were simultaneously recorded (Vigilance II, Edwards Lifesciences). Five criteria, in order to evaluate whether a PCWP measurement was valid, have been described elsewhere. If the PCWP measurement was unreliable, then the left ventricular end-diastolic pressure was measured and used. Additional derived parameters included PVR (PVR=[mPAP −PCWP]/CO), transpulmonary pressure gradient (TPG=mPAP −PCWP), DPG (DPG=pulmonary arterial diastolic pressure −diastolic PCWP), and pulmonary arterial compliance (PAC) (PAC=stroke volume/pulse pressure), where pulse pressure=systolic PAP −diastolic PAP.

Blood samples (taken in the supine position) were obtained in the morning to measure the levels of N-terminal pro-B-type natriuretic peptide (NT-proBNP) before and 6 months after randomization.

The PADN procedure was performed only in the pericon-junctional area between the distal main trunk and the ostial left branch. The following ablation parameters were programmed at each point: temperature >45° C., energy <20 W, and time 120 s. The hemodynamic parameters were monitored and recorded continuously throughout the procedure. After the procedure, oral warfarin was prescribed for 1 month and adjusted to an international normalized ratio of 1.5 to 2.5 for patients with atrial fibrillation. Aspirin (100 mg per day) and clopidogrel (75 mg per day) were prescribed for 1 month for patients with sinus rhythms or for patients with atrial fibrillation with contraindications for warfarin. For a sham PADN procedure in the sildenafil group: the PADN catheter was positioned at the target sites and connected to a generator (as in the actual PADN procedure), but ablation was not performed. To simulate the true PADN procedure, discussions among the operator, technician, and nurses as well as beep sounds from the generator were recorded on a cell phone from a previous PADN procedure. This recording was played during the sham procedure, leading the patient to believe that a PADN procedure was being performed.

Functional capacity was determined before, 1 week, 1 month, 3 months, and 6 months after treatment using the standard 6MWD test according to the guidelines of the American Thoracic Society protocol (FIG. **38**). Patients avoided heavy meals 2 h before testing and were also instructed to avoid caffeine, alcohol, tea, and intense physical exercise within the previous 24 h. Before each test, patients walked as far as possible for 6 min without speaking; rests were allowed, but the patients were told to resume walking as soon as they were able. During the test, patients were given feedback at the end of every minute with encouragement. Dyspnea was assessed using the Borg scale at peak exercise during 6MWD test. The 6MWD measurement and the World Health Organization classification of dyspnea were recorded by a physician who was unaware of the treatment allocation.

Patients were contacted every month by telephone after hospital discharge during the 6-month follow-up period. An office visit at a participating center was scheduled for any patient who was suspected of having worsening symptoms. A repeat 6MWD measurement (within 2 weeks) was required for any patient who showed a reduction of >15% on the 6MWD.

The primary endpoint was the change in the 6MWD at 6-month follow-up evaluation. The secondary endpoint was the change in PVR (measured using pulmonary hemodynamics during RHC). The safety endpoint was the occurrence of pulmonary embolism (PE), defined as: 1) suspected PE (including a new intraluminal filling defect on computed tomography, magnetic resonance imaging, or a pulmonary angiogram; a new perfusion defect of at least 75% on a V/Q lung scan; or an inconclusive spiral computed tomography/pulmonary angiogram/lung scan with the demonstration of deep vein thrombosis in the lower extremities via venography); or 2) fatal PE (including PE based on objective diagnostic testing, autopsy, or death not attributed to a documented cause for which deep vein thrombosis/PE could not be ruled out). Clinical worsening was defined as any occurrence of the following: 1) worsening of symptoms defined as either failure to improve (persistent symptoms and signs of acute HF during treatment) or recurrent symptoms and signs of acute HF, pulmonary edema, or cardiogenic shock after initial stabilization since randomization, either of which requiring increased use of diuretics (as outpatient or inpatient), addition of a new intravenous therapy (diuretics, inotrope, or vasodilator) or mechanical support; 2) rehospitalization due to worsening HF requiring intravenous pharmacological agents (inotrope or vasodilator), mechanical ventilation, mechanical support or ultrafiltration, hemofiltration, or dialysis; 3) referral for heart/lung transplantation (rapidly progressive disease despite maximal medical therapy); and 4) all-cause death. Worsening of HF status was documented by monitoring nurses, clinicians and coordinators on a standardized case report form. Clinical events were blindly assessed by a clinical event committee.

Among 865 screened patients, 387 patients with HF had a systolic PAP >45 mm Hg measured by echocardiography. Among them, 112 patients (28.9%) met all the inclusion and exclusion criteria; however, 2 died soon after echocardiographic screening, and 10 did not consent to participate. Of the remaining 100 patients, 98 were then randomly assigned to the PADN group (n=48) or the sildenafil (plus sham PADN) group (n=50) (FIG. **32**). Two patients were excluded because of erroneous repeat randomization by the study nurses.

Baseline clinical, echocardiographic, and hemodynamic characteristics were similar between the 2 groups (Tables 9, 10, and 11). In general, 38.8% of patients were classified with HFpEF and 61.2% with HFrEF; 52% of patients had atrial fibrillation. The time interval from HF to PH varied from 0.3 years to 9.8 years. Of the 98 patients, 3 patients were defined as IpcPH according solely to PVR criterion (2 in the PADN group and 1 in the sildenafil group) (Table 9). In total, 35 (73.0%; p=0.068) in the PADN group and 29 patients (58.0%) in the sildenafil group had a transpulmonary pressure gradient of >12 mm Hg (Table 10).

TABLE 9

Baseline Demographic and Clinical Characteristics

Empty Cell	Sildenafil Group (n = 50)	PADN Group (n = 48)	p Value
Age, yrs	63.0 ± 12.3	63.7 ± 11.8	0.772
Male	30 (60.0)	30 (62.5)	0.838
Resting heart rate, beats/min	75.4 ± 13.1	76.6 ± 13.8	0.658
Atrial fibrillation	29 (58.0)	22 (45.8)	0.312
Height, cm	164.7 ± 8.4	165.7 ± 8.1	0.578
Weight, kg	68.9 ± 14.2	67.1 ± 14.0	0.536
Body mass index, kg/m^2	25.3 ± 4.6	24.4 ± 4.4	0.290

TABLE 9-continued

Baseline Demographic and Clinical Characteristics

Empty Cell	Sildenafil Group (n = 50)	PADN Group (n = 48)	p Value
Body surface area, m^2	1.86 ± 0.21	1.84 ± 0.21	0.696
Anemia	8 (16.0)	9 (18.8)	0.793
Positive biomarker†	11 (22.0)	10 (20.8)	1.000
Systolic blood pressure, mm Hg	125.2 ± 15.1	126.7 ± 14.4	0.604
Diastolic blood pressure, mm Hg	75.8 ± 10.0	79.3 ± 10.9	0.102
Mean blood pressure, mm Hg	92.2 ± 10.6	95.1 ± 10.3	0.181
Etiology			
Ischemic cardiomyopathy	8 (16.0)	5 (10.4)	0.554
Previous myocardial infarction	4 (8.0)	4 (8.3)	1.000
Hypertrophic cardiomyopathy	3 (6.0)	3 (6.3)	1.000
Hypertension	33 (66.0)	28 (56.0)	0.275
Diabetes	13 (26.0)	12 (25.5)	0.607
Symptom			
Dyspnea	46 (92.0)	43 (89.6)	0.738
Fatigue	48 (96.0)	42 (87.5)	0.155
Chest pain	4 (8.0)	2 (4.2)	0.678
Syncope	2 (4.0)	1 (2.1)	1.000
Pleural effusion	7 (14.0)	3 (6.3)	0.318
Serum creatinine, mmol/l	91.2 ± 40.8	84.4 ± 37.9	0.400
eGFR, ml/min/1.73 m^2	101.5 ± 39.0	108.1 ± 37.1	0.391
<60 ml/min/1.73 m2	8 (16.0)	3 (6.2)	0.200
Heart failure			
Duration, yrs‡	3.0 (1.1-12.0)	2.5 (1.2-12.1)	0.831
Classification			0.813
HFpEF	19 (38.0)	19 (39.5)	
HFrEF	31 (62.0)	29 (60.5)	
PVR-defined CpcPH	49 (98.0)	46 (95.8)	0.746
PH duration, yrs§	1.0 (0.4-9.8)	0.85 (0.3-9.5)	0.818
Medications			
ß-adrenergic receptor blocker	38 (76.0)	33 (68.8)	0.346
Nitrates	5 (10.0)	4 (8.3)	1.000
Diuretics	42 (84.0)	43 (89.6)	0.554
Digoxin	24 (48.0)	17 (35.4)	0.226
ACEI or ARB	34 (68.0)	31 (64.6)	0.846
NYHA functional class			0.665
II	2 (4.0)	2 (4.2)	
III	38 (76.0)	40 (83.3)	
IV	10 (20.0)	6 (12.5)	

Values are mean ± SD, n (%), or median (interquartile range).
ACEI = angiotensin-converting enzyme inhibitor;
ARB = angiotensin receptor blocker;
CpcPH = combined pre- and post-capillary pulmonary hypertension;
eGFR = estimated glomerular filtration rate;
HF = heart failure;
HFpEF = heart failure with preserved ejection fraction;
HFrEF = heart failure with reduced ejection fraction;
NYHA = New York Heart Association;
PADN = pulmonary artery denervation;
PH = pulmonary hypertension;
PVR = pulmonary vascular resistance.
* Defined as hemoglobin <13 g/dl for men and <11 g/dl for women.
† Defined as serum troponin ≥1 times increase of normal upper limit.
‡ Time interval from the diagnosis of heart failure to recruitment.
§ Time interval from the diagnosis of PH to recruitment.

TABLE 10

Echocardiographic and Hemodynamic Measurements

	Sildenafil Group			PADN Group			
Empty Cell	Baseline (n = 50)	6-Month (n = 45)	p Value	Baseline (n = 48)	6-Month (n = 46)	p Value	p Value*
Echocardiographic measurements							
Systolic PAP, mm Hg	57.7 ± 7.7	58.3 ± 7.0	0.546	58.3 ± 7.9	52.2 ± 7.5	<0.001	0.017
Pericardial effusion, mm	2.1 (0-13)	2.2 (0-15)	0.668	1.9 (0-12)	0.96 (0-7)	0.012	0.010
LA diameter, mm	53.1 ± 9.3	55.4 ± 9.8	0.107	52.6 ± 9.2	50.5 ± 9.6	0.103	0.004
LVDd, mm	59.8 ± 12.3	60.7 ± 12.3	0.213	58.4 ± 13.1	57.1 ± 13.0	0.291	0.019
LV Tei index, %	0.59 ± 0.09	0.58 ± 0.09	0.441	0.61 ± 0.10	0.49 ± 0.07	0.009	0.036
LV ejection fraction, %	44.5 ± 16.5	42.3 ± 15.7	0.102	43.2 ± 15.4	47.9 ± 14.3	0.055	0.050
% of increase	—	−4.8	—	—	+10.4	—	0.031
E/E' ratio	17.66 ± 6.81	17.88 ± 6.04	0.873	18.04 ± 7.25	10.58 ± 3.17	0.010	0.011
TAPSE, mm	15.3 ± 4.9	15.1 ± 2.7	0.802	15.8 ± 3.6	19.7 ± 2.8	0.022	0.017
RV Tei index, %	0.44 ± 0.12	0.45 ± 0.10	0.503	0.49 ± 0.17	0.38 ± 0.11	0.014	0.016
RA long-axis diameter, mm	60.4 ± 12.4	59.6 ± 10.7	0.657	59.7 ± 13.5	58.2 ± 11.1	0.664	0.561
RA short-axis diameter, mm	48.6 ± 11.5	46.9 ± 12.7	0.234	48.7 ± 10.4	46.9 ± 10.2	0.128	0.986
Hemodynamic measurements via right heart catheterization							
RA pressure, mm Hg	13.8 ± 5.6	13.1 ± 4.1	0.322	13.8 ± 7.3	11.0 ± 5.1	0.122	0.189
Systolic PAP, mm Hg	56.5 ± 15.2	52.4 ± 11.3	0.196	58.7 ± 19.5	44.6 ± 19.2	<0.001	<0.001
Mean PAP, mm Hg	36.9 ± 10.8	34.4 ± 7.9	0.133	38.8 ± 10.6	28.6 ± 6.5	<0.001	0.037
Cardiac output, l/min	2.56 ± 0.74	2.51 ± 0.72	0.564	2.61 ± 0.76	3.09 ± 0.81	0.021	0.017
Cardiac index, l/min/m^2	1.67 ± 0.79	1.72 ± 0.64	0.089	1.72 ± 0.84	2.52 ± 0.70	0.038	0.035
PVR, Woods units	6.25 ± 3.23	6.09 ± 2.94	0.590	6.38 ± 3.19	4.18 ± 1.51	<0.001	0.001

TABLE 10-continued

Echocardiographic and Hemodynamic Measurements							
	Sildenafil Group			PADN Group			
Empty Cell	Baseline (n = 50)	6-Month (n = 45)	p Value	Baseline (n = 48)	6-Month (n = 46)	p Value	p Value*
PCWP, mm Hg	20.9 ± 5.58	19.1 ± 6.1	0.909	22.2 ± 6.6	16.1 ± 6.2	0.013	0.041
TPG, mm Hg	16.1 ± 4.6	15.3 ± 3.8	0.101	16.5 ± 4.7	12.9 ± 3.9	0.001	0.002
>12 mm Hg	29 (58.0)	25 (55.6)	0.530	35 (73.0)	17 (38.6)	0.001	0.047
DPG, mm Hg	10.4 ± 3.2	9.86 ± 1.74	0.120	10.9 ± 3.7	6.8 ± 1.2	0.011	0.042
PAC, ml/mm Hg	1.96 ± 0.65	1.95 ± 0.86	0.944	1.92 ± 0.86	3.9 ± 0.96	<0.001	<0.001

Values are mean ± SD, median (interquartile range), or n (%).

DPG = diastolic pressure gradient; LA = left atrial; LV = left ventricle; LVDd = left ventricular end-systolic diameter; PAC = pulmonary arterial compliance; PAP = pulmonary arterial pressure; PCWP = pulmonary capillary wedge pressure; RA = right atrial; RV = right ventricle; RVP = right ventricular pressure; TAPSE = tricuspid annual plane systolic excursion; TPG = transpulmonary pressure gradient; VTI = velocity time integral; other abbreviations as in Table 9.

*Indicates a comparison between two 6-month subgroups.

TABLE 11

Clinical Follow-Up			
Empty Cell	Sildenafil Group (n = 50)	PADN Group (n = 48)	p Value
Diuretics dosage (total), mg/day			
Before enrollment	40 (0 to 90)	40 (0 to 80)	0.754
At 6 months	60 (20 to 155)	24 (0 to 140)	0.030
Titration	24 (48.0)	6 (12.5)	0.031
Target drugs			
Monotherapy (sildenafil)	50 (100.0)	0 (0.0)	NS
Combined with prostacyclin analog	1 (2.0)	0 (0.0)	NS
Calcium channel blocker	26 (52.0)	20 (41.7)	0.604
Endothelin receptor antagonist	0 (0.0)	0 (0.0)	NS
NT-proBNP, pg/ml			
Before PADN	1,345 (145 to 14,293)	1,601 (104 to 13,876)	0.803
At 6 months	1,345 (31 to ~9,563)	809 (25 to ~5,004)	0.001
Net reduction, %	−6.2 (−82 to ~54)	−47.5 (−99 to ~33.1)	0.003
NYHA functional class, at 6 months	2.51 ± 0.75	2.13 ± 0.57	0.012
n	45	46	
Class I	0 (0.0)	10 (20.0)	
Class II	28 (63.6)	25 (54.3)	
Class III/IV	16 (36.4)	11 (23.9)	
Borg index, score	1.19 ± 0.66	1.09 ± 0.58	0.548
Clinical worsening	20 (40.0)	8 (16.7)	0.014
All-cause death	5 (10.0)	2 (4.2)	0.436
Rehospitalization	14 (28.0)	6 (12.5)	0.052
Worsening of heart failure	18 (36.0)	7 (14.6)	0.016
Heart transplantation	1 (2.0)	0 (0.0)	NS

Values are median (interquartile range), n (%), n, or mean ± SD.

NT-proBNP = N-terminal pro-B-type natriuretic peptide; other abbreviations as in Table 9.

*Used in 1 patient at 162 days after randomization.

The baseline 6MWD was comparable between the 2 groups (FIG. **33**). In the PADN group, the mean increment of the 6MWD at the 6-month follow-up was 83 m (21.4% increase, least square mean difference 66 m, 95% CI: 38.2 to 98.8; p<0.001), significantly higher than 15 m (a 4.9% increase in median value) in the sildenafil group (FIG. **33**). Eighteen patients showed a reduction in the 6MWD at the end of the follow-up period, including 6 (12.5%) in the PADN group (3 [6.3%] having a reduction of >15% in the 6MWD, HR: 2.947, 95% CI: 1.152 to 4.501; p<0.001) (FIG. **33**) and 12 (26.7%) in the sildenafil group (7 [14%] having a reduction of >15% in 6MWD). Of the 91 surviving patients, the mean increase, percentage increase, and the absolute mean value of the 6MWD in the PADN group were 85.1 m, 50.2%, and 442.4 m, respectively. The corresponding values in the sildenafil group were 20.1 m, 6.8%, and 373.5 m, respectively. All comparisons were statistically significantly higher in the PADN group (p<0.001 for all). However, the change of the 6MWD in both HFpEF and HFrEF subgroups in either the PADN or sildenafil group was comparable (FIG. **34**). There was no significant difference in 6MWD at each timing point of follow-up between patients with EFpHF or EFrHF subgroups in either PADN or Medication group (FIG. **34**). However, at 6 months follow-up, the increase of 6MWD in the PADN group was significantly higher than that in the Medication group (Table 11). By Cox regression analysis, a decrease of 1 SD in the 6MWD significantly predicted the occurrence of clinical worsening (corresponding HR: 3.023, 95% CI: 1.052 to 8.742; p=0.040), but not the prediction of all-cause death, worsening of HF, and rehospitalization (Table 12).

TABLE 12

Adjusted Prediction of 1 SD Decrease in 6MWD for Clinical Events

Empty Cell	Hazard Ratio	95% Confidence Interval	p Values
Clinical worsening	3.023	1.052-8.742	0.040
Worsening of heart failure	2.550	0.875-7.431	0.086
All-cause death	36.730	0.045-29,703.261	0.291
Rehospitalization 6MWD = 6-min walk distance.	1.880	0.628-5.623	0.259

*p Values were calculated with the use of a Cox proportional model, adjusted by conventional baseline demographic variables (all listed in Table 1) and echocardiographic or hemodynamic measurements (all listed in Table 10 in context).

At 6 months, PADN treatment was associated with a significantly lower PVR than in the sildenafil group (4.2±1.5 WU vs. 6.1±2.9 WU; p=0.001). The average reduction of PVR from baseline to 6-month RHC was 29.8% in the PADN group and 3.4% in the sildenafil group (HR: 4.73, 95% CI: 2.05 to 10.89; p<0.001) (Table 10), which was consistent with the increase of CO and PAC.

At the 6-month follow-up, clinical worsening was reported in 28 patients (Table 11, FIG. **35**): 20 (40.0%) in the sildenafil group and 8 (16.7%) in the PADN group (HR: 2.690, 95% CI: 1.184 to 6.113; p=0.018) (FIG. **35**), primarily driven by the protocol defined worsening of HF (36.0% vs. 14.6%, HR: 2.743, 95% CI: 1.145 to 6.571; p=0.024) (FIG. **35**). The PADN procedure was associated with significant improvements in all hemodynamic parameters (Table 10), except for right atrial pressure which tended to be lower, but there was no significant difference. PAC was significantly improved at 6 months after PADN, in parallel with the absolute increase in the 6MWD (FIG. **36**A-FIG. **36**F). However, PVR was unchanged after 6 months in the sildenafil group (FIG. **36**A-FIG. **36**F). The correlation of baseline pulmonary arterial compliance (PAC) with baseline 6-minute walk distance (6MWD) was weak (R^2=0.042, FIG. **36**A), however, after 6 months treatment, the correlation of PAC with absolute increase of 6MWD in was significantly improved (R2=0.160, FIG. **36**B) in the PADN group but not in the Sildenafil group (FIG. **36**C). In contrast, correlation of baseline PAC with pulmonary vascular resistance (PVR, FIG. **36**D) was equally improved at 6 months after treatment in either PADN (FIG. **36**E) or Sildenafil (FIG. **36**F) group, this also indicated the positive treatment effect of sildenafil on PAC and PVR.

These results were in line with the lower requirement for diuretic titration, the reduction of NT-proBNP, Borg index, and improvement of cardiac function (Table 11). Of the 48 patients in the PADN group, 4 (8.3%) were nonresponders, defined as a reduction of mPAP or systolic PAP <10% post-PADN, and 3 patients showed a post-PADN PCWP higher than the baseline value (but no worsening of symptoms). For these 3 patients, repeat RHC was performed 1 week after PADN, and the temporary increment of PCWP decreased thereafter. At 6 months, 6MWD measurement was a statistically significant predictor of clinical worsening or all-cause death (FIG. **37**A-FIG. **37**D). The prediction of baseline 6MWD for clinical worsening (FIG. **37**A) or all-cause death (FIG. **37**B) was significantly enhanced by using 6-month 6MWD to predict (FIG. **37**C, FIG. **37**D).

At the 6-month follow-up, **2** fatal pulmonary embolisms were reported, with one at 72 days after randomization in the PADN group and the other at 36 days in the sildenafil group. There were 7 deaths: 2 in the PADN group (one died of pump failure at 6 days, the other died suddenly at 29 days) and 5 in the sildenafil group (1 died suddenly at 17 days, and the remaining 4 died of pump failure at 17, 93, 100, and 154 days).

After a 6-month follow-up, PADN resulted in a significant increase in the 6MWD, consistent with the significant improvements in PVR, other hemodynamic parameters, and cardiac function. Post hoc analysis demonstrated significantly less frequent clinical worsening with PADN compared with sildenafil therapy. A decrease of 1 SD in the 6MWD strongly predicted the occurrence of clinical worsening.

Neurohumoral overactivation in HF with PH is clinically demonstrated by increased circulating catecholamine levels and impaired heart rate variability, which may indicate the potential of using local denervation for patients with CpcPH. In an experimental study, we further found that both the localization of PA nerve trunk (at the left lateral wall of main PA) and a shorter distance between nerve trunk and PA intimal surface anatomically favor the performance of PADN at this specific location. Furthermore, PADN was tested in a single-center registry of patients with idiopathic PAH and PH secondary to left-sided HF, demonstrating beneficial effects on hemodynamic parameters and exercise capacity. In the present randomized study, PADN treatment (plus standard anti-HF medications) was associated with a significant increase in 6MWD at the 6-month follow-up, which was in parallel to the improvement in pulmonary hemodynamics and cardiac functions, compared with the effects of sildenafil plus standard medications, which further confirmed our previous reports. A sham PADN procedure was performed on patients in the sildenafil group to minimize or eliminate the placebo effect. Blinding may not have been complete due to the open administration of sildenafil in only 1 of the randomized groups.

The 6MWD was selected as the primary endpoint in previous studies of patients with PAH, and a >15% reduction in the 6MWD is a criterion for a clinical event. An 83-m increase in 6MWD achieved by PADN treatment was observed in the study (FIG. **33** and FIG. **38**). The results demonstrated that both 6MWD at 6-month follow-up and 1-SD decrease in 6MWD strongly predicted clinical worsening and further enhanced the prognostic importance of 6MWD for CpcPH patients. PADN resulted in equally improved 6MWD in patients with either HFrEF or HFpEF. Both diastolic and systolic cardiac functions were significantly improved after PADN procedure.

As used herein, the term "animal" is intended to include human beings and other animals such canines, other mammals, etc. As used herein, the terms "live", "living", "live animal" are intended to exclude methods of euthanasia, surgery performed on dead animals including dissection and autopsies, or other techniques for disposing of dead bodies.

While at least a plurality of different embodiments are disclosed herein, it should be appreciated that a vast number of variations exist. It should also be appreciated that the embodiments described herein are not intended to limit the scope, applicability, or configuration of the claimed subject matter in any way. Rather, the foregoing detailed description will provide those skilled in the art with a convenient road map for implementing the described embodiments. It should be understood that various changes can be made in the function and arrangement of elements or steps without departing from the scope defined by the claims, which includes known equivalents and foreseeable equivalents at the time of filing this patent application.

What is claimed is:

1. A method for treating a heart disease or appearance or worsening signs of heart failure, the method comprising:

i. positioning an ablation device in a pulmonary artery trunk of a patient, the pulmonary artery trunk including a distal portion of a main pulmonary artery, a proximal portion of a left pulmonary artery, and a proximal portion of a right pulmonary artery, and

ii. ablating a target tissue in the pulmonary artery trunk to affect an increase in one or more of 6-minute walk distance (6MWD) or cardiac output from at least 6 months after the ablating to 2 years after the ablating,

wherein the target tissue comprises at least one of the distal portion of the main pulmonary artery, the proximal portion of the left pulmonary artery, or the proximal portion of the right pulmonary artery; and

wherein ablating the target tissue comprises ablating one or more of a first ablation site at a left lateral apex of the distal portion of the main pulmonary artery, a second ablation site at an anterior side of the left lateral apex of the distal portion of the main pulmonary artery, or third ablation site at a posterior side of the left lateral apex of the distal portion of the main pulmonary artery.

2. The method of claim **1**, wherein the increase in one or more of 6-minute walk distance (6MWD) or cardiac output at least 6 months after the ablating is about 15%.

3. The method of claim **1**, wherein ablating the target tissue comprises applying at least one of radiofrequency (RF) energy, microwave energy, ultrasound energy, focused ultrasound energy, ionizing energy, electroporation, a drug, a chemical agent, or cryoablation to the target tissue.

4. The method of claim **1**, wherein positioning the ablation device comprises positioning an expandable ablation element of the ablation device adjacent the target tissue and wherein ablating the target tissue comprises ablating the target tissue with the ablation element positioned adjacent the target tissue, the ablation element comprising one or more ablation electrodes.

5. The method of claim **1**, wherein ablating the target tissue causes disruption of sympathetic nerves at the pulmonary artery trunk.

6. The method of claim **1**, wherein positioning the ablation device in the pulmonary artery trunk of the patient comprises advancing the ablation device into a femoral vein of the patient, upwardly into an inferior vena cava of the patient, then upwards into a right atrium of the patient, then down into a right ventricle of the patient, and then up through a pulmonary semilunar valve of the patient to the main pulmonary artery trunk.

7. A method for treating a heart disease or appearance or worsening signs of heart failure, the method comprising:

i. positioning an ablation device in a pulmonary artery trunk of a patient, the pulmonary artery trunk including a distal portion of a main pulmonary artery, a proximal portion of a left pulmonary artery, and a proximal portion of a right pulmonary artery, and

ii. ablating a target tissue in the pulmonary artery trunk to affect a reduction in mean pulmonary artery pressure and a reduction in systolic pulmonary artery pressure,

wherein the target tissue comprises at least one of the distal portion of the main pulmonary artery, the proximal portion of the left pulmonary artery, or the proximal portion of the right pulmonary artery.

8. The method of claim **7**, wherein the reduction in mean pulmonary artery pressure and a reduction in systolic pulmonary artery pressure is about 15%.

9. The method of claim **7**, wherein ablating the target tissue comprises applying at least one of radiofrequency (RF) energy, microwave energy, ultrasound energy, focused ultrasound energy, ionizing energy, electroporation, a drug, a chemical agent, or cryoablation to the target tissue.

10. The method of claim **7**, wherein positioning the ablation device comprises positioning an expandable ablation element of the ablation device adjacent the target tissue and wherein ablating the target tissue comprises ablating the target tissue with the ablation element positioned adjacent the target tissue, the ablation element comprising one or more ablation electrodes.

11. The method of claim **7**, wherein ablating the target tissue comprises ablating one or more of a first ablation site at a left lateral apex of the distal portion of the main pulmonary artery, a second ablation site at an anterior side of the left lateral apex of the distal portion of the main pulmonary artery, or third ablation site at a posterior side of the left lateral apex of the distal portion of the main pulmonary artery.

12. The method of claim **7**, wherein ablating the target tissue causes disruption of sympathetic nerves at the pulmonary artery trunk.

13. The method of claim **7**, wherein positioning the ablation device in the pulmonary artery trunk of the patient comprises advancing the ablation device into a femoral vein of the patient, upwardly into an inferior vena cava of the patient, then upwards into a right atrium of the patient, then down into a right ventricle of the patient, and then up through a pulmonary semilunar valve of the patient to the main pulmonary artery trunk.

* * * * *